



**SOARING  
UPWARDS**  
MALAYSIAN HIGHER EDUCATION



FRGS REPORT

ACTIVE DRAG REDUCTION TECHNIQUE  
FOR ENHANCING THE LIQUID-LIQUID  
MIXING INTENSITY IN MICROMIXERS

(FRGS/1/2016/TK02/UMP/02/1)

(RDU 160120)

HAYDER A. ABDULBARI

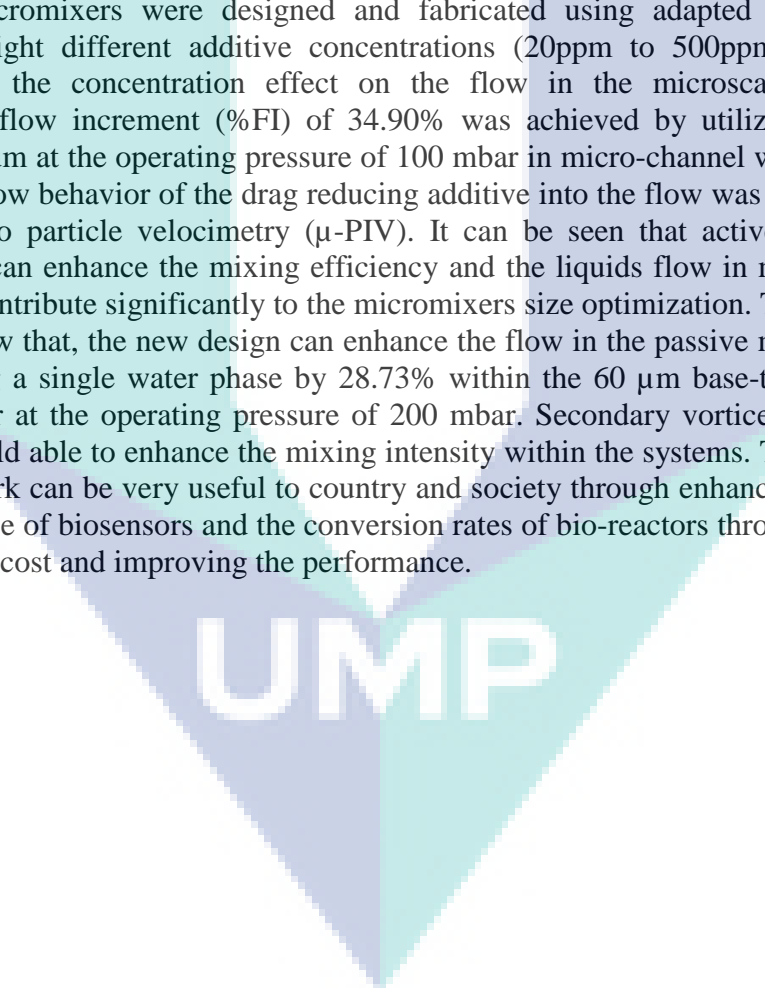
UMP

UNIVERSITI MALAYSIA PAHANG

49T

## ABSTRACT

The advancement of microfluidic devices in the past two decades have had a considerable impact on many academic and industrial fields like biomedical diagnostics, drug development, food and chemical industries. Most of the microfluidics devices consist of microchannels for liquids transportation and mixing, and the design of these channels highly controls the liquids interactions especially in the case of micromixers. The flow in the micromixers is always strictly laminar, and the mixing intensity will depend only on the molecular diffusion between the two phases. Such poor mixing efficiency will affect the micromixers design and size. Optimizing the micromixers size and design is directly related to the media type, micromixers shapes, and flowing conditions. Enhancing the liquids flow in micromixers using active drag reduction techniques will be implemented in the present work. In this work, the addition of soluble polymeric additives (Xanthan gum) function as a drag reducing agent (DRA) on the flow behavior in micromixers was investigated. Seven different geometries of Y-shaped micromixers were designed and fabricated using adapted soft lithography method. Eight different additive concentrations (20ppm to 500ppm) were used to investigate the concentration effect on the flow in the microscale devices. The maximum flow increment (%FI) of 34.90% was achieved by utilizing 500 ppm of Xanthan gum at the operating pressure of 100 mbar in micro-channel with width of 500  $\mu\text{m}$ . The flow behavior of the drag reducing additive into the flow was also investigated using micro particle velocimetry ( $\mu$ -PIV). It can be seen that active drag reduction technique can enhance the mixing efficiency and the liquids flow in micromixers, and that will contribute significantly to the micromixers size optimization. The experimental results show that, the new design can enhance the flow in the passive micromixer when introducing a single water phase by 28.73% within the 60  $\mu\text{m}$  base-to-height ribletted micromixer at the operating pressure of 200 mbar. Secondary vortices were observed which would able to enhance the mixing intensity within the systems. The results of the present work can be very useful to country and society through enhancing the detection performance of biosensors and the conversion rates of bio-reactors through reducing the fabrication cost and improving the performance.

The logo for UMP (Universitas Muhammadiyah Purwokerto) is a large, stylized letter 'U' composed of four triangular segments in shades of blue and teal. The letters 'U', 'M', and 'P' are printed in white across the center of the 'U'.

## TABLE OF CONTENT

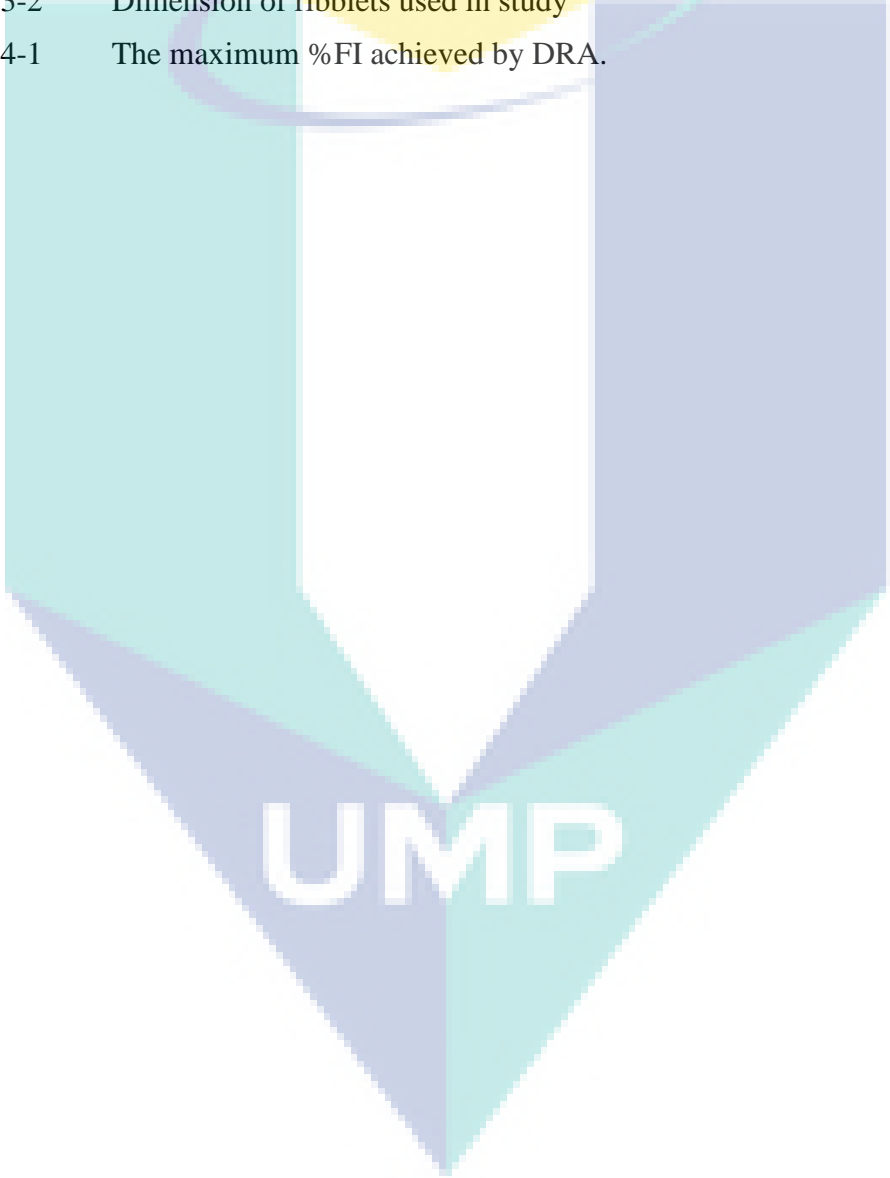
<b>ABSTRACT</b>	<b>iii</b>
<b>TABLE OF CONTENT</b>	<b>iv</b>
<b>LIST OF TABLES</b>	<b>vii</b>
<b>LIST OF FIGURES</b>	<b>viii</b>
<b>LIST OF SYMBOLS</b>	<b>xi</b>
<b>LIST OF ABBREVIATIONS</b>	<b>xii</b>
<b>CHAPTER 1 INTRODUCTION</b>	<b>1</b>
1.1 Motivation	1
1.2 Statement of Problems	4
1.3 Objectives	5
1.4 Research Scopes	5
<b>CHAPTER 2 LITERATURE REVIEW</b>	<b>7</b>
2.1 Micromixer	7
2.1.1 Active Micromixer	8
2.1.2 Passive Micromixer	11
2.1.2.1 Lamination	11
2.1.2.2 Injection Molding	12
2.1.2.3 Surface- Chemistry Technology	12
2.1.2.4 Obstacle Barrier	13
2.2 Drag Reduction	14
2.3 Active Drag Reduction Technique	16

2.3.1	Insoluble Additives (Suspended solids)	16
2.3.2	Soluble Additives	18
2.4	Flow in Microchannels	27
2.5	Microchannels Fabrication Technology	28
2.5.1	Machining	29
2.5.2	Embossing	30
2.5.3	Injection molding	32
2.5.4	Etching	33
2.5.5	Soft Lithography	34
2.6	Particle Image Velocimetry	36
<b>CHAPTER 3 METHODOLOGY</b>		<b>40</b>
3.1	Materials	40
3.1.1	Natural Polymers	40
3.1.2	Working Fluid	40
3.1	Natural polymer solution preparation	41
3.2	Fabrication of Microchannels	41
3.3	Natural Polymer Characterization Analysis	47
3.3.1	Morphology Analysis	47
3.3.2	Rheology Study	47
3.4	Experimental Set-Up	47
3.5	Experimental Procedure	48
3.6	$\mu$ -PIV Measurement	49
<b>CHAPTER 4 RESULTS AND DISCUSSION</b>		<b>51</b>
4.1	Characterization of Natural Polymer	51

4.1.1	Morphological Analysis	51
4.1.2	Rheology Study	52
4.2	Experimental Flow Enhancement Results	56
4.2.1	Effect of Mucilage Concentration	56
4.2.2	Effect of Length in Micro-channels	60
4.2.3	Effect of Width in Micro-channels	65
4.2.4	Summary	69
4.2.5	Flow Enhancement for Passive Micromixer	70
4.3	Result and Discussions for Micro-PIV	71
4.3.1	The CCD Images	71
4.3.2	Velocity Profiles for Active Micromixers	73
4.3.3	Velocity Profiles for Passive Micromixers	78
<b>CHAPTER 5 CONCLUSIONS AND RECOMMENDATIONS</b>		<b>83</b>
5.1	Conclusions	83
5.2	Future work	84
<b>REFERENCES</b>		<b>85</b>
<b>APPENDIX A Publications and awards</b>		<b>116</b>

## LIST OF TABLES

Table 2-1	Summary of synthetic polymeric as drag reducing additives in enhancing fluid flow in pipeline system	24
Table 2-2	Summary of natural polymeric as drag reducing additives in enhancing fluid flow in pipeline system	26
Table 2-3	Summary of fabrication of microchannel technologies	35
Table 3-1	The schematic of Y-shaped micro-channels.	41
Table 3-2	Dimension of ribblets used in study	44
Table 4-1	The maximum %FI achieved by DRA.	70



UMP

## LIST OF FIGURES

Figure 2-1	Classification of active micromixers by Chi-Yen (2011) and Nguyen et. al (2004)	8
Figure 2-2	Microphotograph of the DEP micromixer	9
Figure 2-3	Schematic diagram of channel with multiple side channels	10
Figure 2-3	Classification of passive micromier	11
Figure 2-5	Schematic diagram of the experiment for DR using PAM-based polymer	28
Figure 2-6	Experimental setup of laser machining	30
Figure 2-7	Schematic diagram of hot embossing equipment	31
Figure 2-8	Soft lithography process involving silicon master	35
Figure 2-9	Basic PIV setup comprised of transparent test section with the particle seeded fluid, a laser source producing a light sheet; charge coupled device (CCD) camera imaging the particles in the sheet, and a computer to process and analyze information	37
Figure 3-1	The monosaccharides present in xanthan gum.	40
Figure 3-2	Fabricated Y-shaped micro-channels	43
Figure 3-3	Overall dimension of designed microchannel with ribblets profile	44
Figure 3-4	Fabrication steps of the micro-channel.	46
Figure 3-4	Schematic diagram of experimental setup consisted of (a) computer (b) pressure and vacuum controller (c) reservoir containing solution (d) flow sensor (e) custom made microchannel (f) beaker as storage tank	48
Figure 3-5	Schematic diagram of $\mu$ -PIV setup	50
Figure 4-1	Cryo-TEM image of xanthan gum solution	52
Figure 4-2	Viscosity of various xanthan gum concentrations as a function of shear rate with DI water as control	53
Figure 4-3	Shear stress of various xanthan gum concentrations as a function of shear rate with DI water as control	54
Figure 4-4	G' and G'' curves of xanthan gum solutions at the concentration of (a) 20 ppm, (b) 50 ppm, (c) 100 ppm, (d) 150 ppm, (e) 200 ppm, (f) 300 ppm, (g) 400 ppm, and (h) 500 ppm as a function of sweep frequency	56
Figure 4-5	%FI of various Xanthan gum concentrations varying the operating pressure in micro-channel having the tail length of 70 mm.	57
Figure 4-6	%FI of various Xanthan gum concentrations varying the operating pressure in micro-channel having the tail length of 60 mm.	58
Figure 4-7	%FI of various Xanthan gum concentrations varying the operating pressure in micro-channel having the tail length of 50 mm.	58

Figure 4-8	%FI of various Xanthan gum concentrations varying the operating pressure in micro-channel having the tail length of 40 mm.	59
Figure 4-9	%FI of various Xanthan gum concentrations varying the operating pressure in micro-channel having the width of 500 $\mu\text{m}$ .	59
Figure 4-10	%FI of various Xanthan gum concentrations varying the operating pressure in micro-channel having the width of 300 $\mu\text{m}$ .	60
Figure 4-11	%FI of various Xanthan gum concentrations varying the operating pressure in micro-channel having the width of 200 $\mu\text{m}$ .	60
Figure 4-12	%FI of Xanthan gum in various tail length of micro-channel by varying the operating pressure having the concentration of 20 ppm.	61
Figure 4-13	%FI of Xanthan gum in various tail length of micro-channel by varying the operating pressure having the concentration of 50 ppm.	62
Figure 4-14	%FI of Xanthan gum in various tail length of micro-channel by varying the operating pressure having the concentration of 100 ppm.	62
Figure 4-15	%FI of Xanthan gum in various tail length of micro-channel by varying the operating pressure having the concentration of 150 ppm.	63
Figure 4-16	%FI of Xanthan gum in various tail length of micro-channel by varying the operating pressure having the concentration of 200 ppm.	63
Figure 4-17	%FI of Xanthan gum in various tail length of micro-channel by varying the operating pressure having the concentration of 300 ppm.	64
Figure 4-18	%FI of Xanthan gum in various tail length of micro-channel by varying the operating pressure having the concentration of 400 ppm.	64
Figure 4-19	%FI of Xanthan gum in various tail length of micro-channel by varying the operating pressure having the concentration of 500 ppm.	65
Figure 4-20	%FI of Xanthan gum in various width of micro-channel by varying the operating pressure having the concentration of 20 ppm.	66
Figure 4-21	%FI of Xanthan gum in various width of micro-channel by varying the operating pressure having the concentration of 50 ppm.	66
Figure 4-22	%FI of Xanthan gum in various width of micro-channel by varying the operating pressure having the concentration of 100 ppm.	67
Figure 4-23	%FI of Xanthan gum in various width of micro-channel by varying the operating pressure having the concentration of 150 ppm.	67
Figure 4-24	%FI of Xanthan gum in various width of micro-channel by varying the operating pressure having the concentration of 200 ppm.	68
Figure 4-25	%FI of Xanthan gum in various width of micro-channel by varying the operating pressure having the concentration of 300 ppm.	68
Figure 4-26	%FI of Xanthan gum in various width of micro-channel by varying the operating pressure having the concentration of 400 ppm.	69
Figure 4-27	%FI of Xanthan gum in various width of micro-channel by varying the operating pressure having the concentration of 500 ppm.	69
Figure 4-28	Flow enhancement of micromixer against pressure.	71

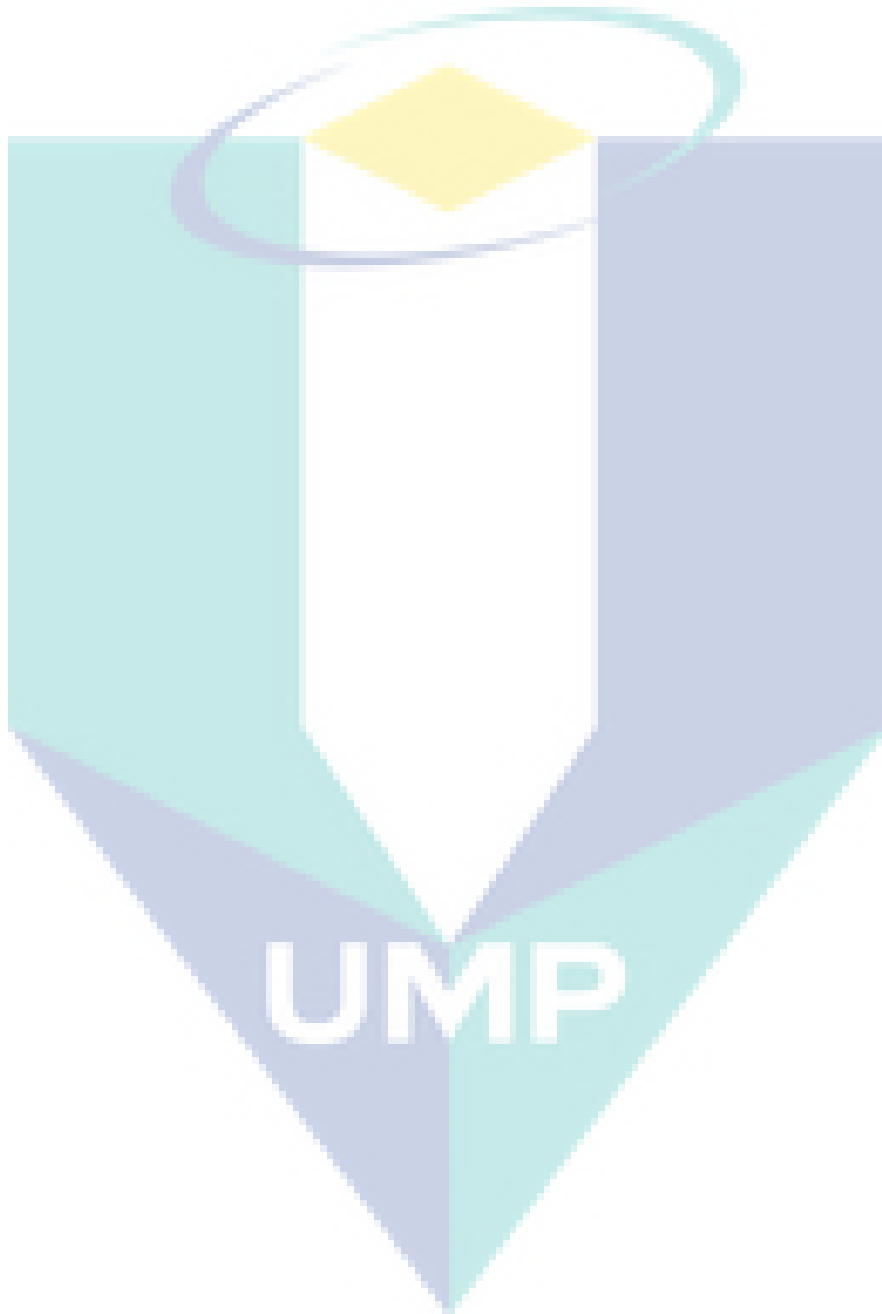
Figure 4-29	Schematic of the 500 $\mu\text{m}$ width micro-channel consist measured regions of (a) Y-shaped (b) straight channel	72
Figure 4-30	CCD images at the Y-shaped region having the (a) DI water and concentration of (b) 20 ppm (c) 50 ppm (d) 100 ppm (e) 150 ppm (f) 200 ppm (g) 300 ppm (h) 400 ppm, and (i) 500 ppm	72
Figure 4-31	CCD images at the straight region having the (a) DI water and concentration of (b) 20 ppm (c) 50 ppm (d) 100 ppm (e) 150 ppm (f) 200 ppm (g) 300 ppm (h) 400 ppm, and (i) 500 ppm	73
Figure 4-32	Velocity profiles at the Y-shaped region having the (a) DI water and concentration of (b) 20 ppm (c) 50 ppm (d) 100 ppm (e) 150 ppm (f) 200 ppm (g) 300 ppm (h) 400 ppm, and (i) 500 ppm	75
Figure 4-33	Velocity profiles at the straight channel region having the (a) DI water and concentration of (b) 20 ppm (c) 50 ppm (d) 100 ppm (e) 150 ppm (f) 200 ppm (g) 300 ppm (h) 400 ppm, and (i) 500 ppm	77
Figure 4-34	Image of $\mu\text{PIV}$ of 60micron ribblets with inlet pressure of 400mbar and 450mbar respectively	79
Figure 4-35	Image of $\mu\text{PIV}$ of 60micron ribblets with inlet pressure of 800mbar and 850mbar respectively	80
Figure 4-36	Image from $\mu\text{PIV}$ of 40 mircon ribblets of 250mbar inlet pressure at part 2 showing the formation of eddies.	81
Figure 4-37	Image from $\mu\text{PIV}$ of 60 mircon ribblets of 350mbar inlet pressure having both dead zone and eddies formation	81

UMP

## LIST OF SYMBOLS

### *Subscripts*

*a* after drag reducing additive addition  
*b* before drag reducing additive addition



## LIST OF ABBREVIATIONS

%DR	Percentage of drag reduction
%FI	Percentage of flow rate increment
APG1214	Alkyl Polyglycoside
CMC	Carboxymethylcellulose
DI water	Deionized water
DR	Drag reduction
DRA	Drag reducing additives
DSC	Differential Scanning Calorimeter
F	Flow rate
FTIR	Fourier Transform Infrared
HF	Hydrogen fluoride
HNO <sub>3</sub>	Nitric acid
ID	Inner diameter
IR laser	Infrared laser
KOH	Potassium hydroxide
MEMS	Microelectromechanical systems
NaAMPS	Sodium 2-acrylamido-2-methylpropane sulphonic acid
PA	Polyamide
PAM	Polyacrylamide
Poly(AM-co-AA)	Poly(acrylamide-co-acrylic acid)
PCI	Percutaneous coronary intervention
PDMS	Polydimethylsiloxane
PEG	Polyethylene glycol
PEO	Polyethylene oxide
PiB	Polyisobutylene
PIV	Particle Image Velocimetry
PMMA	Polymethyl methacrylate
ppm	Parts per million
Re	Reynolds number
RIE	Reactive-ion etching
SDS	Sodium Dodecyl Sulphate
SEM	Scanning Electron Microscope
T <sub>g</sub>	Glass transition temperature
XG	Xanthan gum
μ-PIV	Micro Particle Image Velocimetry

## CHAPTER 1

### INTRODUCTION

#### 1.1 Motivation

Micromixer is an essential component in sample preparation stage of a chemical analysis before proceeding to any chemical or biological reactions. This miniature device brings benefit including utilizes small amount of biological or chemical reagent resulting in reducing the consumption of expensive reagents (e.g. enzymes, chemical standards etc.) thus attractive to be used in many chemical and biological procedures (Wong et.al., 2004).

Micromixer is greatly applied in various industries field such as analytical chemistry and biochemistry. This situation has led to increasing of attention from many researches on the modification of the micromixer design to improve the efficiency of the mixing. Micromixers are usually classified into two major groups namely active and passive micromixers (Victorov et.al., 2015)

Due to this micro size of the micromixer; the microfluidic system has laminar flow behaviour where molecular diffusion is the most dominant in mixing mechanism (Wang et.al., 2002). This mechanism resulting in slower mixing process (Hossain et.al., 2015) where the complete mixing between two fluids in a simple mixer required a longer time and a longer mixing length. Thus, active micromixers require external forces to enhance the mixing performance.

The enhancement of fluid flow in pipes and conduits has always attracted much attention in many industries due to its high economic impact. Drag reduction (DR) as a technique or phenomena, gained much interest since the pioneering work of Toms (Truong, 2001) in the 1940s; when he reported a significant low friction factor with the addition of minute quantities of poly(methyl methacrylate) in mono chlorobenzene

flow, later known as “Toms effect”. Nowadays, active DR is defined as the reduction of the skin friction in turbulent flows through the addition of small quantities of long-chain flexible polymers (White & Mungal, 2008). Hence, DR techniques can be beneficial in the industries by minimizing the energy input and operating costs such as pumping station capital costs, while maintaining the throughput and optimizing the production.

Many researchers have started to introduce and investigate different types of drag reducing additives (DRA) such as long chain polymers (Abubakar, Al-Whaibi, Al-Wahaibi, Al-Hashmi, & Al-Ajmi, 2014; Al-Sarkhi, 2012; Benzi, 2010; Iaccarino, Shaqfeh, & Dubief, 2010; Resende, Kim, Younis, Sureshkumar, & Pinho, 2011), and surfactants (Drzazga, Gierczycki, Dzido, & Lemanowicz, 2013; Li, Kawaguchi, Yu, Wei, & Hishida, 2008; Qi *et al.*, 2011; Rózański, 2011; Tuan & Mizunuma, 2013; Yu & Kawaguchi, 2006) for the enhancement of liquid flow in pipes and channels. The active DR additives were proven to have high DR performance even when used in a minute quantity, usually in parts per million (ppm). They have been greatly utilized in different industrial applications such as the 1300 km USA Alaskan pipeline (Al-Sarkhi, 2010; Burger, Munk, & Wahl, 1982; Li, Yu, Wei, & Kawaguchi, 2012), firefighting, transportation of suspensions and slurries, heat exchanger, airplane tank filling, marine systems, and medical applications (Al-Sarkhi & Hanratty, 2001; Mavros, Ricard, Xuereb, & Bertrand, 2011; Thais, Gatski, & Mompean, 2013; Walsh, Muzychka, Walsh, Egan, & Punch, 2009; Yang & Ding, 2013).

Polymers as DRA play a vital role in both industries and researchers due to their availability in the market and economic feasibility. However, most of the investigated polymeric DRA such as polyacrylamide (PAM) and polyethylene oxide (PEO) are synthetic polymers which are also used as flocculants for wastewater treatment (Brostow, Lobland, Pal, & Singh, 2009). These synthetic polymers are mostly non-biodegradable and considered as not environmentally friendly products. Besides, artificial DRAs show a low shear stability, where it is a serious drawback in industries as most of the fluid flows are under turbulence mode. Researchers thereby started to investigate natural polymers as potential DRAs in an attempt to replace the existing synthetic polymers.

Most studies have proved that DR is effective in the turbulent regime, but in 1976, Driels and Ayyash (1976), observed a significant DR through the addition of

polymers to laminar flows. Since then, DR also established its path into many critical and health effective applications as blood flow enhancement. Recently, there is an incredible enthusiasm on the use of microfluidics technology as an economical and reliable method for the testing of different theoretical phenomena related to engineering (Fiorini & Chiu, 2005) and medical (Boussommier-Calleja, Li, Chen, Wong, & Kamm, 2016; Kozminsky, Wang, & Nagrath, 2016; Tay, Pavesi, Yazdi, Lim, & Warkiani, 2016) fields. The microfluidic technologies manipulate the small volume of fluids in a microchannel, and thus, can be precise in flow control and was useful in experimental works such as DR (Abdulbari & Ming, 2015; (Abdulbari & Ming, 2015; Ming, Abdulbari, Latip, & Heidarini, 2016). Microfluidics technologies carried lots of advantages including high-throughput experiments due to the low consumption of expensive reagents and lower cost associated with easily-available microfluidic materials.

As for passive micromixers, the devices usually are modified to achieve chaotic advection thus no require any of external energy. These modifications include split and recombine (SAR) and addition of obstacles such as ribs and grooves on the channel interior (Victorov et.al., 2015, Chia-Yen Lee et.al., 2011, Stroock A.D et.al., 2002 and Nguyen et.al., 2004).

Micromixer which is developed by the principle of SAR, have better mixing efficiency. However, high pressure drop as the drawback was observed when utilizing this type of micromixer. The high pressure drop is due to the complex design of the SAR-based micromixer (Schonfel et.al., 2004). To design a passive micromixer with high mixing efficiency, pressure drop across the micromixer needed to be considered. Having a high pressure drop process needs external force or energy to be applied to the process. Without doing so, mixing might take a longer time due to the complexity of the design which acts as an obstacle to the flow of the fluid. Having extra energy or force to the process also means the process is costly.

As mentioned before, micromixer has great number of application in many industries and have recently gain tremendously interest among researchers. However, decades ago there are less understanding regarding the physical mechanism in terms of flow and mixing within the micro scale dimension. To fulfill such situation, many researchers have performed measurements and quantification using micro-Particle

Image Velocimetry ( $\mu$ -PIV). One of them include Goncalo et.al (2008) used  $\mu$ -PIV to characterize the flow kinematics inside a Dantec Dynamics microchannel that possesses rather rough walls and a very irregular cross-section shape instead of using measured bulk flow properties.

## 1.2 Statement of Problems

Since the nineties of the past century, microfluidic systems, such as lab-on-a-chip and micro-total analysis systems have gained the attention of a vast number of researchers due to their enormous academic and industrial impacts (Zhang, Xing, and Li, 2007). Compared with large mixing devices, micromixers offer advantages regarding lower sample consumption, a cheaper manufacturing cost, and higher throughput. Micromixers are considered as the heart of many common applications such as; sample preparation and analysis, DNA hybridization, biosensors and biological and chemical synthesis (Hessel, Löwe, & Schönfeld, 2005). In micromixers, the flow is always considered laminar due to the small characteristic dimensions of the channel and low fluid velocities and that means low flow intensity (low turbulence) (Sampaio, Lopes, & Semiao, 2015). The only mixing mode (mass transfer mode) in the micromixers is through diffusion across the interface separating the two fluids (two phases), and that was the primary motivation for the massive research efforts spotted in the literature regarding flow and mixing behavior at the microscale (Aoki, Umei, & Yoshida, 2011; Calado, dosSantos, & Semiao, 2016; Poole, Alfateh, Gauntlett, 2013). The laminar flow mode and the characteristics of the flow media (fluids physical properties) in micromixers will directly affect the device design where longer channels are needed to achieve good mixing efficiency. All these factors will influence the microchip cost and performance. In the present work, active flow enhancement (drag reduction) technique will be implemented and applied by utilizing the addition of polymeric additives in minute quantities to the main flow system in micromixer. The main experimental rig will consist of, micromixers (designed and fabricated for the purpose of this work) with different designs and shapes, micro flow meters, a microscope with high-speed camera, a micro-PIV system for flow characterization, pumps and pressure sensors. The present work aim is to investigate the effect of these additives on the mixing efficiency and their relation to the micromixers design and the liquids flow and rheological properties. It is expected that the experimental results will

introduce a new vision in designing the micromixers and how very low concentrations of polymeric additives (in ppm) can affect and optimize these designs in a way that can result in more compact micromixers with high mixing efficiency.

The present work aims to introduce and investigate the performance of the natural polymers (Xanthan gum) to enhance the laminar flow in a customized microchannel. Seven Y-shaped micromixers with different geometries were designed and fabricated using adapted soft lithography approach. A micro-particle image velocimetry ( $\mu$ -PIV) experiment was designed and used to obtain the velocity and mixing profile after the introduction of the additives into the liquid flow in the microfluidic system. In this study also, the mixing intensity within passive micromixers with microriblets were investigated.

### **1.3 Objectives**

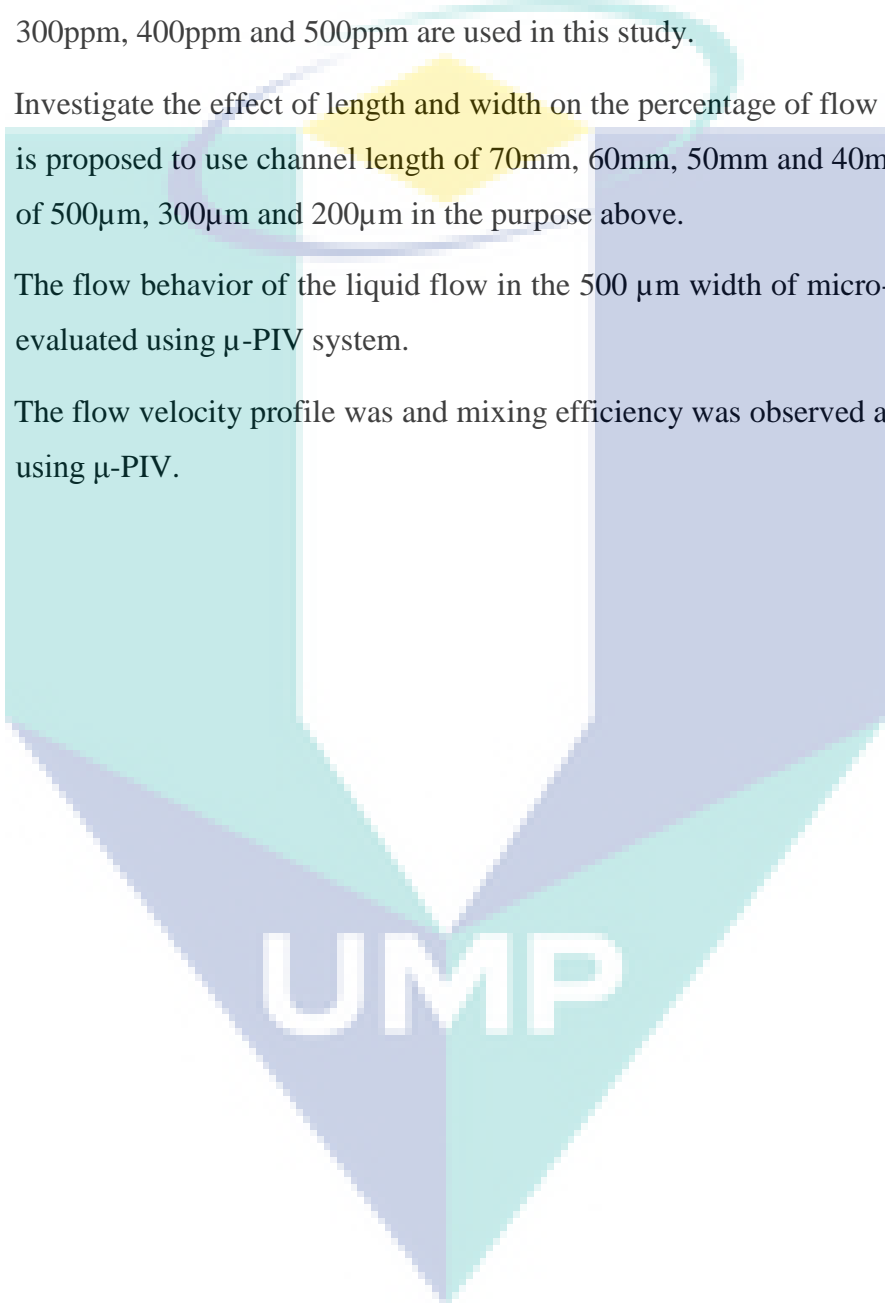
The objectives of the research project are:

1. To design and fabricate micromixers that having different geometries using adapted soft lithography approach.
2. To investigate the flow enhancement performance with the addition of Xanthan gum as natural polymer in the micromixers system under different conditions by varying parameters such as concentration, operating pressure and geometry of the micromixers.
3. To investigate the mixing behavior of liquids in micromixers after adding organic polymers using  $\mu$ -PIV system.
4. To investigate the mixing performance in passive micromixers using  $\mu$ -PIV techniques.

### **1.4 Research Scopes**

1. Design and fabricate seven models of Y-shaped micromixers with different dimensions using adapted soft lithography approach.

2. Design and fabricate seven models of passive micromixer varying the base and height of the riblets (0.00mm, 0.01mm, 0.02mm, 0.04mm, 0.06mm, 0.08mm, and 0.10mm).
3. Elucidate the effect of concentration on DR performance in reducing the drag in fluid flow. The concentration of 20ppm, 50ppm, 100ppm, 150ppm, 200ppm, 300ppm, 400ppm and 500ppm are used in this study.
4. Investigate the effect of length and width on the percentage of flow increment. It is proposed to use channel length of 70mm, 60mm, 50mm and 40mm and width of 500 $\mu$ m, 300 $\mu$ m and 200 $\mu$ m in the purpose above.
5. The flow behavior of the liquid flow in the 500  $\mu$ m width of micro-channel was evaluated using  $\mu$ -PIV system.
6. The flow velocity profile was and mixing efficiency was observed and evaluated using  $\mu$ -PIV.

The logo for UIMP (Universiti Malaysia Perlis) is a large, downward-pointing arrow shape. It is composed of four triangular sections meeting at a central point. The top-left and bottom-right sections are light blue, while the top-right and bottom-left sections are a darker, muted blue. The letters 'UIMP' are printed in white, bold, sans-serif font across the center of the arrow.

UIMP

## CHAPTER 2

### LITERATURE REVIEW

#### 2.1 Micromixer

Micromixer has established its path in various applications in both academic and industries including analytical, chemistry and biological field such as biotechnology and biomedical. Mixing in these miniature devices bring numerous advantages such as low cost at mass production, reduce amount of biological or chemical reagent and et the usage of sample or reagent and low amount of waste produced. (Bayraktar et.al, 2006). However, due to the micro scale of microfluidic devices, the flow in micromixer is mainly laminar flow (low Re). Thus, the diffusion of molecules become dominant in the mixing process. This phenomenon resulting in prolong the mixing time and required a longer channel to achieve the desire mixing profile.

Researchers started to manipulate the micromixer design such as adding obstacles to create the chaotic flow in the system thus increase the mixing efficiency (Abraham et. al., 2002). Several authors also introducing transverse component of flow which will subsequently reduce the mixing length as it 'stretch and fold' the fluid along the channel to enhance the mixing efficiency (Robin et. al., 2000).

Generally micromixers can be categorized into two major groups, namely active and passive micromixers. Active micromixers require external forces such as pressure, temperature, electrohydrodynamics, megnetohydrodynamic and acoustics. Active micromixers also have sub categories which are based on the type of disturbances required for the mixing process. On the other hand, no external energy required for passive micromixers indicates that the mixing process depends on diffusion or chaotic advection. Parallel lamination, serial lamination, injection, chaotic advection and droplets are the sub categories of passive micromixers.

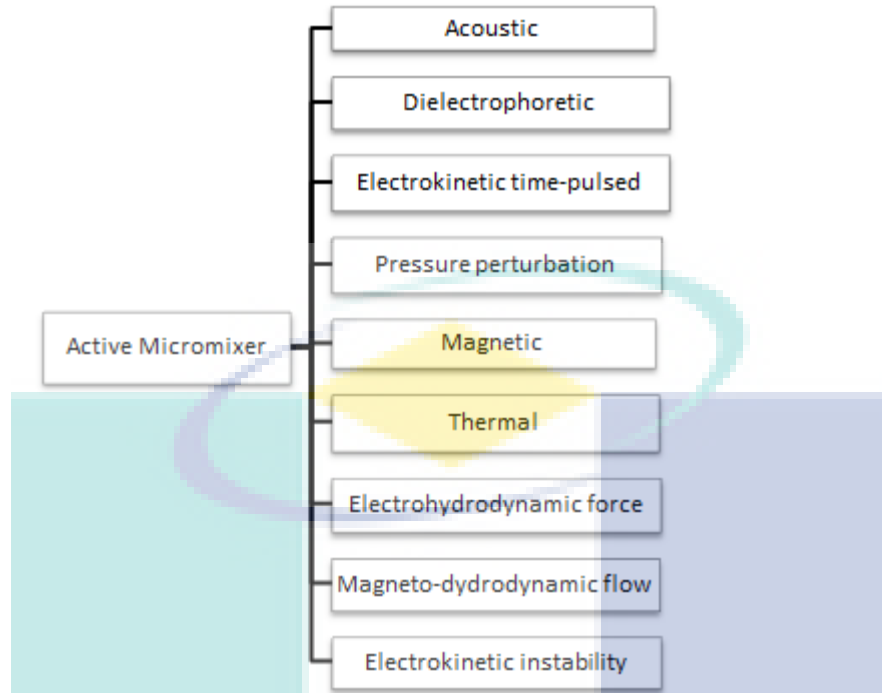


Figure 2-1 Classification of active micromixers by Chi-Yen (2011) and Nguyen et. al (2004)

The structure of active micromixers is often complicated and the fabrication process is usually complex. The operation of micromixers also required external sources thus, making the whole system both difficult and costly. Besides fluid delivery system, there are no other external forces or energy acting on the passive mixers to enhance the mixing process, thus making the microchannel system simple, less expensive due to its simple design and structurally stable. Based on that description, passive micromixer is chosen for this research.

### 2.1.1 Active Micromixer

Active micromixers use an external field that generates disturbances for the mixing process. Such disturbances will induce effects on pressure, temperature, electrohydrodynamics, dielectrophoretics, electrokinetics, magnetohydrodynamics and acoustics (Nguyen and Zhigang, 2004).

Acoustic disturbance use embedded ultrasonic transducers which is applied to generate acoustic waves. This waves will promote turbulence flow and thus allow the fluid inside the micromixer to mix. Chi-Yen (2011) investigate the mixing performance where the mixing inside embeded ultrasonic transducer micromixers achived a high

performance. However, the downside of this system, besides generating acoustic waves, it also generates heat energy which may result in an unwanted reaction within the fluids or samples.

Polarized particles were induced by non-uniform alternating electrical fields. This happens when dielectrophoretic (DEP) is applied (Yaralioglu, 2004). When dipole moments were generated between particles, net force was generated and drove the particles to be in motion. When this electrical field is applied precisely within a space, time and velocity profile, saddle point regions are generated. This saddle point is a region where particles are stretched and folded about a virtual quasi-static point. Such behaviour enhances the mixing effect (Chi-Yen, 2011).

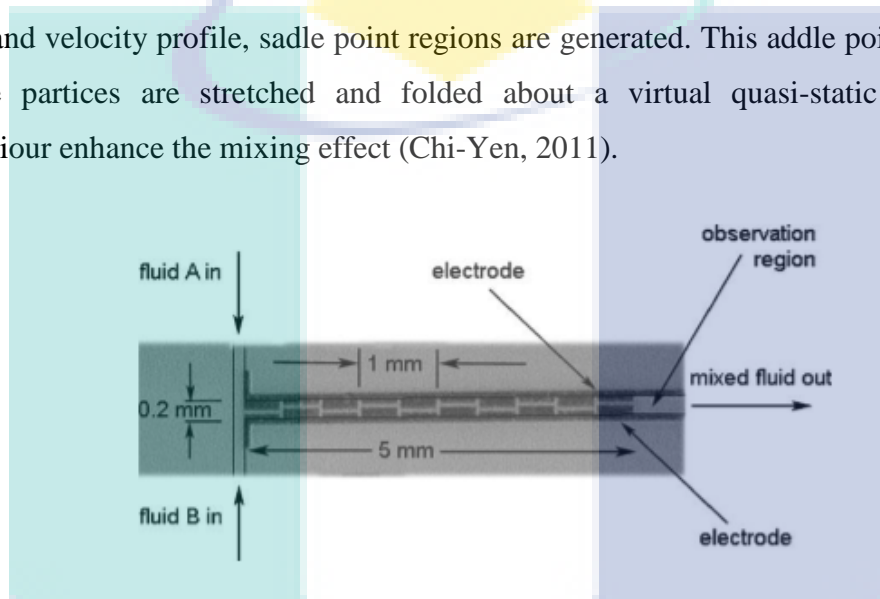


Figure 2-2 Microphotograph of the DEP micromixer

Source: Campisi *et al.*, 2009

By applying an electrokinetic driving force, the fluid within the micromixers will be transported and at the same time, periodic perturbations will be induced (Chi-Yen, 2011). There are a few factors which can enhance its performance such as larger contact area, time and chaotic flow behaviour of the fluid (Chen *et al.*, 2008)

Perturbations are generated by velocity pulse (Niu *et al.*, 2003). Within this system, it usually comprises of a main channel and a few side channels. Due to the velocity pulsing from the side channel, the fluid inside the main channel will be experiencing chaotic movement or flow and thus enhance the mixing within the microchannel.

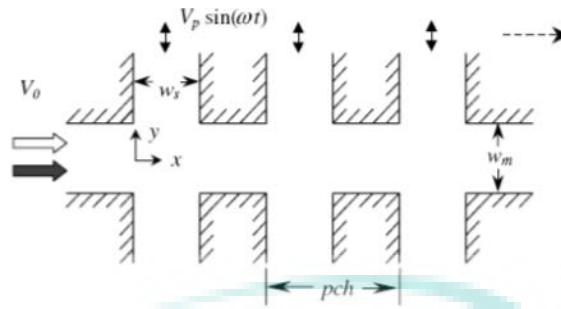


Figure 2-3 Schematic diagram of channel with multiple side channels

Source: Niu *et al.*, 2003

El Moctar *et. al* proposed a micromixer design with two fluids of same physical properties (viscosity and density) but differ in electrical properties and they were injected by syringe pump. To create a transversal secondary flow, the electrodes embedded were arranged at 90° angle (perpendicular) to the interface between the fluid. The results obtained showed a satisfactory mixing properties when certain appropriate voltage and frequency were applied.

Many researchers used MHD flow effect to enhance mixing in microfluidic system. Such researchers include Wang *et. al* (2008) introduced a micromixer where the fluid containing magnetic articles was allowed to flow in the system. Micromixer with magnetic particles within the fluid inside the micromixer was introduced. Mixing inside the micromixer occurred when the magnetic particle actuation was being manipulated. High mixing efficiency was observed at the higher operating frequency for high magnitude of magnetic force in smaller diameter microchannel. MHD flow also can be induced by Lorentz force. This force is generated by either DC or AC electrical and magnetic fields as developed by Bau *et. al*. Such MHD flow will promote a chaotic flow within the fluid and thus enhance the mixing.

Huang *et. al.* (2006) examine the effect of electrokinetic instability on the mixing efficiency profile. Unfortunately such design require high voltage and therefore not suitable for process which may not come into contact with high voltage process.

As explained above, active micromixer requires external actuators or forces and therefore, there are complexity in its design as it need to include integrated components. Besides, the external power sources also needed to be consider for active micromixer and leads to higher research cost. In this research, the focus is drawn to passive

micromixer as its design is not complicated thus does not require complex fabrication methods and is also inexpensive.

### 2.1.2 Passive Micromixer

Passive micromixers gain a lot of attention in various industries and also in researches. As discussed in Section 2.1.1, passive micromixers are easy to be fabricated due to their simple design as well as less expensive as compared to active micromixers. Numerous researches have done to improve the mixing efficiency of micromixers by allowing the chaotic flow of the fluid (Nimafar et al., 2012).

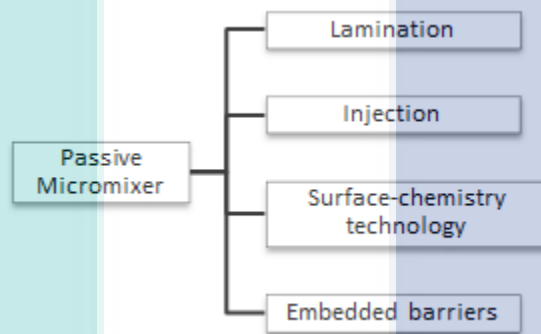


Figure 2-4 Classification of passive micromixer

Source: Nguyen et al. (2004)

To induce such behaviour, the smooth surfaces of the mixer need to be altered. (Nguyen et al., 2004). Most of the researches used the idea of splitting, stretching, folding and breaking the flow to enhance mixing process. Such condition will promote the chaotic flow of the fluid (turbulent) and thus improve the mixing process. Obstacles or barriers are also embedded in the mixer to provide such flow. From numerical investigation conducted by Wong et al. (2003) the mixing process is improved by the introduction of static mixing elements (SMEs) to the system.

#### 2.1.2.1 Lamination

To enhance mixing in microfluidic system, mixing path needs to be reduced and the contact surface within the fluids needs to be increased. Lamination has sub-categories which are parallel and serial lamination. As for parallel lamination, the inlet is split

into certain number of channel called substreams and then are joint to form one stream called laminae. The basic design which use these concepts are T-mixer and Y-mixer (Kamholz et.al., 1999).

As T-mixer depends solely on molecular diffusion, increasing the Reynolds number of the fluid flow may result in shorter mixing length, thus making the design shorter in length (Yi M, 2003). Having high Reynolds number will promote chaotic advection behaviour of the fluid and this will induce vortices within the fluid. The more vortices, the better the mixing effect. The mixing can be further enhance by modifying the T-mixer by embedded the obstacles which also generate vortices and promote chaotic advection.

Serial lamination micromixers on the other hand also use the same concept as parallel lamination that is split and rejoin the channels in order to enhance the mixing process (Nguyen et.al.,2004). Serial lamination differ from parallel lamination where the inlet channels are first horizontally joined, then vertically. After several times splitting and joining stages, liquid layers can be laminated.

#### **2.1.2.2 Injection Molding**

This type of micromixer almost similar to that of parallel lamination type. The injection concept is applied when the splitted solute flow were injected into solvent flow (Nguyen et.al.,2004). To improve the mixing effect, array of nozzles were introduced on top of the channel. These nozzles will create microplumes of solutes, thus reduce the mixing length and also increase contact surface within the flow.

#### **2.1.2.3 Surface- Chemistry Technology**

Due to the minute scale, surface force and high friction during the fluid flow usually generate a high pressure gradient. The substrate used to fabricate the micromixer also contribute to the reduction of fluid flow within the channel. Silicon dioxide which is the substrate used to fabricate the micromixer have deprotonated silanol group ( $\equiv\text{Si-O}^-$ ) on the surface which give negatively charged property to the surface of the channel. This negatively charge surface will attract positively charged fluid and thus forming a layer called diffuse layer (Chi-Yen, 2011). By applying

electrical field, the positively charged layer will move. The bulk fluid will be dragged by the moving diffuse layer creating electro-osmotic flow (EOF) (Zheng, 2000).

#### 2.1.2.4 Obstacle Barrier

One of the effective techniques for enhancing the mixing performance in micromixers is the insertion or creation of flow destruction obstacles (chaotic advection methods) that will change the flow pattern along the microchannel (Chen & Li, 2017; Hossain, Ansari, & Kim, 2009; Jeon & Shin, 2009; C.-Y. Lin, Meng, & Fu, 2011; Schönfeld, Hessel, & Hofmann, 2004). The chaotic regime in the system can disperse the fluids effectively by creating eddy-based flow patterns in regular flow fields (Jen, Wu, Lin, & Wu, 2003; Jiang, Drese, Hardt, Küpper, & Schönfeld, 2004; Y. Lin, Gerfen, Rousseau, & Yeh, 2003; Wang, Iovenitti, Harvey, & Masood, 2002) and stretches or folds fluid volumes (Lu, Chen, Liao, & Hsieh, 2009; Ottino & Wiggins, 2004). It is important to note that stretching increases the length of the interface while folding constrains the fluid to fill a finite region (Kelley & Ouellette, 2011). When the length of the fluid boundary grows exponentially with time due to the stretching-folding mechanism, the diffusion will enhance and this results in a higher mixing performance (Sarkar, Narváez, & Harting, 2012). Park et al. (Jang Min, Kyoung Duck, & Tai Hun, 2010) investigated the mixing performance of a micromixer with two hexahedron blocks as obstacles which were placed along the base of the channel. They observed that the mixing efficiency was enhanced by increasing the micromixer aspect ratio (H/W) as this structure caused more uniform stretching effects over the cross sectional of the micromixer. Wu et al. (Shih-Jeh, Hsiang-Chen, & Wen-Jui, 2014) observed a 100% complete mixing in 0.08 seconds when cylindrical obstacles were embedded within their micromixer system. Cortes-Quiroz et al. (Cortes-Quiroz, Azarbadegan, Zangeneh, & Goto, 2010) reported a high mixing index up to 0.83 through a grooved micromixer with a staggered herringbone structure, and that the mixing performance increased with the groove width. Kim et al. (D. S. Kim, Lee, Kwon, & Ahn, 2005) proposed a new integrated micromixer by combining both SAR and chaotic advection mechanisms. They reported that the advection mechanism was dominant at higher Re and this reduced the thickness of the lamellar structures, hence reduced the mixing time. The combination of both mechanisms was found to demonstrate a high level of mixing efficiency (up to 0.9) over a wide range of Re. Subsequently, other studies reported

high mixing performance of more than 90% by using different geometries such as ribs-shaped (B. S. Kim et al., 2011), diamond-shaped (Tseng, Yang, Lee, & Hsieh, 2011), trapezoidal blade (Le The et al., 2015), and Tesla structure (Hossain, Ansari, Husain, & Kim, 2010; Yang et al., 2015).

Wang et al (2006) reported a numerical investigation on many obstacles arrangements. It is found that eddies or recirculation does not occur at low Reynolds number. However, at high Reynolds number, with the presence of embedded obstacles or barriers, the results show an improvement in mixing performance.

Despite these various results on high mixing efficiency, researchers are still faced with several issues such as high pressure drop and structure complexity. Jeon and Shin (Jeon & Shin, 2009) encountered a high pressure drop (119 Pascal) in their zigzag-type micromixer due to the drastic change of the flow direction ( $90^\circ$ ) although the mixing index was highest (0.96) compared to others. In contrast, the micromixer without any obstacles encountered minimum pressure drop (60 Pascal) although with a low mixing performance of 55%. The basic micromixer, both T and Y-shaped, takes a longer mixing time and a longer channel to attain a higher mixing performance and mixing mechanism depends solely on the interface between the two parallel flowing liquids.

## **2.2 Drag Reduction**

In engineering, most of the flow encountered is in the turbulent mode. Turbulent flows are characterized by a random and irregular fluctuation in the swirling regions of the fluid called eddies, throughout the flow. These flow regimes are preferable in industries as the fluctuation of fluids provide an additional mechanism for momentum and energy transfer and thus, enhance the mass and heat transfer. Turbulent flows experience some problems such as energy losses due to high frictional forces causing a significant pressure drop across the transportation system. To overcome this, operators increase the number of pumping station along the pipelines which contributes to higher operating costs and also affect the lifespan of pipes.

For the past few decades, DR techniques have been introduced and investigated by researchers and implemented in various industries. The DR methods can be

categorized into two main groups namely: passive DR and active DR. Passive DR can be achieved by altering the surface of the pipes or conduits without the introduction of any foreign substance or additives in the flow system. By applying manipulators with particular dimensions into the wall or surface, the turbulent structures will be shifted away from the wall and hence, reducing the drag force. There are two types of manipulators: the external layer manipulators and the internal layer manipulators. Thin plates are introduced at the outer part of the flow as external manipulators, and this method is proven to be ineffective in the reduction of the total drag in the turbulent boundary layers.

As for the internal layer or thinner layer manipulators, the geometry of the wall is altered by small stream-oriented striations such as compliant walls (Gad-El-Hak, 2003), oscillating walls (Choi & Clayton, 2001; Skote, Mishra, & Wu, 2015), dimples (Kim, Moon, & Kim, 2011; van Nesselrooij, Veldhuis, van Oudheusden, & Schrijer, 2016), and riblets (Viswanath, 2002; Walsh, 1983). Several authors have been inspired by the pioneering work of Gray (1936) and started to investigate the performance of the compliant coating in DR. Kramer (1960) observed a maximum DR of up to 60 % with the use of a compliant coating. However, other researchers were not able to achieve promising results when they tried to reproduce using the same method (Blick, 1969; Choi *et al.*, 1997; Gad-el-Hak, 1998; Puryear, 1962). This technique has been effectively used in the marine vehicles but yet to be applied for DR in pipes with turbulent flows. Dimples are widely used in heat transfer applications due to the high contact area of the structures. However, few studies have claimed that dimples do not have significant DR performance when compared to its heat transfer effect (Lienhart, Breuer, & Köksoy, 2008; Rohlf, Haustein, Garbrecht, & Kneer, 2012) which contradicted some other studies (Hofmann, Stern, & Myska, 1994; Kroppe & Lipus, 2010).

Among the passive DR techniques, the riblets gained most attention from researchers. Riblets are the longitudinal microgrooves that were designed and etched into wall surfaces to reduce the drag of fluid flow and increase the surface area for enhanced momentum and heat transfer. Various riblets designs were introduced and among them, the most common designs are the V-shaped, U-shaped and L-grooves. The protrusion height and lateral spacing is the key to determining the effectiveness of

riblets on DR performance; sharp pointy tips that protrude at an optimal height perform better (Walsh & Lindemann, 1984). Although there is a broad investigation on riblets, there is no promising significant effect on DR, most observed DR is less than 10 % (Chamorro, Arndt, & Sotiropoulos, 2013; El-Samni, Chun, & Yoon, 2007; Martin & Bhushan, 2016; Neumann & Dinkelacker, 1991; Park & Wallace, 1994; Walsh, 1982) or with adverse effect (Boomsma & Sotiropoulos, 2015).

The introduction of the passive means of DR is a more environmentally friendly approach towards the enhancement of fluid flows in the long pipeline system. This technology is a permanent way of reducing drag which involves the restructuring of the inner surface of the pipes and conduits. However, passive DR has some disadvantages such as high cost of altering the inner surface of the ducts, and the performance so far recorded is still unsatisfactory. Thus, active DR is widely used in the industries as they can achieve about 4 - 8 times more DR performance than the passive DR. The addition of foreign substances such as polymers, surfactants, microbubbles, powders or particles, and fibers as DRA can significantly reduce drag even when used in minute quantities. The following sections will focus on the review of DR achieved by the addition of DR additives.

## **2.3 Active Drag Reduction Technique**

Active DR is achieved by the addition of foreign substances into the core of the turbulent flow in pipes and conduits to reduce the turbulent friction. These DRAs can be categorized into two main groups namely: insoluble and soluble additives. Fiber is the most common insoluble DRA while surfactants and polymers are greatly used as soluble DRA by researchers and in the industries. This section provides an overview of both insoluble and soluble additives in the enhancement of turbulent flows in pipeline systems.

### **2.3.1 Insoluble Additives (Suspended solids)**

It is believed that insoluble additives are chemically and mechanically stable thus suitable to be used in various applications such as improve performance of the ion-exchange membrane (MacKinnon *et al.*, 2007), drilling industry (Alsabagh, Abdou, Ahmed, Khalil, & Aboulrous, 2015), and flow enhancer. In 1931, Forrest and Grierson

(Forrest & Grierson, 1931) observed that reduction of energy loss after the addition of the wood pulp fiber suspension to the turbulence water flow. Since then, different type of suspended solids such as pulpwood, sand, fibers, fine grains and silts are investigated and well known for their feasibility as DRA. There are some suspended solids obtained from the industrial production process such as slag, a main by-product from tin production showed massive impact in DR technique. Kamarulizam, Bari, and Arumugam (2011) reported that a maximum of 60% DR can be achieved by introducing nanomolar of slag to the liquid circulation system. Author also reported that variables such as fluid velocity, pipe diameter and the concentration of the additives influenced the efficacy of the DR where these results showed agreement with other literature (Abdulbari, Nour, Kor, & Abdalla, 2011; Abdulbari, Wang Ming, & Mahmood, 2017).

A higher fluid velocity resulting in greater degree of turbulence which creating a better platform for the suspended solid to perform as DRA thus increases the efficacy of DR. This phenomenon can be also observed in smaller pipe diameter where higher velocity of the fluid can be achieved thus increases the occurrences of eddies in the conduits resulting in providing an environment that suitable for the insoluble additives to perform as DRA. Higher concentration of the additives in the liquid flow indicating that more particles were involved in suppressing the turbulence elements known as eddies thus increase the flow rate of the liquid.

Due to the inert properties of suspended solids that do not react with other material and do not produce any toxic substances, these particles are preferably in industries as DRA for their environment perspective. Most of these additives can be obtained from natural resources thus cause less pollution or harmful effect to the living organisms around the area. However, there is some difficulties in utilizing these insoluble additives as they carry few disadvantages including creating plugging problems in smaller pipe and difficulties in separation of the particles from the main flow of the transportation..

## 2.3.2 Soluble Additives

### 2.3.2.1 Surfactants

Numerous studies have been conducted on different types of soluble DRA, mainly surfactants (Drzazga *et al.*, 2013; Li *et al.*, 2008; Qi *et al.*, 2011; Rózański, 2011; Tuan & Mizunuma, 2013; Yu & Kawaguchi, 2006), and long-chain polymers (Abubakar *et al.*, 2014; Al-Sarkhi, 2012; Benzi, 2010; Iaccarino *et al.*, 2010; Resende *et al.*, 2011) for wide industrial application (Al-Sarkhi & Hanratty, 2001; Mavros *et al.*, 2011; Thais *et al.*, 2013; Walsh *et al.*, 2009; Yang & Ding, 2013). This is due to their low cost and high availability in addition to their effectiveness even when used in minute amounts.

Since the publication from Dodge and Metzner in 1959, surface-active molecules, also known as surfactants have received impressive enthusiasm for utilization as effective flow enhancers (Savins, 1967). These compounds produce worm-like micelles (Suksamranchit & Sirivat, 2007) with their hydrophilic heads exposed to water while the hydrophobic tails shield the interior end of the micelles from the water. The surfactants have unique self-assembly properties with the capability of repairing damaged structures in a matter of seconds after the disappearance of the high shear. This property permits the use of surfactants in many industries especially in recirculation system such as district heating and cooling systems. The self-assembly of surfactants is mediated by the hydrophobic effect, van der Waals, hydrogen bonding, or electrostatic interactions (for charged surfactants) that exists between the molecules and the aim is to restore the DR performance (Malcher & Gzyl-Malcher, 2012; Mulligan, 2005). The strong vorticity fluctuation or formation of eddies near the wall disappears with the introduction of surfactants (Kawaguchi, Segawa, Feng, & Li, 2002; Li *et al.*, 2008; Yu, Li, & Kawaguchi, 2004).

There are other variables that affect the performance of surfactants in DR, some of which include the property of the surfactants and fluid conditions. The non-ionic and cationic surfactants exhibit higher DR efficacy compared to the anionic surfactants (Ushida *et al.*, 2011; Ushida, Hasegawa, & Narumi, 2010). The repulsion against the wall generates displacements that result in the accumulation of anions and cause the anionic surfactants to have little impact in DR. A surfactant will lose its ability as DRA

when the temperature and velocity of the fluid is out of the effective range (Prajapati, 2009; Xia, Liu, Qi, & Xu, 2008). Huang *et al.* (2016) reported that the DR performance of surfactants increase in the presence of microgrooves because these structures increase the drag in the liquid flow, and thus, enhance the flow enhancement performance of the surfactant. Researchers have proposed that surfactant has a massive impact on heat transfer and DR applications. The addition of a small amount of organic acid to a surfactant solution can improve the drag reducing abilities and reduce the degradation rate caused by the continuous circulation of the surfactant (Tamano, Ikarashi, Morinishi, & Taga, 2015).

The relationship between the pipe diameter and the DR performance of surfactants has also attracted research attention. Eskin (2017) revealed that DR efficacy was inversely proportional to the pipe diameter and also affected by the type and concentration of additive. The results agreed with the earlier report of Matras and Kopiczak (2015). However, it has been observed that DR performance can increase with an increase in the diameter of a pipe with minimal surface roughness (Dosunmu & Shah, 2014). Authors have also shown that the addition of salt into a surfactant solution can enhance the DR efficiency due to the presence of longer micelles.

The addition of surfactant to polymer solutions has also been considered, utilizing the advantages of both additives for drag reduction. Reis, Oliveira, Pires, and Lucas (2016) proved that the efficiency of polymer-surfactant complexes was higher when compared with the pure polymers itself; the performance of polymers as DR agents depend on their molecular weight, intrinsic viscosity, molecular size, and molecular distribution. From the results, the complexes showed higher resistance to shear rate than the components alone. Their results agreed with the report of (Matras & Kopiczak, 2015), proving that the addition of surfactants to polymers can result in a significant extension of the DR zones. Also, the complexes combine and intensify the positive features of the pure polymers and surfactants, leading to effectiveness in a wider range of flow. Despite the effectiveness of the surfactants, they cause some adverse environmental problems due to the involvement of tetra-ammonium in the molecules, and the slow rate of anaerobic degradation (Li *et al.*, 2012). Some surfactants also possess some uncertain properties like surfactant toxicity, long-term stability, and post-separation techniques.

### 2.3.2.2 Synthetic Polymeric Additives

Polymeric DRA is the most widely studied and have been used in industries for decades to reduce frictional drag in turbulent flows. The property of the polymers such as long linear chain polymer with no side branched, and a higher degree of polymerization of low molecular weight monomers (Virk, 1975) are crucial in their DR performance. The configuration of the polymer molecules also influenced their DR performance as it can change due to the rotation of the chemical bonds or thermodynamic motion of the molecules (de Bessa & Ortiz, 2006). The most common investigated polymers are polyethylene oxide (PEO), polyacrylamide (PAM), polymethyl methacrylate (PMMA), and polyisobutylene (PiB). These additives have been greatly investigated in DR fundamental studies due to their low cost and high availability. Studies have concluded that a minute amount of polymers that satisfies the earlier mentioned attributes can achieve a DR of up to 75 % (Sun, Wu, Wei, Bai, & Ma 2014). However, there is limited information on the mechanism of DR using polymers in spite numerous published assertions that very small amount of high molecular weight polymer can enhance fluid flow in pipeline systems.

Researchers are also having concerns regarding other variables that might be affecting the DR performance of the investigated polymers. Some of these factors include the concentration of the additives (Karami & Mowla, 2012), molecular weight (Virk, 1975), and chemical nature of polymers (Kulicke, Kötter, & Gräger, 1989). A higher concentration of additives in the core of the turbulent flow has a strong effect on the DR performance. However, experimental works have demonstrated that upon a critical point (so-called critical concentration), a continuous increase in the concentration of the additives cannot increase the DR efficacy of the additive (Nesyn, Konovalov, Vetrova, & Menshov, 2015; Oliver & Bakhtiyarov, 1983). Since 1960, several authors have reported the influence of the molecular weight of polymers on the DR efficacy (Martin & Shapella, 2003; Shanshool & Al-Qamaje, 2008). It was also reported that higher molecular weight polymers gave higher DR performance (Gampert & Wagner, 1985; Kim, Kim, Lim, Chen, & Chun, 2009; Virk, 1975). Hunston and Reischman (1975) proposed that polymers with a high molecular weight can interact with bigger vortices thus, increasing the efficiency of DR. Long linear polymers have also been reported to be highly efficient in DR with greater resistance towards high

shear stress (Singh, Jain, & Lan, 1991). A maximum percentage DR of up to 80 % was reported by Sifferman and Greenkorn (1981) through the utilization of polymers with greater flexibility, polyethylene in this case.

Zhang, Lim, and Choi (2016) investigated the relationship of the molecular weight, concentration and rotational speed on the performance of poly(acrylamide-co-acrylic acid) [poly(AM-co-AA)] using the rotating disk apparatus instead of a pipe flow. From the results, the high molecular weight polymer showed an excellent flow enhancement performance. An increase in the concentration of the polymer solution increased the shear viscosity of the solution, resulting in an increase in the DR; yet, beyond the critical point, there was a significant increase in the shear viscosity, leading to a lower DR performance. The DR efficacy reduced at a high rotational speed due to the degradation of the polymers with the increasing of the violent turbulent flow. It was also observed that higher molecular weight polymers have high resistance towards degradation when compared with the lower molecular weight polymers at the same rotational speed.

The performance of an anionic soluble binary polymer mixture in the enhancement of flow has been examined and compared with the performance of the individual polymers (Eshrati *et al.*, 2017). The binary polymer mixture and the individual polymers showed a high DR efficiency at a high Re. From the results, the binary polymer mixture achieved greater flow enhancement when compared with the lower molecular weight polymers. Also, a mixture of high and low molecular weight polymers was observed to have better DR efficacy than the mixture of high and medium molecular weight polymers. Eshrati and coworkers (2015) investigated the effect of oil fractions in DR performance and reported that an increase of the oil fraction in the continuous phase of the test section resulted to the negative DR. The authors concluded that the DR performance was enhanced by using more flexible polymer chains with high molecular weight and lower charge density.

The DR performance of a polymer after the addition of salt solution into the polymer system has been reported (Le Brun, Zadrazil, Norman, Bismarck, & Markides, 2016). The authors observed that the sodium 2-acrylamido-2-methylpropane sulphonic acid (NaAMPS) groups in the polymer (PAM) enhanced the efficiency of the polymer in reducing the drag while maintaining resistance to degradation due to high shear

stress. However, increasing the concentration of salt in the polymer solution led to an increase in the dynamic viscosity of the solution which lowered the efficiency of the polymer in reducing the frictional drag (Le Brun *et al.*, 2016). It was also reported that the DR performance was intensified by increasing the concentration of the salt and the  $Re$ .

Additionally, DR performance is also dependent on the condition of the pipes and ducts. Karami, Mowla (2012) and Vlachogiannis, Hanratty (2004) have revealed that DR efficiency increases with increase in the relative roughness of the pipe although this finding contradicts other reports. Experiments have been conducted using pipes with full rough surfaces (Petrie, Deutsch, Brungart, & Fontaine, 2003). The authors reported that more than 60 % of DR efficacy was observed when using PEO and high additive concentration in a relatively rough pipe system. Ceccio, Dowling, Perlin, and Solomon (2007) claimed that the roughness on the surface of the ducts can induce the mixing of the polymer solution, thereby increasing the polymer degradation rate and resulting in a lower percentage DR.

The size and geometry of channels also affect the DR performance directly. Interthal and Wilsk (1985) reported no linear relationship between the inner diameters (ID) and DR efficacy. From the observations, the percentage DR (%DR) increased from 66 % at 3 mm ID to 80 % at 14 mm ID, but then, decreased to 76 % at 30 mm ID. Karami and Mowla (2012) argued that DR can decrease with an increase in the pipe diameter. Hence, there is no consistency in the variation of DR with pipe diameter. In the industries, coiled tubes are also being used instead of straight pipes. Researchers have reported that DR can decrease with an increase in the curvature ratio (Shah & Zhou, 2003; Zhou, Shah, & Gujar, 2006). Khadom and Hadi reported that the presence of elbows can reduce DR performance when compared with the results obtained in straight pipes (Khadom & Abdul-Hadi, 2014). From the results, the authors demonstrated that the DR efficiency of polymers can increase with an increase in the polymer concentration and  $Re$  in larger pipe diameters.

As discussed earlier, polymers are effective as flow enhancers in the reduction of frictional drag. The polymeric DRAs possess high DR performance with excellent thermal stability, yet most of the investigated polymers are artificial polymers, thus, there are some arguments on the utilization of these polymers in transportation

pipelines. Most of the synthetic polymers are derived from petroleum which is accompanied by non-biodegradable properties, resulting in environmental concern. Synthetic polymeric DRAs are also said to be more expensive than the natural polymer of similar molecular weights. Thus, natural polymeric DRAs started to gain research interest in an attempt to replace the synthetic polymers. Some of the interesting findings using natural polymers on DR will be reviewed in next section.

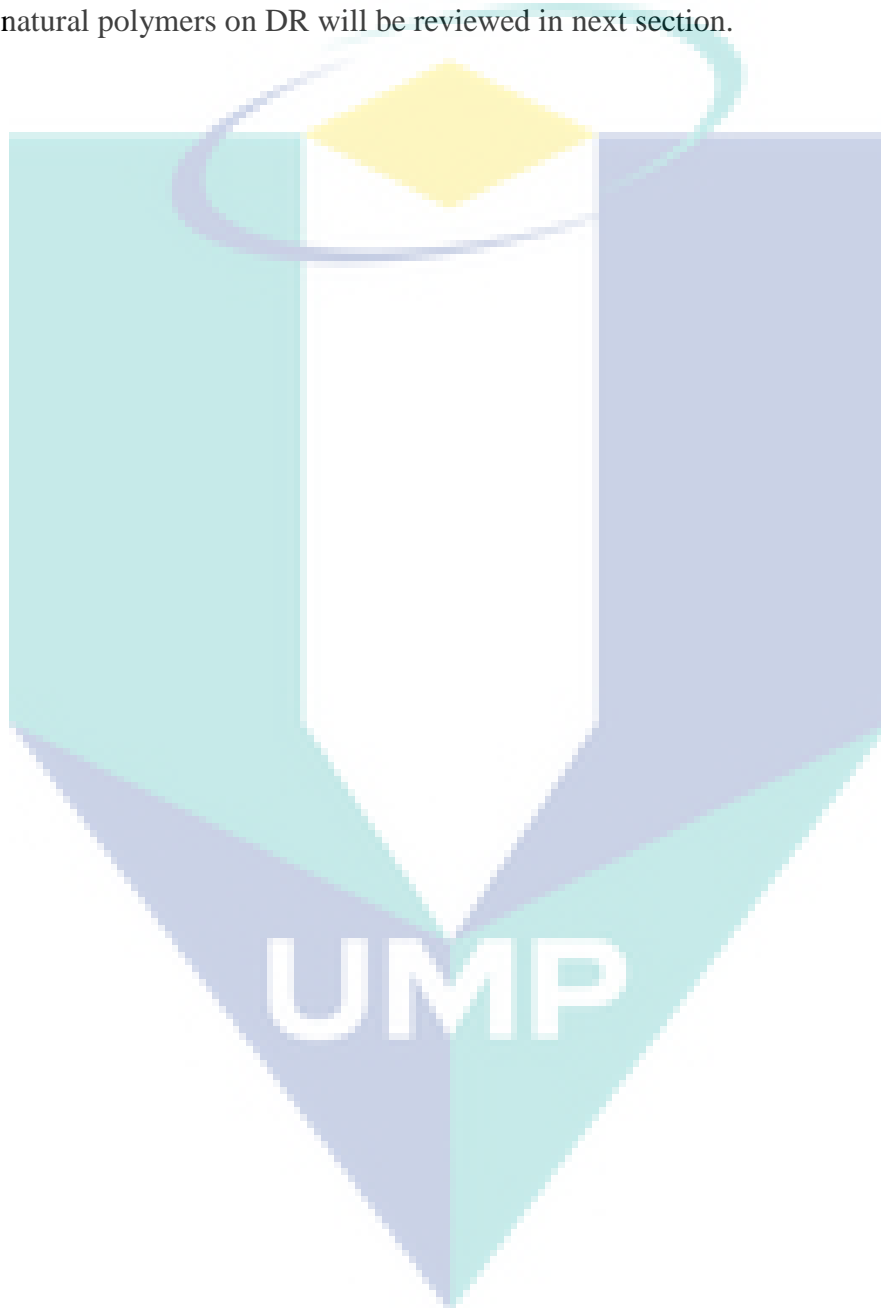


Table 2-1 Summary of synthetic polymeric as drag reducing additives in enhancing fluid flow in pipeline system

Authors	Synthetic Polymers	Concentration (ppm)	Max %DR	Ref.
Karami and Mowla (2012)	Mixture of Polyolefin synthetic rubber, Polyethylene wax, Polyacrylic acid, Aluminium particle, and Propylene glycol	200	44.06	(Karami & Mowla, 2012)
Oliver and Bakhtiyarov (1983)	Separan MG200	0.40	40.6	(Oliver & Bakhtiyarov, 1983)
Nesyn <i>et al.</i> (2015)	Poly-1-octene	2.5	60	(Nesyn <i>et al.</i> , 2015)
Martin and Shapella (2003)	Polyisobutylene (PiB)	1000	70	(J. R. Martin & Shapella, 2003)
Shanshool and Al-Qamaje (2008)	PiB	50	18.7	(Shanshool & Al-Qamaje, 2008)
Kim <i>et al.</i> (2009)	PEO	20	50	(Kim <i>et al.</i> , 2009)
Huntson and Reischman (1975)	Polystyrene	100	55	(Huntson & Reischman, 1975)
Sifferman, and Greenkorn (1981)	POLYOX	3000	80	(Sifferman & Greenkorn, 1981)
Zhang <i>et al.</i> (2016)	Poly(AM-co-AA)	50	≈ 45	(Zhang <i>et al.</i> , 2016)
Eshrati <i>et al.</i> (2017)	AN125SH and 75%AN125SH + 25%AN125VLM	30	44.2	(Eshrati <i>et al.</i> , 2017)
Eshrati <i>et al.</i> (2015)	AN125SH	20	55	(Eshrati <i>et al.</i> , 2015)
Le Brun <i>et al.</i> (2016)	NaAMPS-PAM-10	100	75	(Le Brun <i>et al.</i> , 2016)
Ceccio <i>et al.</i> (2007)	PEO	4000	70	(Ceccio <i>et al.</i> , 2007)
Interthal, W. and H. Wilsk (1985)	Polyacrylamide (PAM)	30	80	(Interthal & Wilski, 1985)
Khadom and Hadi (2014)	PAM	50	40.64	(Khadom & Abdul-Hadi, 2014)

### 2.3.2.3 Natural Polymeric Additives

Most of the natural polymeric DRAs can be extracted easily from resources such as microorganisms and plants in nature. These organic substances, when used in minute quantities, can reduce drag by up to 70 %. Xanthan gum (XG), produced from the fermentation of *Xanthomonas campestris* is one of the most investigated natural polymeric DRA. From the literature, XG has shown excellent DR performance (Bewersdorff & Singh, 1988; Hong, Choi, Zhang, Renou, & Grisel, 2015; Kim, Choi, Kim, & Jhon, 1998; Tian *et al.*, 2015) and even suitable for use under high temperatures (Sohn, Kim, Choi, & Jhon, 2001).

Recently, researchers have emphasized on the investigation of biopolymers extracted from local plant sources as they do not harm the environment by contaminating the soil. Kaur, Singh, and bt. Jaafar (2013) synthesized carboxymethylcellulose (CMC) from banana peels and tested its potential as a DRA. From the study, the authors reported that the temperature of reaction when synthesizing the biopolymer affected the DR performance of the CMC. They studied a range of temperature and concluded that a temperature at 55 °C had a higher percentage yield of CMC and thus, gave the highest DR. Prolonged heating at a high temperature will permanently degrade or depolymerize the cellulose chains, resulting in a decrease in the percentage DR. The authors also observed that the %DR reduced over the duration of 14 days due to the degradation of the biopolymer as CMC is an organic element made up of cellulose.

Abdulbari and co-workers (Abdulbari *et al.*, 2010; Abdulbari *et al.*, 2012; Kamarulizam & Man, 2011; Kamarulizam, 2012) were among the earliest researchers who reported the use of Okra mucilage as a drag reducer and these were a milestone in the field of DR. From the observations, a maximum % DR of up to 70 % was achieved by using Okra mucilage. The %DR increased with an increase in the mucilage concentration. Abdul also pointed out that a higher %DR was observed in the bigger ID pipes. The %DR reduced with an increase in the Re. They also reported up to 63 % of DR efficacy when using only 400 ppm of Aloe vera mucilage. From the work of Coelho, Barbosa, Soares, Siqueira, and Freitas (2016), a high DR efficacy of 74 % was also observed when using 1600 ppm of Okra solution. Japper-Jaafar, Escudier, and Poole (2009) concluded in their study that flexible polymers provide greater %DR than

the rigid rod-like polymers. In the industries, coiled tubes are also being used instead of only the straight pipes. Researchers have reported that DR can decrease with an increase in the curvature ratio (Shah & Zhou, 2003; Zhou *et al.*, 2006).

Zakaria and Nabil (2012) also introduced the usage of natural polymers extracted from hibiscus leaves as effective DRA where this polymers are cheap alternative to the existing polymers due to its abundant resource all over Malaysia. The experiments was conducted using an open flow system consisting of a 12.5 m galvanized pipe connected with two pressure gauge. The polymers was injected into the water flow at the injection point for mixing purposes. Authors reported that the drag reduction was higher when utilized higher concentration of hibiscus leaves indicating that the polymers were more effective at higher concentration. Despite the good performance of polymers extracted from hibiscus mucilage, there is limited investigation on these natural polymers in DR operation. These studies also indicate the potential of biopolymers as DRA and as an excellent alternative to the synthetic polymers.

Table 2-2 Summary of natural polymeric as drag reducing additives in enhancing fluid flow in pipeline system

Authors	Natural Polymers	Concentration	Max %DR	Ref.
Abdulbari <i>et al.</i> (2011)	Aloe vera	400 ppm	63	(Abdulbari, Letchmanan, & Yunus, 2011)
Abdulbari <i>et al.</i> (2012)	Okra	1000 ppm	70	(Abdulbari <i>et al.</i> , 2012)
Abdulbari <i>et al.</i> (2010)	Okra	1000 ppm	71	(Abdulbari <i>et al.</i> , 2010)
Coelho <i>et al.</i> (2016)	Okra	1600 ppm	≈ 74	(Coelho <i>et al.</i> , 2016)
Kaur, Singh, and bt. Jaafar (2013)	CMC	100 ppm	21.61	(Kaur <i>et al.</i> , 2013)
Japper-Jaafar <i>et al.</i> (2009)	Scleroglucan	0.075w/w%	55	(Japper-Jaafar <i>et al.</i> , 2009)
Shah and Zhou (2003)	XG	10 lb/Mgal	68	(Shah & Zhou, 2003)
Zhou, Shah, and Gujar (2006)	XG	30 lb/Mgal	80	(Zhou <i>et al.</i> , 2006)

## 2.4 Flow in Microchannels

With the rapid development of microfluidic technology as a new branch of science and technology, there has been a growing interest in the study of microfluidics involving lab-on-chip and microreactor systems. Microfluidic system deals with the fluid flow within the hydraulic diameter ranging from  $10^{-6}$  m to  $10^{-3}$  m. This system have wide applications including sample preparation, separation, reaction, transport, purification, immobilization, biosensing and detection. The fluid behavior is quite different in these micro or even nano scale (You & Guo, 2010) where the flow is always in laminar regime. Factors such as surface tension may become dominant in microfluidic devices. When the size of biological samples is close to the flow channels or needles through which the samples are transported, then the sample flow may not be envisaged on the basis of conventional fluidic systems (Ashraf, Tayyaba, & Afzulpurkar, 2011). Thus, the understanding in the fundamental of the fluid behavior in this systems is very important.

Recently, the remarkable development of the microfluidic techniques drags the attention of enormous numbers of researchers due to its immense industrial and academic impact. Enhancing the flow in microchannel systems using additives is a new challenge that rarely been explored despite its great importance in many applications such as drug delivery (Weibel & Whitesides, 2006; Zhao, 2013), blood flow simulation (Marhefka et al., 2009; Zhao, Marhefka, Antaki, & Kameneva, 2010), mixing (Le The et al., 2015; Nimafar, Viktorov, & Martinelli, 2012), microreactors (Stone, Stroock, & Ajdari, 2004) and biosensors (Barbulovic-N, Yang, Park, & Wheeler, 2008).

In microfluidic system, surfactants as DRA were also used to enhancing the laminar flow in the microchannel. Xia, Liu, Qi, and Xu (2008) utilized Sodium Dodecyl Sulphate (SDS) and Alkyl Polyglycoside (APG1214) in fluid flow enhancement in the microchannel. The higher temperature of the fluid flow promotes the DR in the presence of the both surfactants. From the results, non-ionic APG showed better DR than anionic SDS. These results show agreement with the work of Ushida et al. (Ushida et al., 2011; Ushida, Hasegawa, & Narumi, 2010) where non-ionic surfactant and the cationic surfactant is more effective than anionic surfactants.

Several authors also reported that a minute quantity of polymeric DRA could effectively enhance the laminar flow in the microchannel. Sun, Wu, Wei, Bai, and Ma (2014) investigate the performance of the PAM-based polymer as flow enhancer in the microchannel where they observed more than 50% of DR was achieved. The authors also reported that higher concentration of polymers at low velocities within larger diameter of microchannel have greater flow enhancement performance.

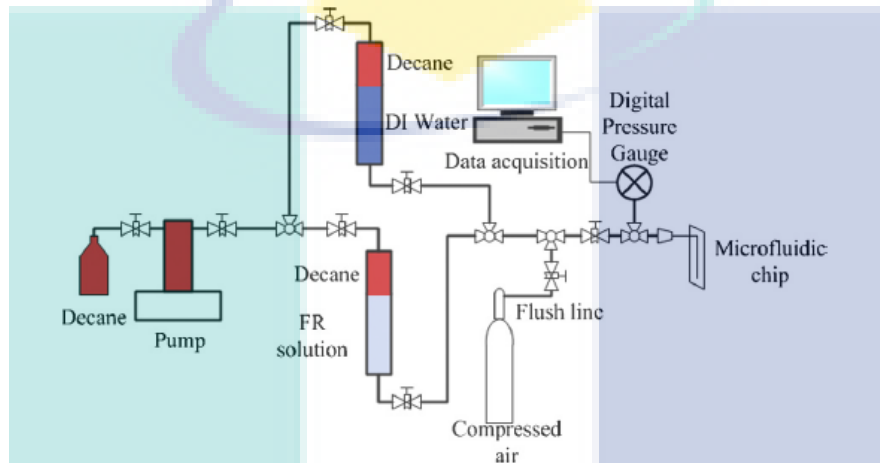


Figure 2-5 Schematic diagram of the experiment for DR using PAM-based polymer  
Source: Sun *et al.* (2014)

Tang, Lu, Zhang, Wang, and Tao (2012) utilized PAM solution to investigate the influence of the microchannel surface in the performance of the flow enhancer. The authors examined three types of different microchannels including fused silica, fused silica square and stainless steel microchannels in investigating the flow behavior of the non-Newtonian fluid. From the results, flow enhancement performance was greater in rough stainless steel microchannel than smooth fused silica microchannels.

It can be seen that polymeric DRA were also effective in enhancing the flow in microchannel, yet there were no literature reporting the utilization of natural polymeric additives in this area.

## 2.5 Microchannels Fabrication Technology

The microfluidic technology involves the use of microchannels with dimensions less than 1 mm and allows precision in the handling of fluids. Since the last decade,

microfluidic technology has significantly developed with a promising future in a wide variety of industries. Due to the use of the micrometer-sized channels, low sample and reagent volumes are used, thus, leading to less waste and environmental problems. Further advantages of the miniaturization of analytical techniques are a reduction of the equipment sizes, shortening of the reaction or analysis time, and the possibility of developing portable devices.

The miniaturization system has provided a new platform for fluid manipulation components (Fiorini & Chiu, 2005) such as pumps, valves, filters, and mixing. Lab-on-chips were also widely used in reactions (deMello, 2006; Truter, Ordonsky, Schouten, & Nijhuis, 2016; Ying *et al.*, 2016) and heat transfer (Lee & Mudawar, 2016; Morgan *et al.*, 2013). In detection techniques, microfluidics plays an important role especially in separation (Nam, Kim, & Kim, 2014), and food analysis (Guo, Feng, Fang, Xu, & Lu, 2015; Muijlwijk, Berton-Carabin, & Schroën, 2016). Other than that, microfluidics is also substantially applicable in clinical (Boussommier-Calleja *et al.*, 2016; Kozminsky *et al.*, 2016; Tay *et al.*, 2016) and cell biology (Grünberger, Wiechert, & Kohlheyer, 2014). Besides, droplet generators (Shah *et al.*, 2008; Zhu & Fang, 2013) in microfluidics are also important in chemical and biological processes.

An ongoing challenge in microfluidics is the rapid prototyping of microchannels for use in academic studies. There are a variety of rapid prototyping methods for the fabrication of microchannels such as wet etching, reactive ion etching, conventional machining (Schaller Bohn, Mayer, & Schubert, 1999), photolithography, soft lithography, hot embossing, injection molding, laser ablation, in situ construction (Beebe *et al.*, 2000), and plasma etching (Rossier *et al.*, 2002).

### **2.5.1 Machining**

Micro-machining is a non-lithography technique which uses milling machines or laser devices (Chang, 2013). Machining does not limit the material of the substrate, but the materials must be soft and ductile to be machined (Ashman & Kandlikar, 2006). Microfluidic devices with the depth of 100 – 300  $\mu\text{m}$  can be machined by commercial  $\text{CO}_2$  laser, where the minimum width of the channel can be up to 85  $\mu\text{m}$  (Klank, Kutter, & Geschke, 2002). The roughness of the microchannel is always the concern of researchers. Huang, Liu, Yang, & Yu (2010) suggested that by preheating polymethyl

methacrylate (PMMA) substrate up to 70 – 90 °C, there can be a reduction in the roughness of the microchannel.

Other methods of machining other than CO<sub>2</sub> laser machining such as an infrared laser (IR laser) (Romoli, Tantussi, & Dini, 2011), foil-assisted CO<sub>2</sub> laser (Chung & Lin, 2011) and direct-write laser (Cheng, Wei, Hsu, & Young, 2004) has been introduced. Machining itself also involves a combination of few techniques of microchannel fabrications such as wet etching, photolithography (Muluneh & Issadore, 2013) and others which require the clean room facilities, thus increasing the cost of fabrication (Martynova *et al.*, 1997; Rodriguez, Spicar-Mihalic, Kuyper, Fiorini, & Chiu, 2003; Xu, Locascio, Gaitan, & Lee, 2000).

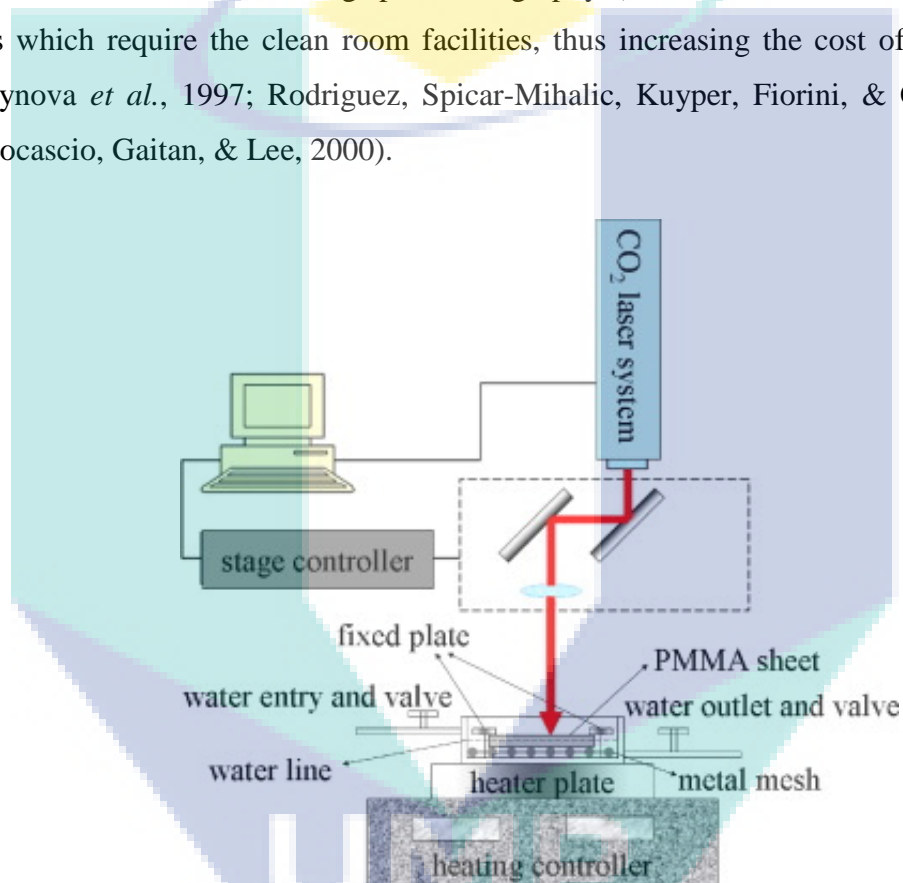


Figure 2-6 Experimental setup of laser machining

Source: Huang *et al.* (2010)

### 2.5.2 Embossing

Embossing, also known as hot embossing is gaining much interest as a method of microchannel fabrication; it involves the imprinting of structures on substrates, usually polymeric material using a preformed master. An embossing force is used to imprint the substrate using the master after the substrate has been heated up to its glass transition temperature (T<sub>g</sub>). The typical emboss temperature for microchannels fabrication is 120 °C and imprint force of 700N (Ishizuka, Mizuno, Harada, & Shoji,

2004). Thus, the material of the master is necessary to withstand multiple high temperature cycles and embossing forces cycles. Nickel has been reported as a suitable material for the stamp; however, it directly increases the cost and does not allow rapid design modification (Becker & Heim, 2000). Besides nickel, researchers have also introduced copper as a master material (Nugen, Asiello, & Baemner, 2008). Authors reported that the stamp produced by the SU-8 on silicon, glass, and polydimethylsiloxane (PDMS) can withstand more than 50 embossing cycles where the stamp fabrication process can be performed in less than 4 hours (Koerner, Brown, Xie, & Oleschuk, 2005).

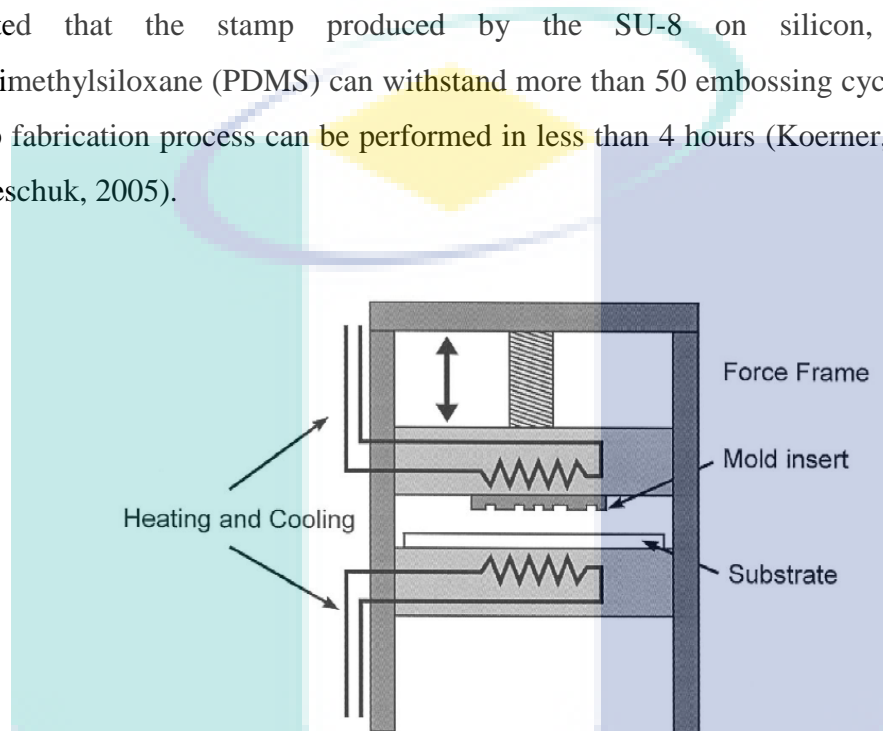


Figure 2-7 Schematic diagram of hot embossing equipment

Source: Becker & Heim (2000)

Embossing process consumes lots of time (Tsao, Chen, Woon, & Lo, 2012) and it is not suitable for prototyping few microchannels for testing purposes. However, it is suitable for medium volume production where fabricated microchannels still under the process of trial and validation and may need some modification of the design. Konstantinou, Shirazi, Sadri, & Young (2016) presented that embossing technique can produce 50 devices per week where this method satisfy the need of design changes without lengthy procedure.

Roller hot embossing is improvised from conventional hot embossing method and PMMA-based can be used as a substrate (Yeo *et al.*, 2010). This method is applicable for mass production of microfluidics devices where it is a continuous process to imprint on flexible sheets and films materials (Kimerling, Liu, Kim, & Yao, 2006; Ting, Huang, Tsai, Chou, & Fu, 2008; Velten, Schuck, Haberer, & Bauerfeld, 2009;

Yeo, Ng, Wang, Wang, & de Rooij, 2009). This technology is gaining interest to for application in industries due to its high production rate, lower cycle time and cost effectiveness (Y. C. Chang, Yang, & Sheh, 2006; Mäkelä, Haatainen, Majander, & Ahopelto, 2007; Metwally, Robert, Salut, & Khan-Malek, 2012; Shih-Jung & Yau-Chia, 2007). The products produced have better uniformity and this technique can also release trapped air bubbles (Zhang, Sahli, Gelin, & Barrière, 2015). Thermoplastic is proven to be a suitable substrate for roller hot embossing method (Ng & Wang, 2008; Shan, Jin, Soh, & Lu, 2009).

### **2.5.3 Injection molding**

Injection molding is a non-photolithography technique that is also widely used in the fabrication of microfluidic devices. Metal mold masters such as brass (Jakeway, de Mello, & Russell) and aluminum (Mecomber, Hurd, & Limbach, 2005; Mecomber et al., 2006; Zhao, Roy, McCormick, Kuhr, & Brazill, 2003) were reported as suitable materials used to replicate microchannels.

The profile of the microchannels such as the width and depth is affected by the operating conditions of injection molding hence, investigation on the optimum conditions for the process started to gain attention (Fu, Tor, Hardt, & Loh, 2011). This method is suitable for fabricating polypropylene microfluidic devices which can be used in biochemistry and medicine field (McCormick, Nelson, Alonso-Amigo, Benvegna, & Hooper, 1997). Besides polypropylene, thermoplastic such as polycarbonate (Liu *et al.*, 2001; Liu *et al.*, 2002), PMMA (Johnson, Ross, Gaitan, & Locascio, 2001; Youdan, 2014), cycloolefin polymers, and copolymers (Mela *et al.*, 2005) can also be used as substrates.

It was also recommended to combine some technique besides injection molding to fabricate the microchannel (Redha *et al.*, 2009). Thus, due to the complexity of molding equipment and high operating temperature and pressure (Çetin, Koska, & Erdal, 2015), injection molding is more suitable for industrial use compare to research application.

## 2.5.4 Etching

Etching is a technology where chemicals are used to remove the surface of the wafer to produce channels. Different etching processes in microchannels fabrication have been developed such as silicon etching, chemical etching, and laser-induced etching. Silicon etching is done by covering the silicon with the patterned mask, and then the silicon is being etched. Silicon can be etched by using different methods such as wet anisotropic, wet isotropic, dry anisotropic, and dry isotropic. The wet anisotropic process always involves the use of basic solutions such as potassium hydroxide (KOH). The concentration of KOH and process temperature are the parameters affecting the quality of the microchannels produced (Kang, Chen, & Hung, 1998). However, this process takes a longer time to complete.

Acidic solutions such as hydrogen fluoride (HF) and nitric acid (HNO<sub>3</sub>) are used in wet isotropic where the composition of the solution affect the final shape of the microchannels (Schwartz & Robbins, 1976). The microchannels produced using this method will have round corners. Also, dry etching process requires a plasma etching machine and the shape of the channels is dependent on the etching conditions (Henri, Han, Meint de, Miko, & Jan, 1996). A strong acid or base is used in chemical etching to develop the microchannels on silicon wafers or glass. Harpole and Eninger (1991) reported that this method is perfect for fabrication of small cross section rectangular microchannels where the silicon wafers can be removed at a very fast rate. Laser-induced etching can be utilized in the fabrication of microchannels where laser light is used to melt the silicon. The silicon is then etched anisotropically in KOH solutions (Alavi, Büttgenbach, Schumacher, & Wagner, 1991, 1992). However, the end products will leave a large opening at the top.

After the surface of the silicon has been removed using one of the methods discussed above, the next step will be to close the channels to make it a close system. Bonding of a glass of silicon wafer on top of the microchannels is the easiest way to close the channel in analytical applications (Harrison, Manz, Fan, Luedi, & Widmer, 1992; Manz et al., 1990; Terry, Jerman, & Angell, 1979). Desired geometry of the microchannels also can be obtained by etching two wafers that each contained one-half of the channels (Paoletti, Gretillat, & Rooij, 1996; Reston & Kolesar, 1994; Tjerkstra et al., 1997b). However, this required expertise to prevent misalignment. The simplicity of

this method and possibility of filling materials especially for chromatographic purposes make it widely used in analytical fields.

However, bonding will cause problems such as the formation of micro-void, high air pressure trapped insides can press the wafers apart, and misalignment. Thus, to replace the bonding method, deposition of a layer to seal the channel was also developed. There are two approaches to complete this process: the first method is done by deposition of a layer of silicon oxide or nitride which is commercially applicable in the inkjet print head (Chen & Wise, 1995), and the second is chemical analysis systems (Kaplan, Elderstig, & Veider, 1994). Transparent materials are also being used to make the channels visible but they crack easily. However, the deposition can cause the wall of the microchannels to be covered.

The produced microchannels can also be closed by burying channels beneath the wafer surface as described by (Tjerkstra et al., 1997a). Reaction-ion etching (RIE) is used to etch a deep narrow trench, and then a layer of silicon nitride is used to cover the wafer surface which will cover the wall and the bottom of the trench. Again, RIE is then utilized to remove the silicon nitride at the bottom of the trench. The wafers are then etched using any method as discussed above and the nitride is etched using 50 % HF. A thick layer of deposition materials such as silicon oxide, silicon nitride or polysilicon on the wafer covers the walls and closes the trench. However, this method is complicated and need some specialized equipment.

### **2.5.5 Soft Lithography**

In most of the laboratory environment, soft lithography is used as rapid prototyping due to the advantages such as low cost and less time consuming (Friend & Yeo, 2010; Martin & Aksay, 2005). The material used in soft lithography is PDMS which has a high optical transparency and high gas permeability, thus, suitable even for cell and biology applications (Faustino, Catarino, Lima, & Minas, 2016). The elastomeric properties of PDMS cause the easy detachment of the elastomer from the wafer and easy bonding to another piece of polymer or glass in the sealing process (Becker & Locascio, 2002; McDonald & Whitesides, 2002). This property is also suitable for fabricating multilayer 3D-structured microchannels (Qin, Xia, & Whitesides, 2010; Ziaie, Baldi, Lei, Gu, & Siegel, 2004).

However, the traditional way of soft lithography involves fabrication of special silicon master composed of photoresist with the design of microchannel on it. This process is much more time-consuming and required clean room facilities, thus, increase the cost (Feng & Tsai, 2010). Due to the hydrophobic nature of PDMS, it required surface molecular property treatments when involving handling of functional macromolecules such as protein adsorption (Wong & Ho, 2009).

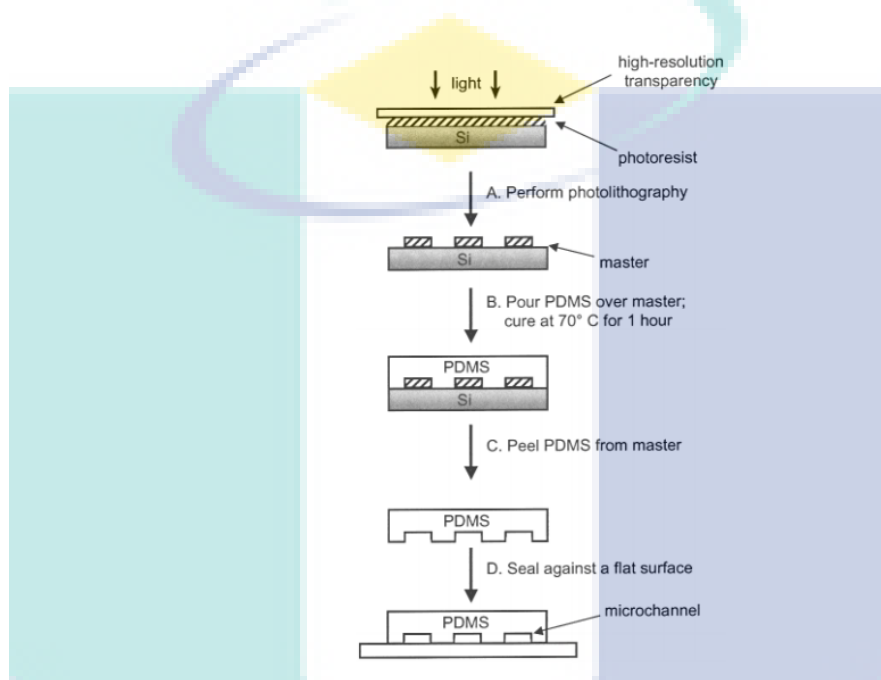


Figure 2-8 Soft lithography process involving silicon master

Source: McDonald & Whitesides (2002)

Table 2-3 Summary of fabrication of microchannel technologies

Authors	Technologies	Advantages/Disadvantages	Ref.
Martynova <i>et al.</i> (1997) Xu <i>et al.</i> (2000) Rodriguez <i>et al.</i> (2003)	Machining	<ul style="list-style-type: none"> <li>Involve combination of few techniques</li> <li>Requires clean room facilities</li> <li>High cost</li> </ul>	(Martynova <i>et al.</i> , 1997; Rodriguez <i>et al.</i> , 2003; Xu <i>et al.</i> , 2000)
Tsao <i>et al.</i> (2012)	Embossing	<ul style="list-style-type: none"> <li>Time consuming</li> </ul>	(Tsao <i>et al.</i> , 2012)
Çetin <i>et al.</i> (2015)	Injection molding	<ul style="list-style-type: none"> <li>Complexity of equipment</li> <li>High operating temperature and pressure</li> </ul>	(Çetin <i>et al.</i> , 2015)

Wong and Ho (2009)	Soft lithography	<ul style="list-style-type: none"> <li>• Involve fabrication of special silicon master composed of photoresist</li> <li>• Time consuming</li> <li>• Requires clean room facilities</li> <li>• Required surface molecular property treatments</li> </ul>	(Feng & Tsai, 2010; Wong & Ho, 2009)
--------------------	------------------	---	--------------------------------------

## 2.6 Particle Image Velocimetry

As earlier discussed in Section 2.3.2, the mechanism of DR by utilizing polymers in blood flow is undetermined yet. Thus, in this study, particle image velocimetry (PIV) technique was used to investigate the possible mechanism of flow enhancement when introducing a minute amount of natural polymer in the working fluid. Particle image velocimetry (PIV) as a flow visualization technique is substantially used to study the fluid motion. PIV can provide flow velocity vector measurements over global (2D or 3D) domains instantaneously. Generally, PIV comprises of four basic components, namely, transparent test section with the particle seeded fluid, a laser source producing a light sheet to illuminate the region of interest, recording hardware consisting of charge coupled device (CCD) camera imaging the particles in the sheet, and a computer to process the recorded images and extract the velocity information from the tracer particle positions (Stamhuis, 2006).

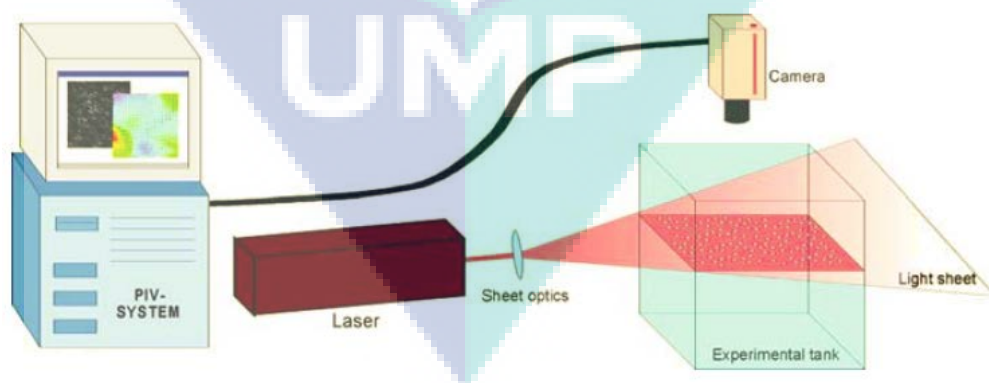


Figure 2-9 Basic PIV setup comprised of transparent test section with the particle seeded fluid, a laser source producing a light sheet; charge coupled device (CCD) camera imaging the particles in the sheet, and a computer to process and analyze information

Source: Stamhuis (2006)

Back in the 1920s, Pitot-static tubes or hot-wire, and anemometers were used to obtain quantitative velocity measurements in fluid flow research. These techniques have disadvantages such as physical probe insertion which will intrude on the flow itself, and the velocity information only obtained at the point occupied by the probe (Prasad, 2000). However, extensive quantitative data (two or more points in the flow field at the same time) is required especially in the application for the verification of theories of turbulence or the evaluation of mathematical models of turbulent flows (Buchhave, 1992). PIV was significantly used in both research and industries after the invention of the laser in the 1960s which led to the development of the laser doppler anemometer that uses a laser probe to enable non-intrusive velocity measurements (Prasad, 2000).

As discussed in Section 2.3, microfluidics has gained great interest in handling the precise volume of fluids or reagents and has a promising future in a wide range of fields. Thus, there is an increasing need for the diagnostic tools to measure or analyze the flow behavior in microfluidic devices. Santiago, Wereley, Meinhart, Beebe, and Adrian (1998) succeeded in conducting the first micro-PIV ( $\mu$ -PIV) experiment by using an epi-fluorescent microscope with a continuous Hg-arc lamp, and a CCD camera to record the flow around a nominally 30  $\mu\text{m}$  diacylinder in a Hele-Shaw flow cell. A 300 nm diameter polystyrene particles were chosen as flow-tracing particles and these particles were large enough to emit sufficient light for recording and to reduce the effects of Brownian motion. This experimental setup has a high spatial resolution and low-light levels which are suitable for investigating the flows around living micro-organisms.

Chinaud, Roumpea, and Angeli, (2015) used  $\mu$ -PIV to study plug formation at a microchannel inlet during the flow of two immiscible liquid. From the observations, the continuous phase resists the flow of the dispersed phase into the main channel, causing

a change in the interface curvature and appearance of the vortex at the tip of the plug during the early stage of plug formation. The interface curvature accelerates the thinning of the meniscus result in plug breakage. This study is important as liquid-liquid flow in microchannel has a great impact on the production of the emulsion, two-phase extractions, and reactions. The understanding of the hydrodynamic characteristics of flow pattern and their transitions, besides consideration of the operating conditions (velocity and phase flow ratio), and geometry of the inlet, enable the design of a micro-scale multiphase system (Jovanovic' et al., 2011; Salim, Fourar, Pironon, & Sausse, 2008; Tsaoulidis, Dore, Angeli, Plechkova, & Seddon, 2013).

In medical applications, fluid dynamics of blood is the main concern where it can affect the microvascular circulation (arteries, ventricles, and capillaries). The circulation is important in maintaining metabolism in tissues, and the flow behavior can be an indicator for the risk of circulatory diseases such as hypertension and stroke (Dintenfass, 1969; Fossum, Høieggen, & Moan, 1997; Lee, Mowbray, & Lowe, 1998; Resch, Ernst, Matrai, & Paulsen, 1992; Toth, Kesmarky, & Vekasi, 1999). Due to the high concentration of red blood cells in the blood, the biophysical behavior of these cells is crucial to determine the blood flow behavior in the circulatory system. Thus, there is great attention in measuring the velocity profile of blood flow either in vivo or in vitro. Back to 80s and 90s, ultrasonic Doppler flow meter (Haywood, Shaffer, Fastenow, Fink, & Brody, 1981) and Laser Doppler Velocimetry (LDV) (Cochrane, Earnshaw, & Love, 1981; Seki, Sasaki, Oyama, & Yamamoto, 1996) were being used to obtain blood velocity measurements. However, these methods only enable researchers to collect qualitative flow structure and information thus, PIV method started to be implemented to get a large amount of quantitative data including spatial distribution information.

There are few factors that needed to take account of to get high accuracy information of blood flow velocity profile when using  $\mu$ -PIV (Pitts & Fenech, 2013). It is important to ensure the concentration of fluorescing tracing particles is high enough so that it is easier for imaging. However, too high concentration of red blood cell will make the fluid opaque leading to difficulties during imaging. This circumstance cannot be overcome by increasing the density of the tracer particles. The authors also suggested that the understanding the characteristics of the red blood cells such as the

density, aggregation, and deformability is also significant to get the data required by researchers. Since the velocity at the center of the channel is at maximum, the tracing particles will be moving together with the red blood cells at the same speed. However, at the wall of the channel, there might be few or no red blood cells present causing phenomena of “cell-free” layer. For the cases of higher magnifications, this phenomenon must be accounted for to collect more accurate data.

Kim *et al.* (2010) observed the motion of red blood cells in a 100  $\mu\text{m}$ -diameter microchannel using confocal microscopy  $\mu\text{-PIV}$  which can measure velocity up to few hundreds  $\mu\text{m}/\text{sec}$ . The interesting aspect of this study is that the authors utilized the red blood cells as the tracing particles replacing the conventional exogenous fluorescent particles. The authors reported that some irregularities in the velocity contour distribution occurred due to the presence of red blood cells. It is suspected that these cells show three-dimensional tumbling, causing out of plane motion. Parabolic velocity profile was obtained when the authors measured the blood flow velocity at a different depth of microchannel. This scenario is due to the three-dimensional cell motion near the tube wall regime because of abrupt shear rate variations. The outcome of this study is expected to be applied in the measurement of in vivo blood flow in capillaries of live animals.

There will be a significant impact on medical and pharmaceutical fields when using  $\mu\text{-PIV}$  for the analysis of the velocity profile of blood flow in order to study the effect of medications, diseases, and therapeutic treatments. These measurements are useful in modern medicine and engineering since the uptake of nutrients and medications is shear-dependent.

## CHAPTER 3

### METHODOLOGY

#### 3.1 Materials

##### 3.1.1 Natural Polymers

Xanthan gum was selected to be used in this study. It is an anionic polysaccharide containing glucose, mannose, acetate, potassium, pyruvate and glucuronate (Sigma–Aldrich, St. Louis, MO). Xanthan gum is a soluble polysaccharide produced by fermentation of the bacteria *xanthomonas campestris*. Xanthan gum powder purchased from Sigma-Aldrich, was used without any further purification and deionised water used as a solvent (Sigma–Aldrich, St. Louis, MO).

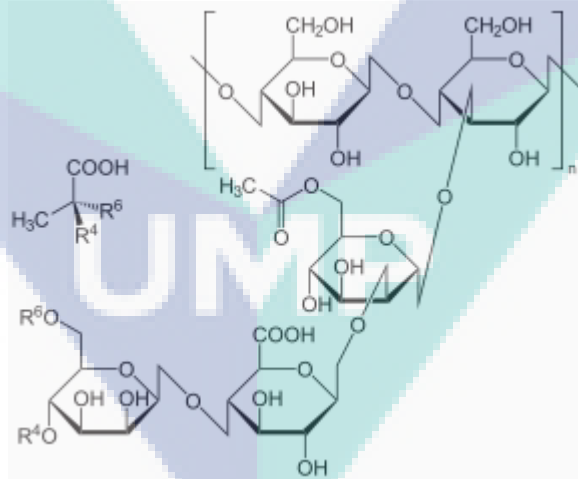


Figure 3-1 The monosaccharides present in xanthan gum.

##### 3.1.2 Working Fluid

In this work, deionized water (DI water) was selected as the working fluid. DI water was collected from the laboratory unit of Center of Excellence for Advanced Research in Fluid Flow (CARIFF), University Malaysia Pahang.

### 3.1 Natural polymer solution preparation

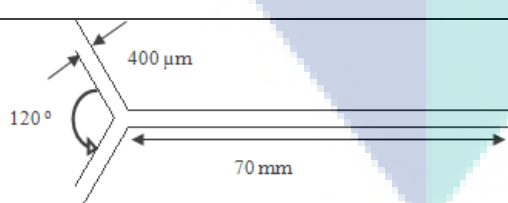
500 ppm of Xanthan gum solution was prepared by diluting the required amount of polymer powder (0.25 g) into 500 ml deionised water. Polymer solution was stirred slowly at room temperature until a homogeneous solution is obtained. Eight different concentrations of Xanthan gum solution were prepared by dilution with additional deionised water to a desired test concentration ranging from 20ppm to 400ppm. Xanthan gum solutions were diluted according to formula below:

$$M_1 V_1 = M_2 V_2 \quad \begin{matrix} 3 \\ .1 \end{matrix}$$

### 3.2 Fabrication of Microchannels

Table 3-1 shows a schematic of Y-shaped PDMS micro-channels. There were seven different Y-shaped micro-channels varies in length of tail and width of channel. The depths of the micro-channels were fixed with 100 micrometer ( $\mu\text{m}$ ). Three micro-channels have same in angle ( $120^\circ$ ) and width ( $400 \mu\text{m}$ ), but contained different in length of the tail (40 mm, 60 mm, 50mm and 70mm). For another three micro-channels were variations of the width ( $200 \mu\text{m}$ ,  $300 \mu\text{m}$ , and  $500 \mu\text{m}$ ) with same in angle ( $120^\circ$ ) and length (50 mm). The fabricated Y-shaped PDMS micro-channels were shown in Figure 3-2.

Table 3-1 The schematic of Y-shaped micro-channels.

No	Design	Angle ( $^\circ$ )	Length (mm)	Width ( $\mu\text{m}$ )
a.		120	70	400

b.		120	60	400
c.		120	50	400
d.		120	40	400
e.		120	50	500
f.		120	50	300
g.		120	50	200

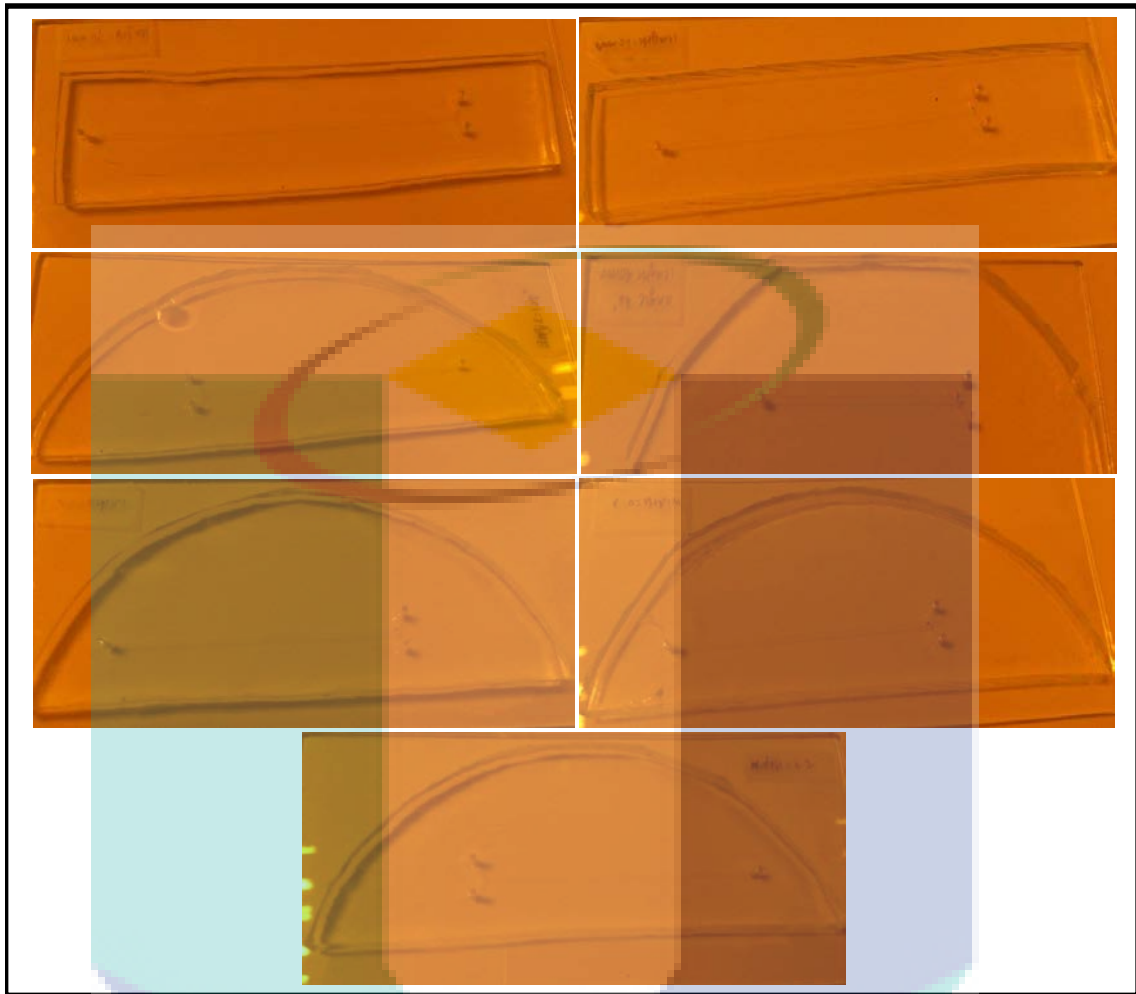


Figure 3-2 Fabricated Y-shaped micro-channels

Furthermore, seven models of passive micromixers having different dimensions of microriblets along the side of the system were designed and fabricated.

The ribblets are in the shape of prism and are embed along walls of the micromixer. They are varied in base and height where the ratio of the base to the height is 1:1, ranging from 0.00mm, 0.01mm, 0.02mm, 0.04mm, 0.06mm, 0.08mm and 0.1mm. Overall dimensions as well as the ribblets dimensions can be seen on Figure 3-3 and Table 3-2.

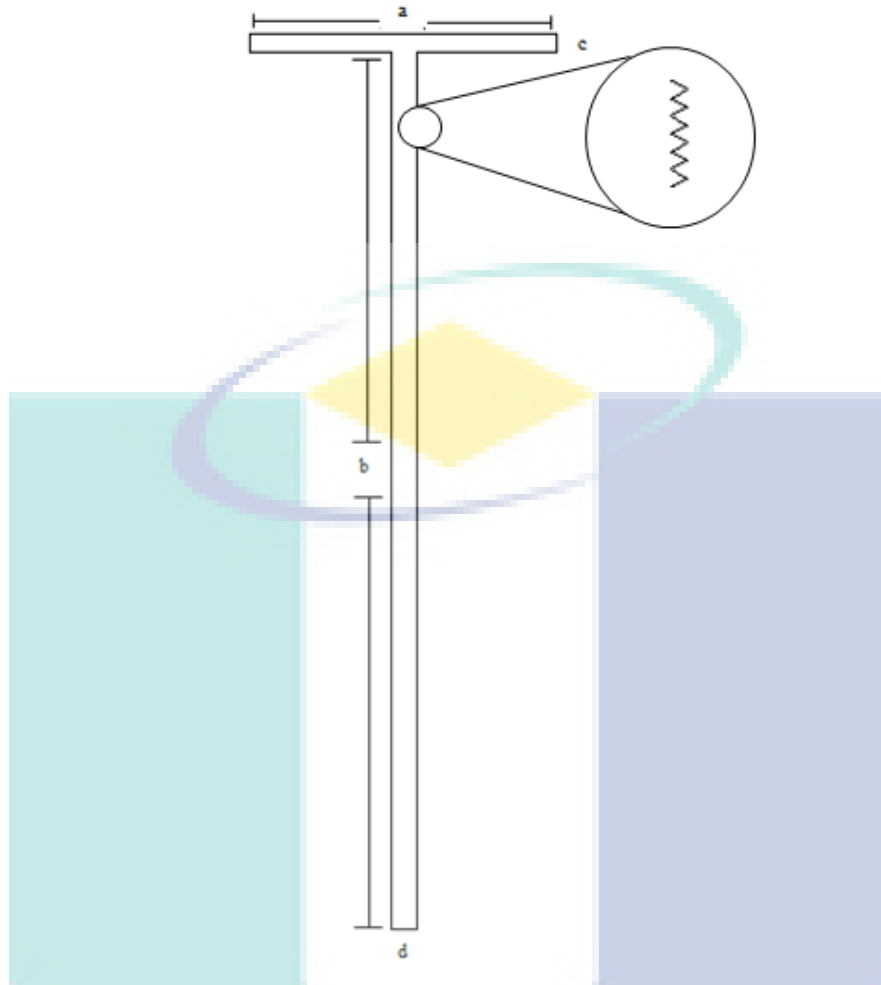
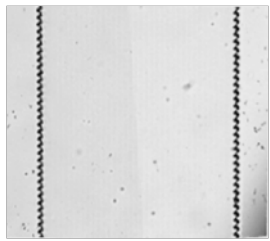
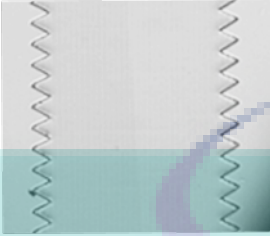
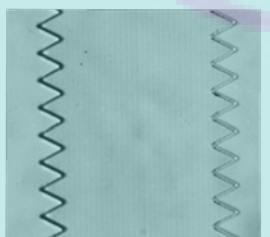
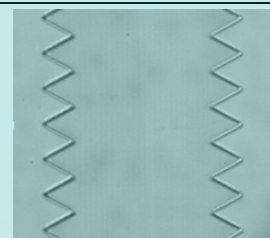


Figure 3-3 Overall dimension of designed microchannel with ribblets profile

Table 3-2 Dimension of ribblets used in study

Model	Total length of inlet channels	Total length of mixing channel	Width of inlet channel	Width of mixing channel
	7 mm	20 mm	0.4 mm	0.6 mm
Microriblets Dimension ( $\mu\text{m}$ )				
Height			Base	
1	0		0	

2		20	20
3		60	60
4		80	80
5		100	100

The fabrication processes of the micro-channels were based on adapted soft lithography techniques as illustrated in Figure 3-4. The material used for micro-channels is PDMS (polydimethylsiloxane).

Firstly, seven Y-shaped of the micro-channels are chosen as the design of the micro-channel. These designs were drawn in Autocad software. A new and clean wafer was taken out and put it as center as possible on the spin coater chuck. 5.50ml of SU-8 was taken out using macro-pipette and put at the center of the wafer. There were two steps to coat the wafer, first with a lower speed at 500rpm for 10 seconds and acceleration of 100rpm/s; then higher speed at 900rpm for 30 seconds and acceleration of 300rpm/s. The setting set was aimed to achieve the SU-8 thickness of 100 $\mu$ m which would be the depth of the micro-channel later on. The wafer was then pre-baked at 65 °C for 15 minutes followed by 95 °C for 2 hours.

After pre-baked, wafer was cooled down to room temperature (25-30 °C). The wafer coated with SU-8 was brought for exposure to obtain the desired design using

micro pattern generator ( $\mu$ PG). The wafer was brought for post exposure bake at 65 °C for 15 minutes followed by 95 °C for 40 minutes. Then, the wafer was cooled down to room temperature (25-30 °C) and soaked in around 80 ml of SU-8 developer with manual agitation for 5 minutes. The wafer was rinsed using isopropanol and dried it using air gun. After that, the wafer was hard baked at 135°C for 2 hours.

The PDMS ( $\approx$  60 g) and curing agent ( $\approx$  6 g) were poured in a disposable plastic cup with a 10:1 ratio by weight. The mixture was mixed vigorously together for 5 minutes at 1000 rpm and degassed at 400 rpm for another 5 min in Thinky mixer. The wafer was cleaned using air gun. Then, the PDMS was poured on the wafer followed by desiccated it under vacuum for 40 minutes to remove all the air bubbles. The PDMS was baked in an oven at 80 °C. After 2 hours, PDMS was peeled off from the wafer using a blade and tweezer to take it out. Inlet and outlet of the micro-channel were punched using a puncher. The glass slide was cleaned using isopropanol then dry using air gun. Both the PDMS and the glass slide were placed in plasma cleaner for 2 minutes.

Lastly, both surfaces were put together (design of micro-channel facing the glass slide) and pressed slightly to let them bond together.

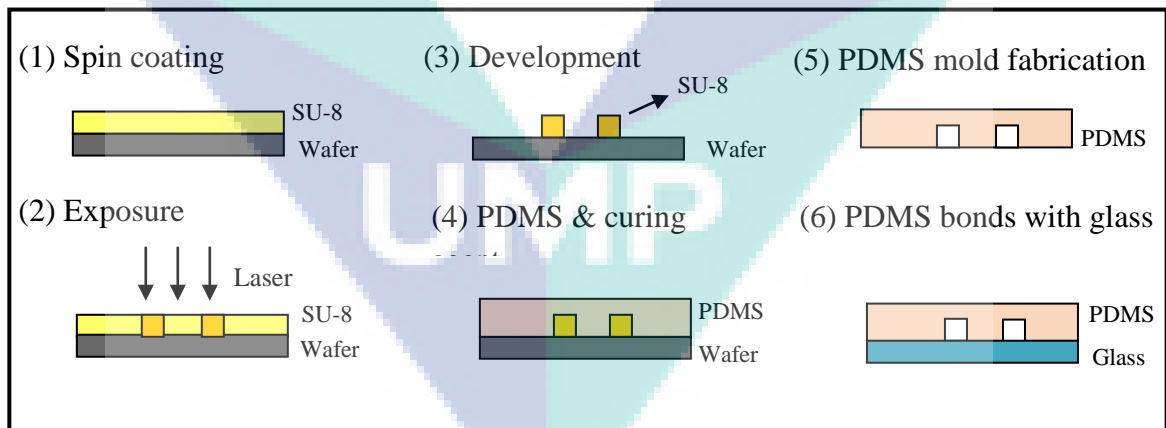


Figure 3-4 Fabrication steps of the micro-channel.

### **3.3 Natural Polymer Characterization Analysis**

#### **3.3.1 Morphology Analysis**

The morphology of Xanthan gum solution was investigated using cryo-TEM technique which was performed in the Center of Excellence for Advanced Research in Fluid Flow (CARIFF), University Malaysia Pahang.

#### **3.3.2 Rheology Study**

The rheological analysis of xanthan gum solution was performed using a rheometer (Malvern Kinexus Lab+, England). The viscosity of the solution was measured using a cone-plate geometry (CP2/60 SR22750SS) with a shear rate of 10 to 250  $s^{-1}$ , with the aid of Toolkit V001 method available in the software rSpace for Kinexus. The viscoelasticity of the xanthan gum solution was also examined. The  $G'$  (storage modulus) and  $G''$  (loss modulus) values of the solution were measured using the method Oscillation 0003 by setting the sweep frequency from 1 to 100 Hz with a shear strain of 30 % using a parallel-plate geometry (PU60 SR3192 SS).

### **3.4 Experimental Set-Up**

An experimental apparatus was erected as shown in Figure 3-4 for obtaining the DR data at a wide range of mucilage concentrations. The experimental setup comprised of a pressure and vacuum controller (model: Elveflow OB1 MK3) connected to a compressor which helped to push the solution out of the reservoir, an Elveflow flow sensor, a customized PDMS microchannel, Polytetrafluoroethylene (PTFE) tubing, and a beaker which served as a collecting tank. The setup started with the connection from the pressure and vacuum controller to a reservoir that contained the solution; then to the inlet of the flow sensor. The outlet of the flow sensor was connected to the inlet of the microchannel made of PDMS. Finally, the remaining solution coming out from the outlet of the microchannel was collected in the beaker. The parameters that were investigated in this work include the effect of additives concentration, type of additives, operating pressure and the clogging location in the microchannel.

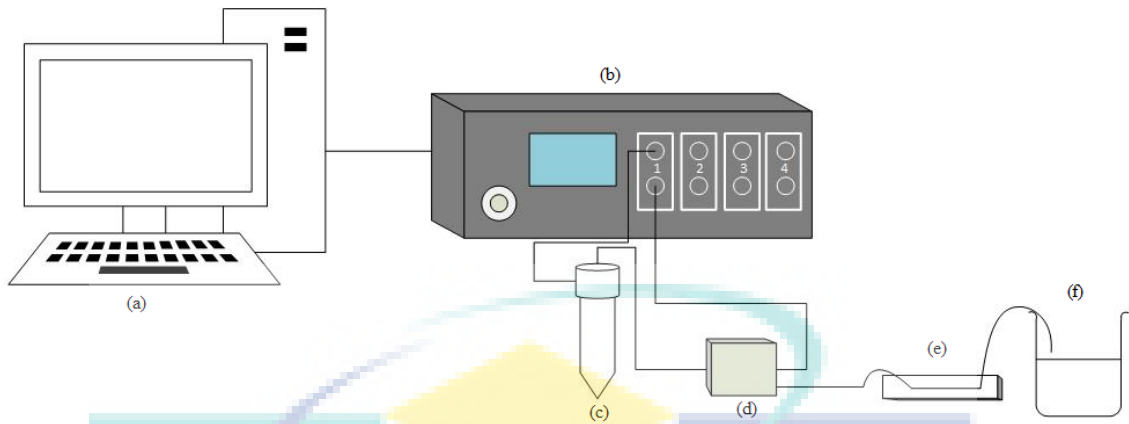


Figure 3-5 Schematic diagram of experimental setup consisted of (a) computer (b) pressure and vacuum controller (c) reservoir containing solution (d) flow sensor (e) custom made microchannel (f) beaker as storage tank

### 3.5 Experimental Procedure

Five different concentrations of each mucilage ranging from 100 ppm to 500 ppm extraction solution were prepared. The weight of the needed mucilage was expressed in weight/weight. The mucilage was weighed accordingly and added to the transport liquid (DI in this case), and then, stirred manually. All the experiments were conducted in an open loop microfluidic system, experimenting on the effect of concentration of extracted mucilage on DR. The procedure began by testing every concentration of the DR agent; the operation started when the solution delivered across the tube length. The Elveflow Smart Interface was used to execute commands to the pressure and vacuum controller to manipulate the required pressure (50 – 500 mbar) for pushing the solution out of the reservoir. By varying the pressure, the flow rate readings across the tube length were recorded. This method was repeated for each mucilage concentrations to check its effect on the DR operation. Each experiment was carried out in triplicates to obtain results with less deviation. The results were presented as the mean of the triplicate measurements. The percentage increase in the flow rate (%FI) was calculated using Equation 3.1.

$$\%FI = \frac{F_a - F_b}{F_a} \times 100 \quad 3.2$$

where

$F_b$  = Flow rate before the addition of DRA ( $\mu\text{L}/\text{min}$ )

$F_a$  = Flow rate after the addition of DRA ( $\mu\text{L}/\text{min}$ )

### 3.6 $\mu$ -PIV Measurement

The velocity profile of the flows in the microchannel was measured with the  $\mu$ -PIV system as illustrated in Figure 3-5, adapting the method proposed by (Hsieh, Lin, & Chen, 2013). The same settings as shown in Figure 3-4 was used to control the flow of liquid into the microchannel. The time-interval between each pair of the image is 8  $\mu\text{s}$ . A double-pulsed Nd: YAG laser emitted light with pulse energy of 200 mJ which was focused on the object plane by a microscope (model: Nikon ECLIPSE Ni-U). The 532-nm incident laser light was expanded and reflected by an epifluorescent filter (dichroic mirror) before illuminating the particles within a volume of fluid through an objective lens. The excitation of the fluorescence and the scattered light by the particles followed the same path, going through the microscope objective and the dichroic mirror. Doped by a fluorescent dye with excitation and emission peak wavelengths of 532 and 590 nm, respectively, the 8  $\mu\text{m}$  diameter Rhodamine B fluorescent particle (MicroVec MV-F07) absorbed the green incident light and emitted red light. In order to obtain accurate instantaneous velocity fields, the volumetric particle concentration was about 0.07 %. The images were recorded using a 5MP CCD camera (model: IMPERX CLB-B2520M-SC) with  $2456 \times 2058$  pixel array. The instantaneous velocity vectors were derived from two-frame cross-correlation, and 40 pairs of frames were averaged to get the mean velocity profiles. The interrogation window was set to  $64 \times 32$  pixels (streamwise  $\times$  spanwise direction) and 50 % overlap.

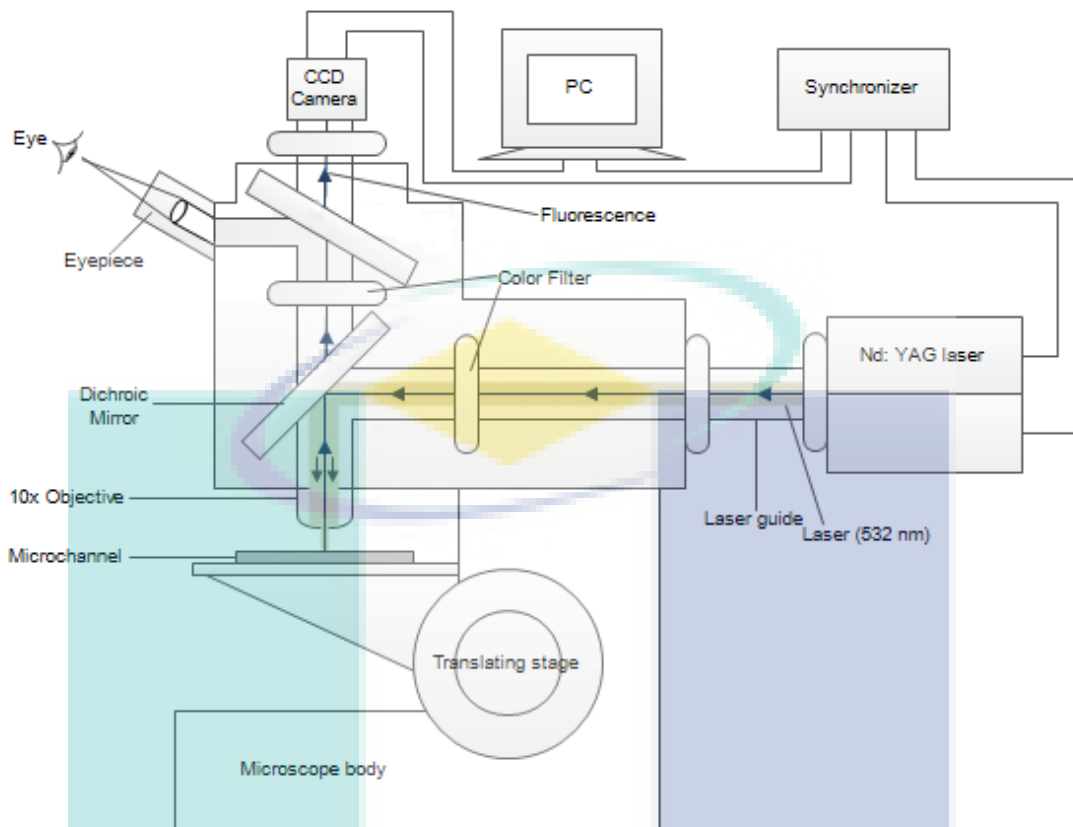


Figure 3-6 Schematic diagram of  $\mu$ -PIV setup

UMP

## CHAPTER 4

### RESULTS AND DISCUSSION

#### 4.1 Characterization of Natural Polymer

##### 4.1.1 Morphological Analysis

The morphology of xanthan gum was illustrated in Figure 4-1. The additives have a distinguished polymeric network as seen in the cryo-TEM image which is similar with the result reported by Mendes et al. (2013). From the figure, the polymers are not only present in single long chains but also interact with other polymer molecules to form branched polymers. However, most of the xanthan gum was found to be in linear chain due to the dilute solution used in this present work. Thus, there is low possibility of the xanthan gum to interact with each other to form larger polymer molecules. This property is important in flow enhancement application as the efficacy of the additives was reported to be higher when utilizing long straight polymers (Singh, Jain, and Lan, 1991).

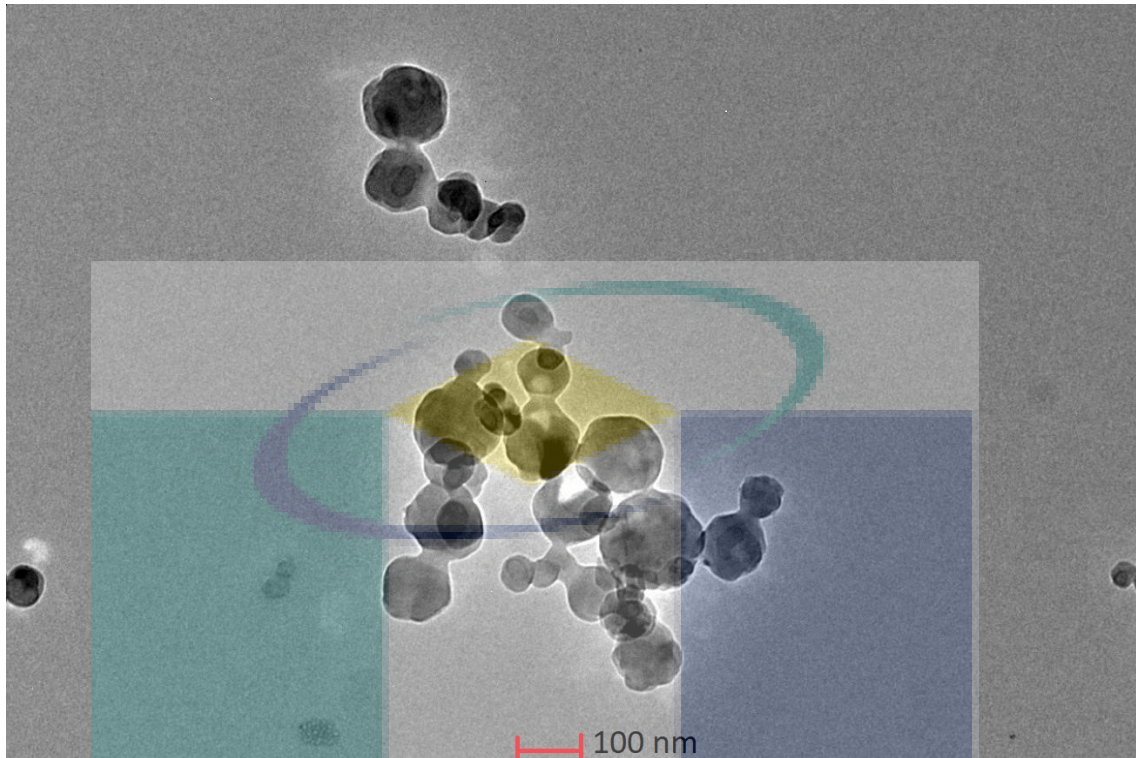


Figure 4-1 Cryo-TEM image of xanthan gum solution

#### 4.1.2 Rheology Study

The viscosity of xanthan gum solution at various concentrations (20 to 500 ppm) as a function of the shear rate is shown in Figure 4-2, whereas the shear stress as a function of shear rate is demonstrated in Figure 4-3. It can be clearly seen that the viscosity of high xanthan gum concentrations increased from 1.4 to 23 cP. The viscosity of 20 ppm of xanthan gum solution was similar to the viscosity of DI water. The results agree with the previous work done by Zaharuddin, Noordin, and Kadivar (2014) where the increasing of the mucilage amount increased the viscosity. From the results, the viscosity of the xanthan gum solution decreased with the increasing shear rate until it plateaued, where continuous increasing of the shear rate did not affect the viscosity of the solution indicating the shear thinning behavior of the xanthan gum solution (Chejara, Kondaveeti, Prasad, and Siddhanta, 2013). Figure 4-3 confirms the shear thinning behavior of the xanthan gum solution where the results deviated from the Newtonian behavior showed by pure DI water. The shear thinning behavior is due to the alignment of the highly anisotropic chains, resulting in the decreasing viscosity of a solution. This non-Newtonian behavior was more visible in higher concentrations of xanthan gum (400 and 500 ppm). From Figure 4-2, the decreasing viscosity with the

increasing shear rate of higher concentration of xanthan gum solution achieved equilibrium plateau slower than in the case of lower concentration of xanthan gum solution.

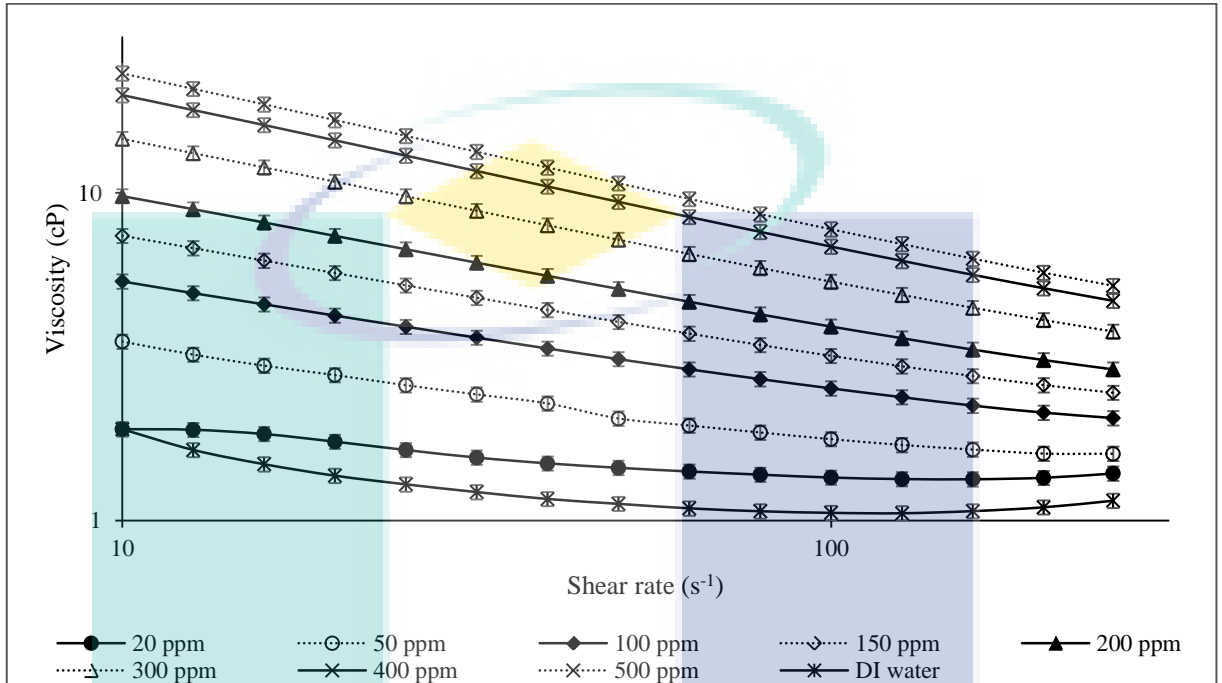


Figure 4-2 Viscosity of various xanthan gum concentrations as a function of shear rate with DI water as control

It was believed the minute amount of the polymeric additives affected the laminar flow through two conjugated mechanisms which are “viscous theory” and “elastic theory”. It was expected that in this case “viscous theory” which was proposed by Lumley (Lumley, 1969, 1973) was more dominant where the introduction of the additives increased the effective viscosity thus increasing the viscous sublayer thickness and resulting in reduced wall skin friction.

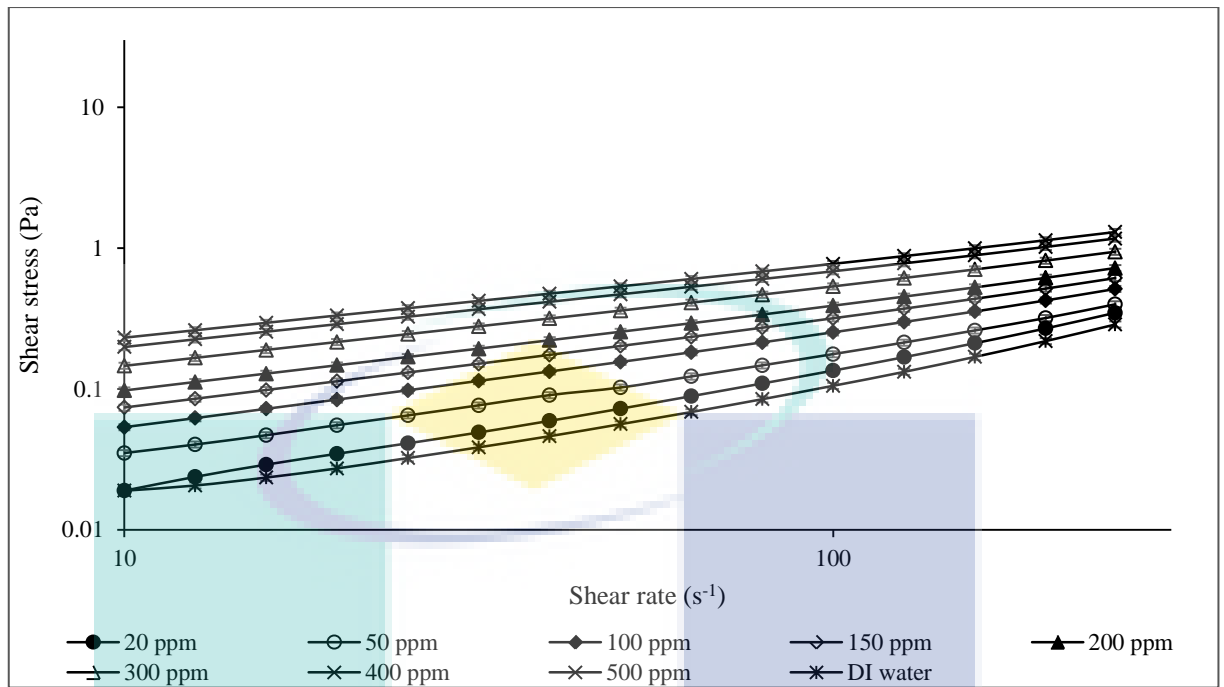
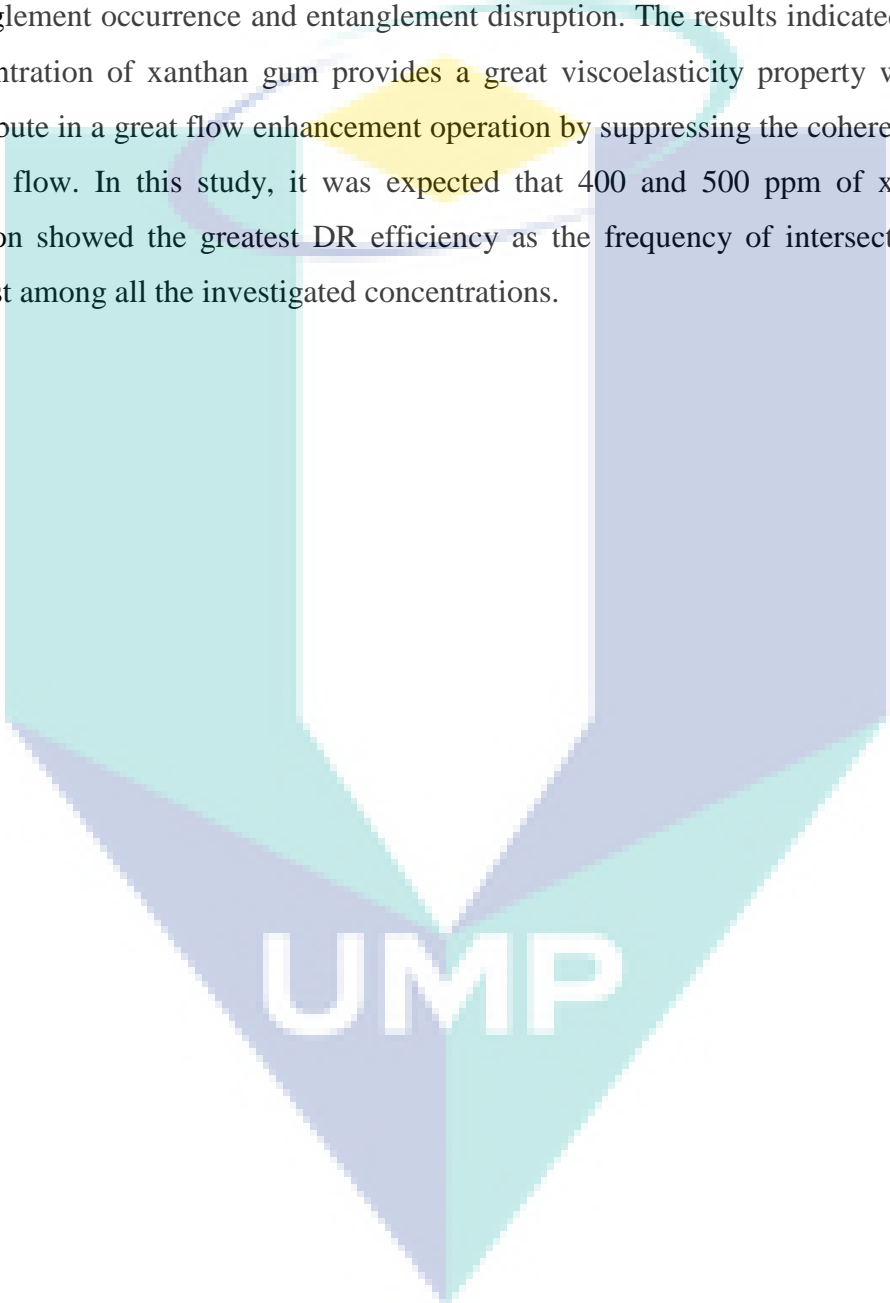


Figure 4-3 Shear stress of various xanthan gum concentrations as a function of shear rate with DI water as control

The elastic and viscous characteristics of a fluid can be determined by subjecting the solution to an oscillatory stress ( $\sigma$ ) and determining the response accordingly. The storage (elastic) modulus,  $G'$ , indicates that the fluid stores the stress energy applied (frequency sweep in this case) as the stress increases, but recovers when the stress energy is removed. Meanwhile, the loss (viscous) modulus,  $G''$ , explains that the stress applied on the fluid is completely lost as heat and the deformation is not recovered after the force is removed.

Figure 4-4 illustrates the viscoelasticity of various concentrations of xanthan gum solution measured at a frequency of 1 to 100 Hz. It can be seen that all the xanthan gum solutions show viscoelasticity properties where the  $G'$  curves crossed with the  $G''$  curves.  $G''$  dominated at lower frequency for all the xanthan gum solutions described the viscous properties of the additives solutions. Crossing over between  $G'$  and  $G''$  started to occur when increasing the frequency. The storage modulus,  $G'$  was higher than the loss modulus demonstrated the elastic properties of the additives and the crossover between both  $G'$  and  $G''$  confirming that the additives have both viscous and elastic properties and believed to have “weak gel” structures (Goh et al., 2016). From Figure 4-4a to c, the crossing over occurred at the frequency of 50 Hz for the lower

concentration of xanthan gum solutions (20 – 100 ppm). Increasing the xanthan gum concentration to 150 ppm and above, the crossing over started at lower frequency which is around 12 Hz. As seen in Figure 4-4d to i, the crossing over of  $G'$  and  $G''$  curves was more frequent when the concentration of the xanthan gum was increased from 100 to 500 ppm where at this point it is believed that the time was insufficient for entanglement occurrence and entanglement disruption. The results indicated that a high concentration of xanthan gum provides a great viscoelasticity property which would contribute in a great flow enhancement operation by suppressing the coherent structures in the flow. In this study, it was expected that 400 and 500 ppm of xanthan gum solution showed the greatest DR efficiency as the frequency of intersection was the highest among all the investigated concentrations.

The logo for UMP (Universitas Muhammadiyah Purwokerto) is a large, downward-pointing arrow shape. It is composed of four triangular sections meeting at a central point. The top-left and bottom-right sections are light blue, while the top-right and bottom-left sections are a slightly darker shade of blue. The letters 'UMMP' are printed in white, bold, sans-serif font across the center of the arrow.

UMMP

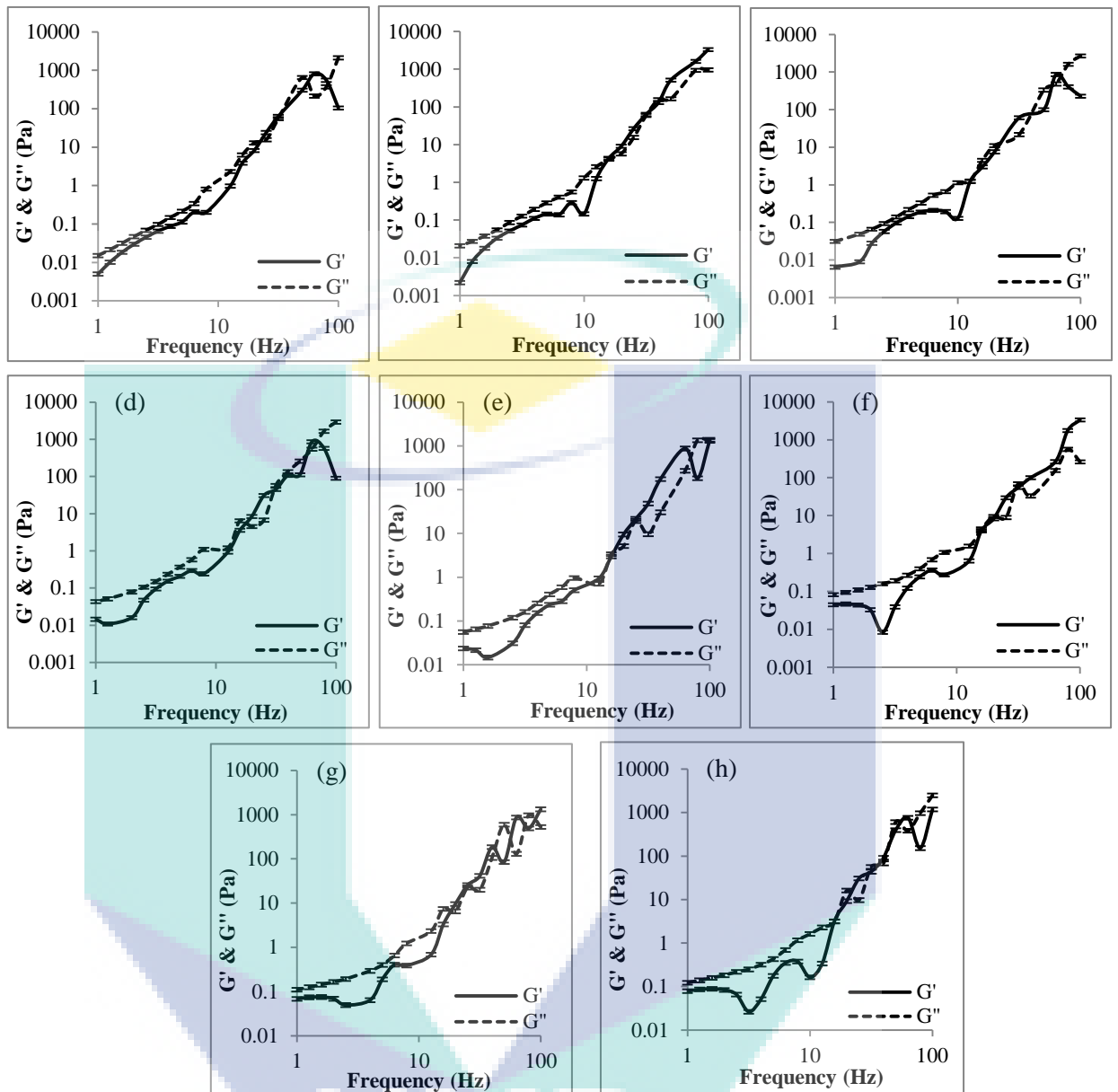


Figure 4-4  $G'$  and  $G''$  curves of xanthan gum solutions at the concentration of (a) 20 ppm, (b) 50 ppm, (c) 100 ppm, (d) 150 ppm, (e) 200 ppm, (f) 300 ppm, (g) 400 ppm, and (h) 500 ppm as a function of sweep frequency

## 4.2 Experimental Flow Enhancement Results

### 4.2.1 Effect of Mucilage Concentration

Figure 4-5 to Figure 4-11 demonstrated the effect of Xanthan gum concentration on %FI varying the operating pressure in micro-channels. The results had highlighted that all the examined solutions did show DR effect in most of the concentrations and flow rates investigated. It is obvious that by increasing the concentration of the DRA,

the %FI significantly increased which indicated that DR happened. By increasing the additives concentration, the polymeric molecules involved in DR operation also increased. Thus, there is more elements available to suppress the turbulence hence reduce the frictional forces across the channels result in increasing of the DR efficiency (Marhefka, 2007; Japper-Jaafar et al., 2009; Bari et al., 2010). It is expected that continuous increasing of the additives concentration will have positive effect on flow enhancement until it reaches its optimum concentration. Beyond this point, continuous increasing of the concentration is expected do not contribute to flow enhancement. For the case of the present work, turbulent flow is not possible in microfluidics devices or micro-channels, and that led to the flow behavior shown in Figure 4-5 to Figure 4-11 for all the solutions investigated. The maximum %FI of 34.90% was achieved by 500 ppm of Xanthan gum at 100 mbar in micro-channel having the width of 500  $\mu\text{m}$ . The minimum value of %FI was observed when the concentration is 20 ppm at 50 mbar which is 4.07% in micro-channel having the length of 50 mm. Turbulent DR experiments usually conducted using pipelines as the increasing of the additives concentrations will lead to an increment in the flow enhancement performance within certain ranges due to the interactive friction flow in the pipe. In the present work, the situation is different with pipeline where no turbulent flow occurs and the effect of the additive concentration in not linear.

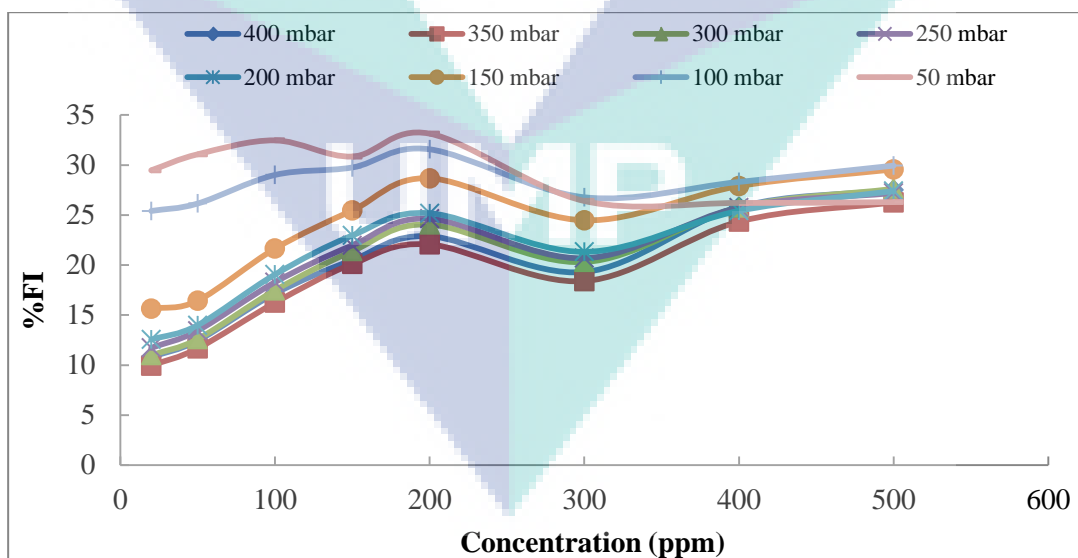


Figure 4-5 %FI of various Xanthan gum concentrations varying the operating pressure in micro-channel having the tail length of 70 mm.

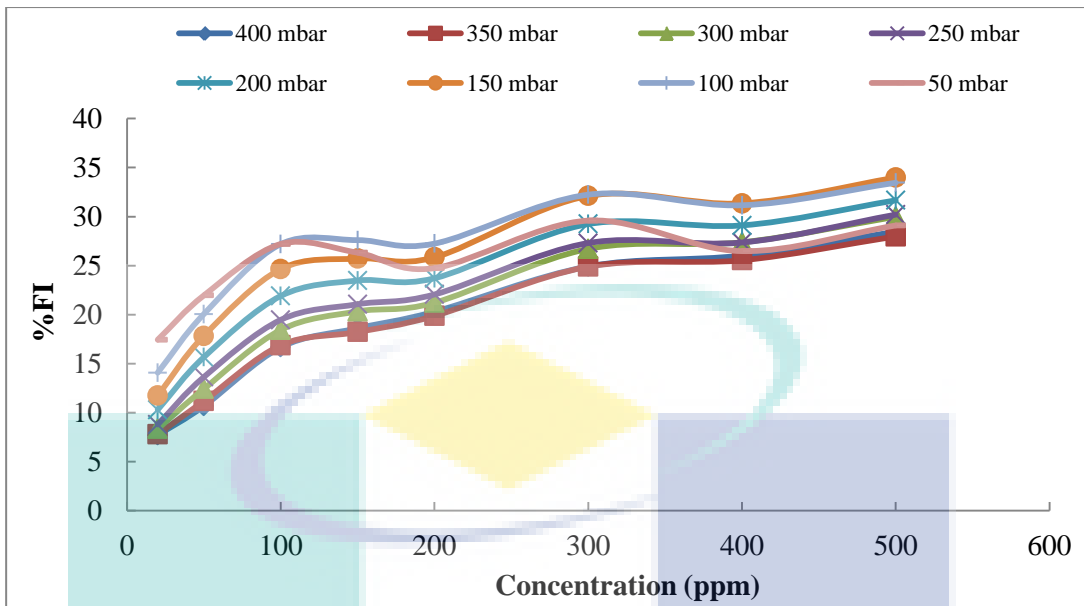


Figure 4-6 %FI of various Xanthan gum concentrations varying the operating pressure in micro-channel having the tail length of 60 mm.

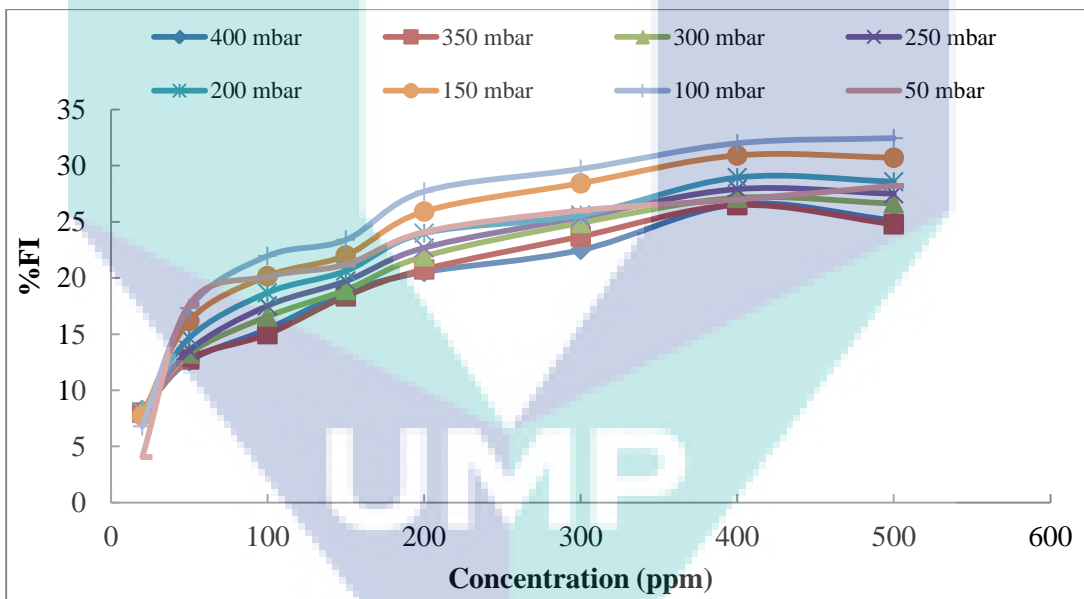


Figure 4-7 %FI of various Xanthan gum concentrations varying the operating pressure in micro-channel having the tail length of 50 mm.

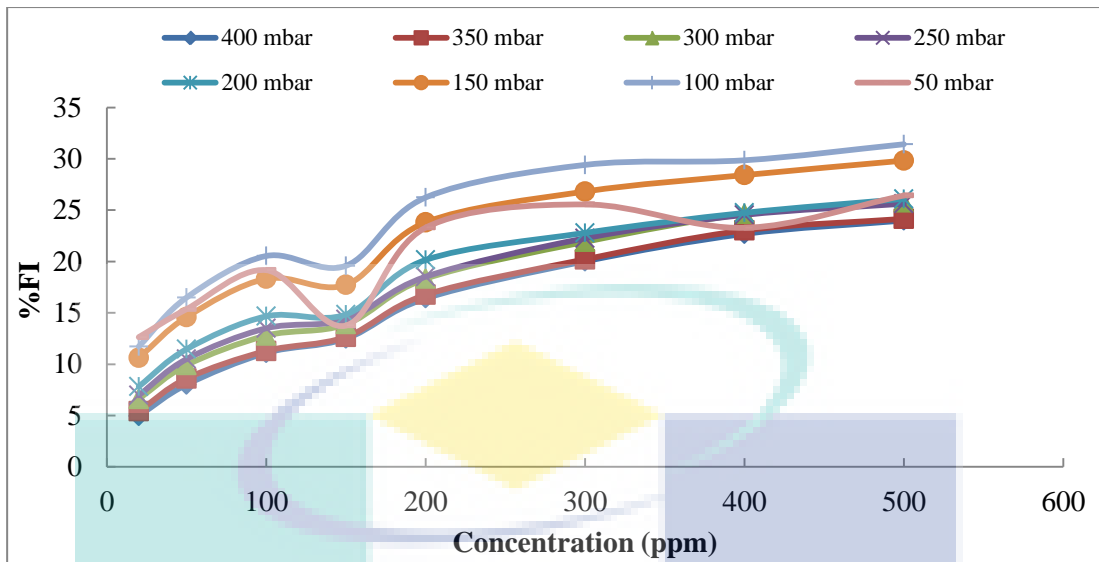


Figure 4-8 %FI of various Xanthan gum concentrations varying the operating pressure in micro-channel having the tail length of 40 mm.

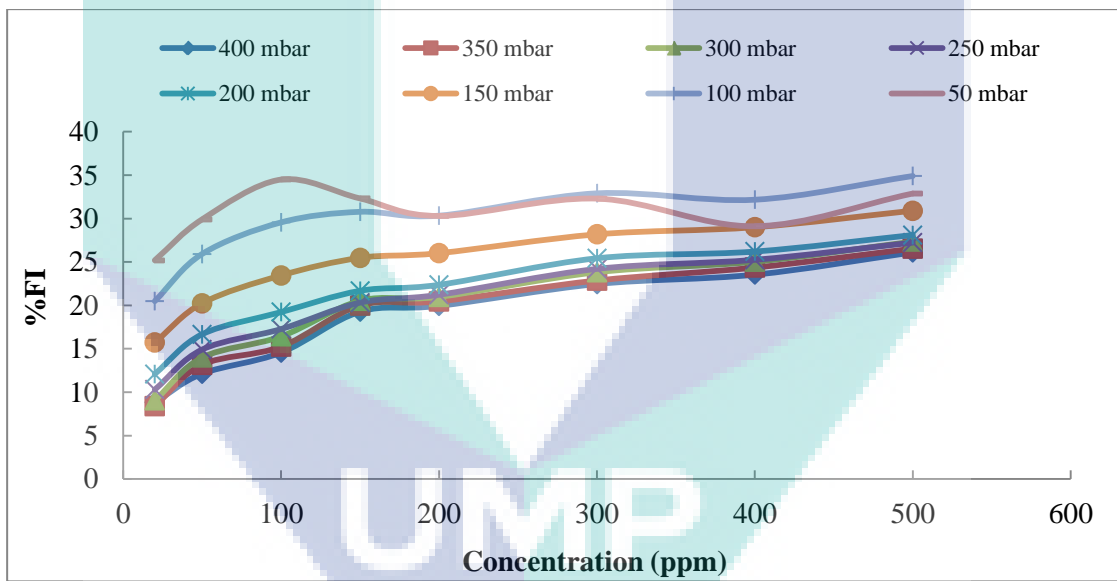


Figure 4-9 %FI of various Xanthan gum concentrations varying the operating pressure in micro-channel having the width of 500 μm.

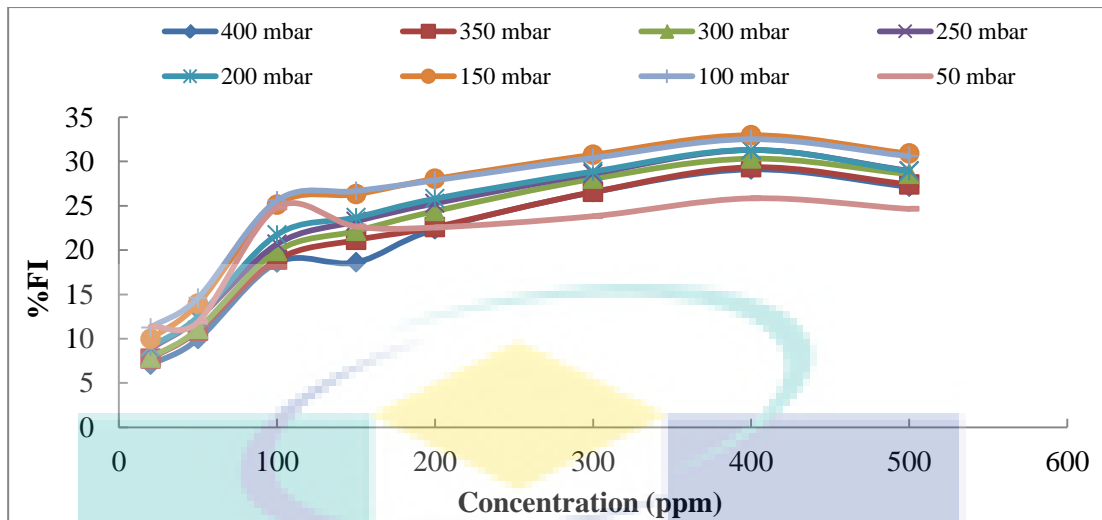


Figure 4-10 %FI of various Xanthan gum concentrations varying the operating pressure in micro-channel having the width of 300  $\mu\text{m}$ .

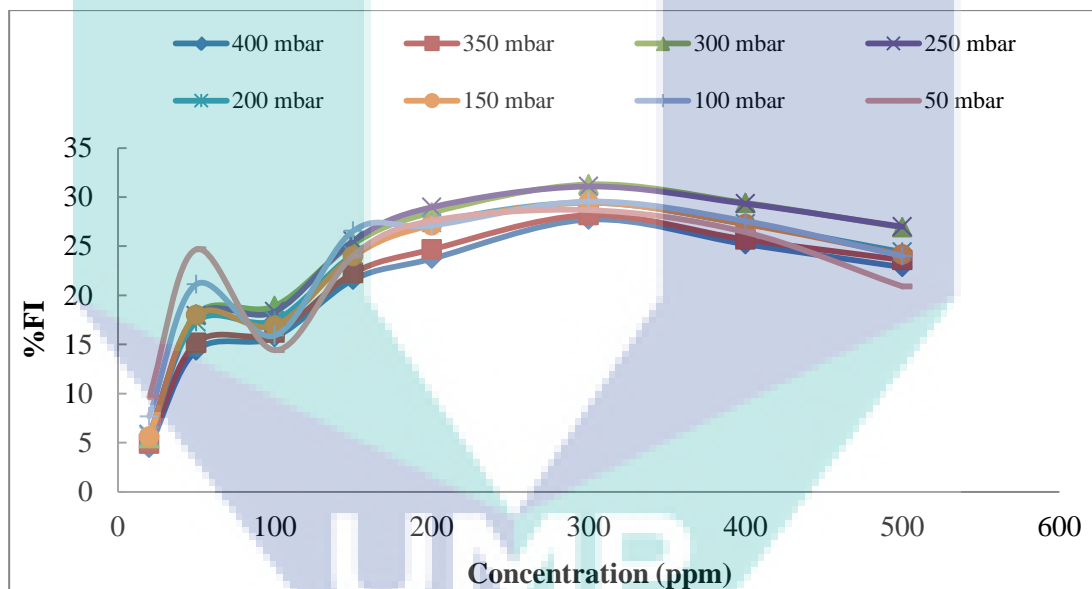


Figure 4-11 %FI of various Xanthan gum concentrations varying the operating pressure in micro-channel having the width of 200  $\mu\text{m}$ .

#### 4.2.2 Effect of Length in Micro-channels

Figure 4-13 to Figure 4-19 showed the %FI as a function of the tail length of the micro-channel by varying the operating pressure. The effect of the tail length is a representation of the relation between the friction force and shear force in the flow against the stability of the polymer. Surprisingly, the %FI is quite stable across the increasing of the channel length at lower Xanthan gum concentration as illustrated in

Figure 4-13 to Figure 4-16. Averagely, the trend of the %FI in these cases increases with the increases of the channel length. In longer channel length, it is expected that the fluid flow experienced higher friction forces hence providing greater platform for the additives to perform resulting in the higher %FI. However, at higher concentration of the Xanthan gum the different behaviour was observed. The %FI increases when increasing the channel but at a certain point ( $\approx 60$  mm) the %FI decreases significantly as shown from Figure 4-17 to Figure 4-19. The trend indicated that at higher concentration of the additives did not have positive effect in enhancing the flow in longer channel. This may due to the complex interaction of other variables (operating pressure, concentration and properties of Xanthan gum, rheological properties of the fluid etc.) with the fluid flow behaviour causing the different trend at higher additives concentration. In these cases, greater friction force is expected to be experienced by the concentrated liquid flow thus the turbulence media might increases. The %FI decreased in longer micro-channel length as the effect of shear degradation start to appear. The effects of the stability of the polymer against the shear force in the flow resulting in a loss of additive's efficiency (Abdul Bari et al., 2011).

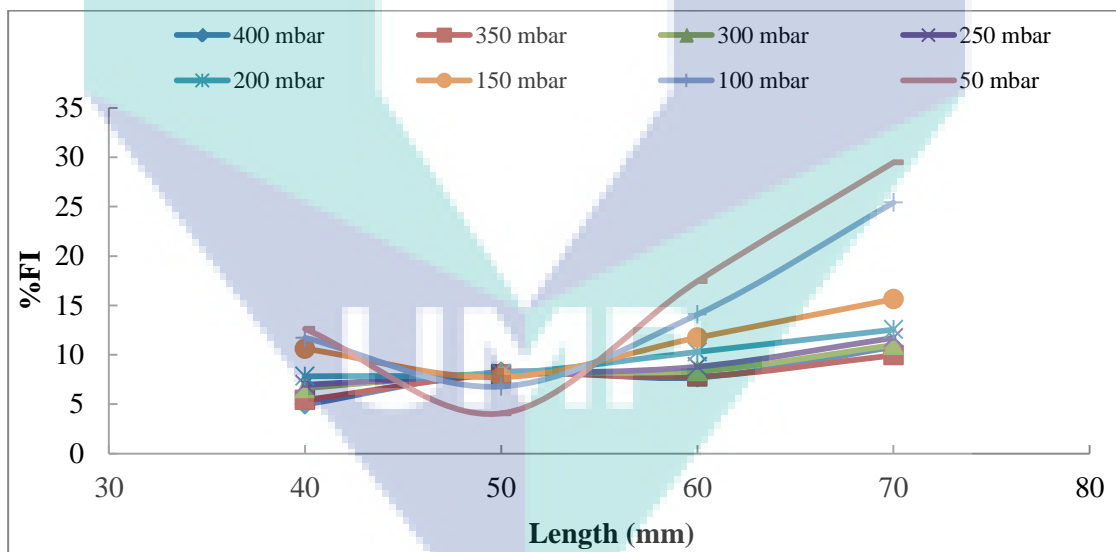


Figure 4-12 %FI of Xanthan gum in various tail length of micro-channel by varying the operating pressure having the concentration of 20 ppm.

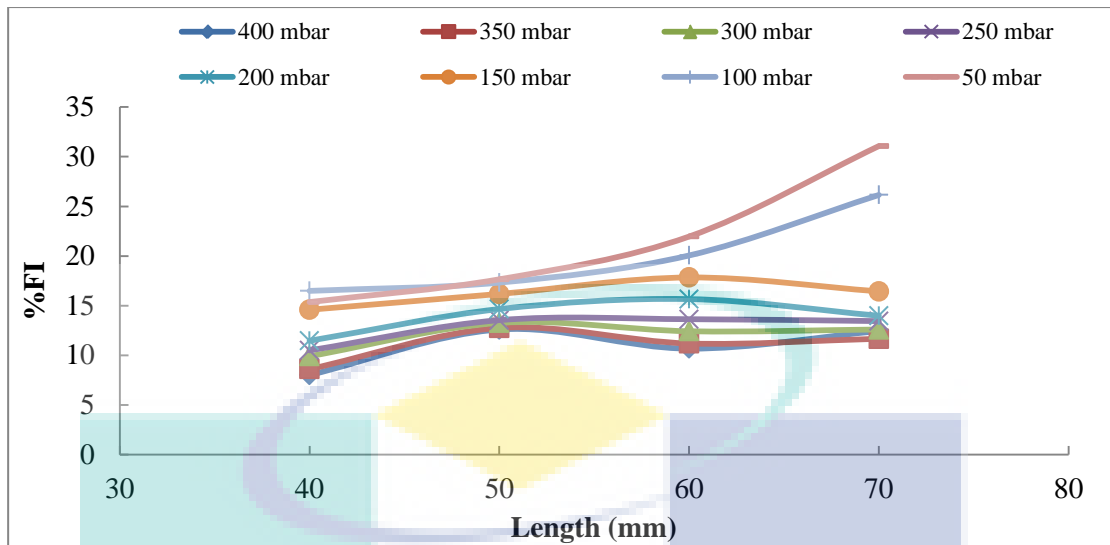


Figure 4-13 %FI of Xanthan gum in various tail length of micro-channel by varying the operating pressure having the concentration of 50 ppm.

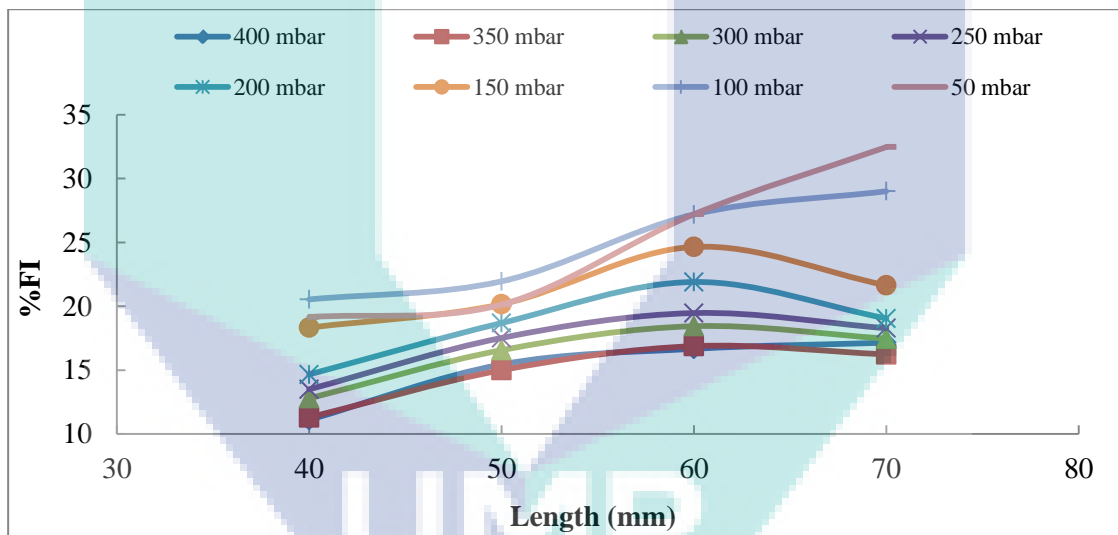


Figure 4-14 %FI of Xanthan gum in various tail length of micro-channel by varying the operating pressure having the concentration of 100 ppm.

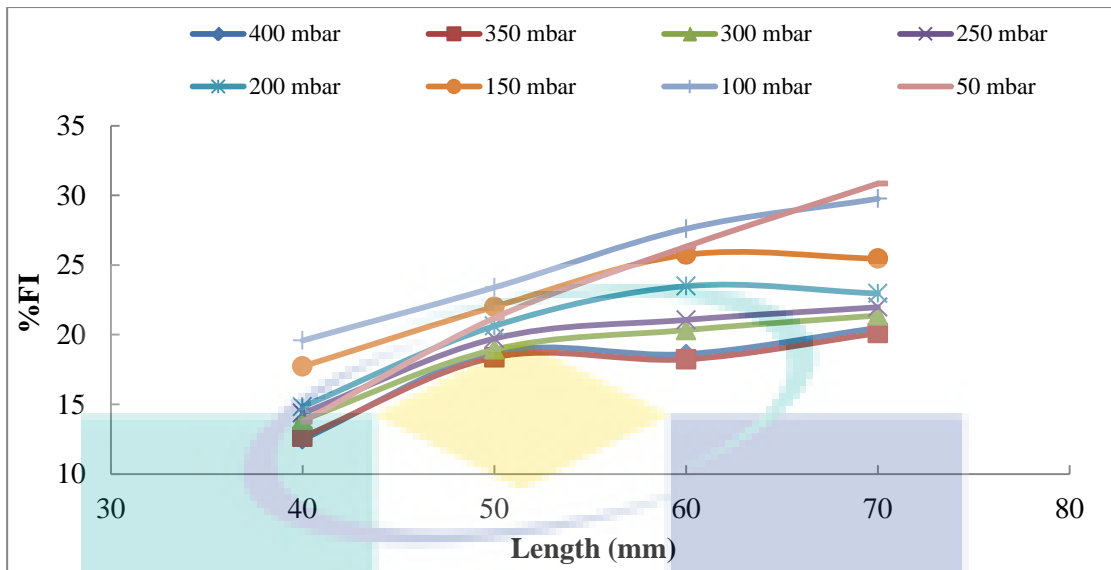


Figure 4-15 %FI of Xanthan gum in various tail length of micro-channel by varying the operating pressure having the concentration of 150 ppm.

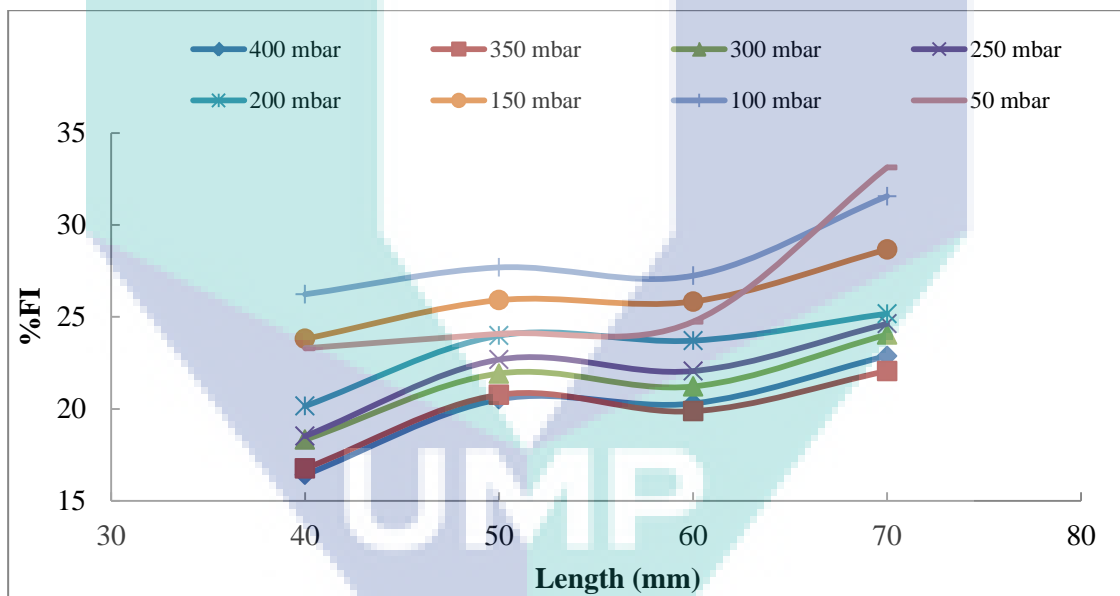


Figure 4-16 %FI of Xanthan gum in various tail length of micro-channel by varying the operating pressure having the concentration of 200 ppm.

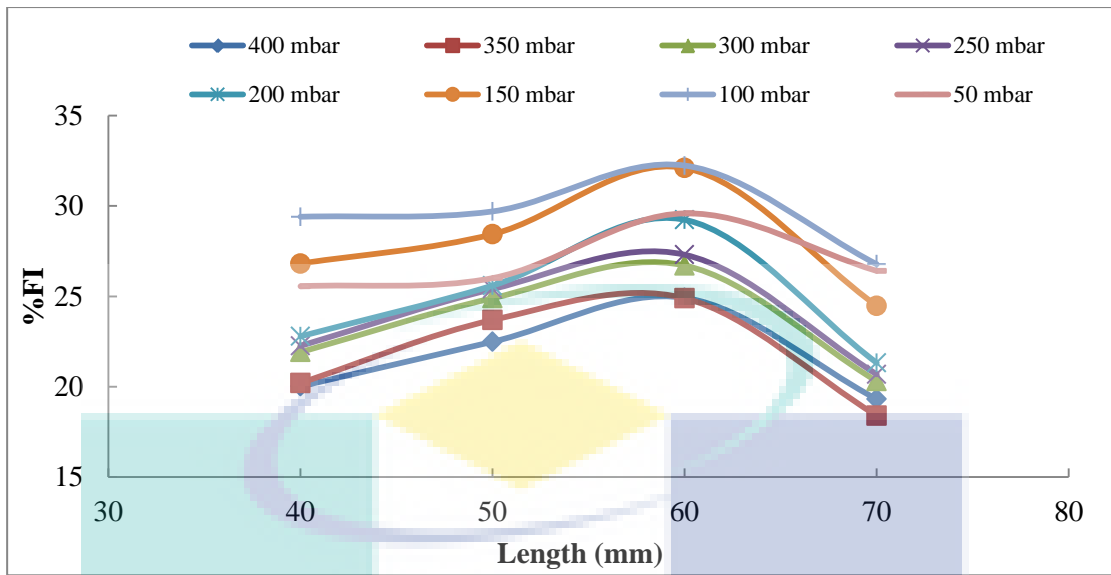


Figure 4-17 %FI of Xanthan gum in various tail length of micro-channel by varying the operating pressure having the concentration of 300 ppm.

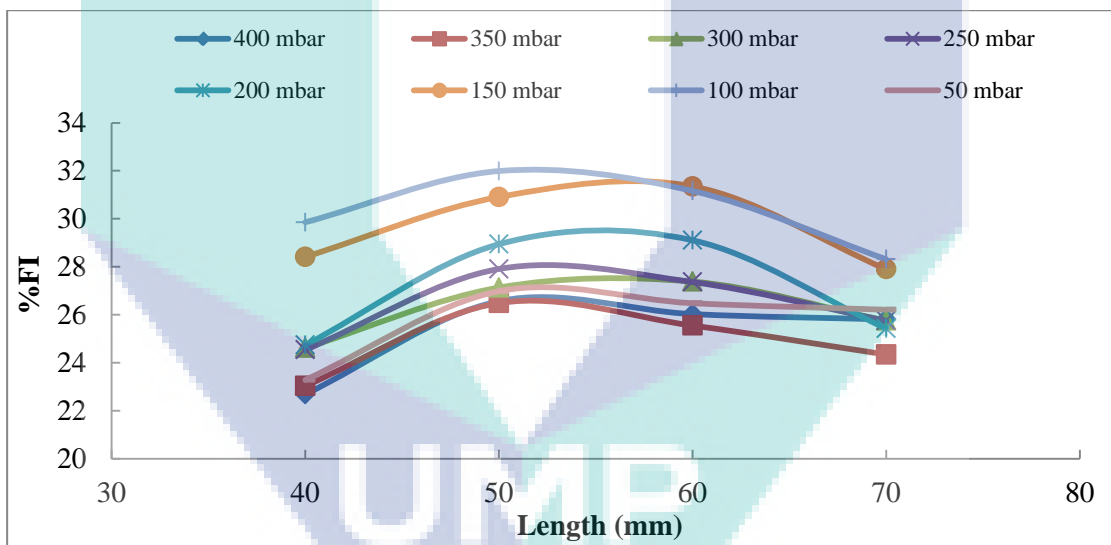


Figure 4-18 %FI of Xanthan gum in various tail length of micro-channel by varying the operating pressure having the concentration of 400 ppm.

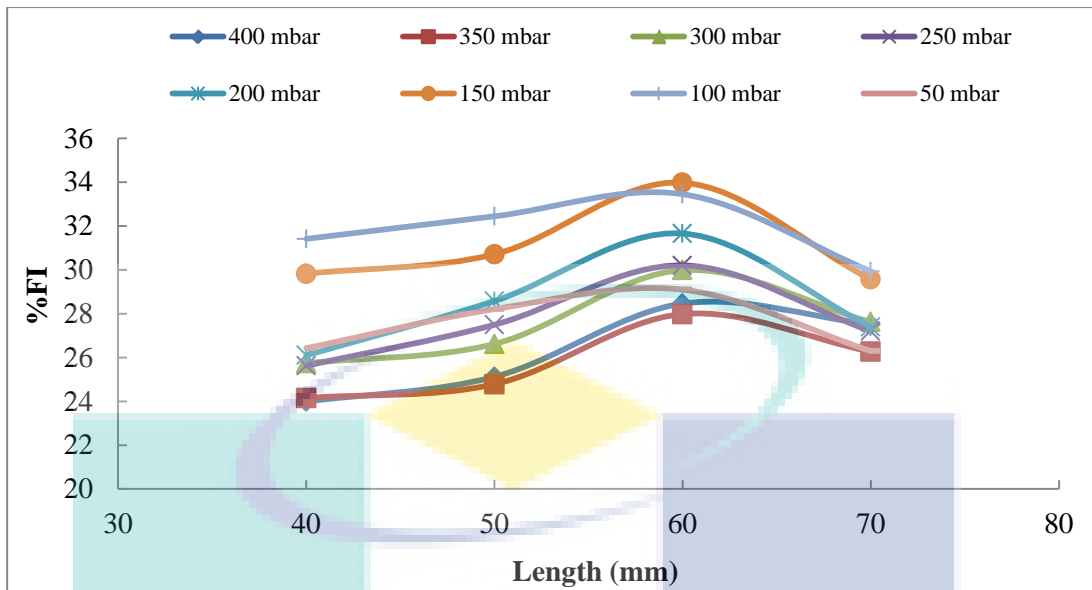


Figure 4-19 %FI of Xanthan gum in various tail length of micro-channel by varying the operating pressure having the concentration of 500 ppm.

#### 4.2.3 Effect of Width in Micro-channels

As demonstrated in Figure 4-20 to Figure 4-27, %FI fluctuated across the increasing of the channel width. However, higher %FI was mostly achieved at smaller width of micro-channel. Smaller channel width resulting in higher fluid velocity inside the micro-channel thus increases the turbulence intensity and eddies are more likely to be produced (Khadom & Abdul-Hadi, 2014). Although laminar flow is reported to present in the micro-channel, transitional even turbulence flow may occur due to the high velocity in the channel. Therefore, higher %FI was observed in smaller channel width where this condition leads to the possibility of eddies creation thus provide bigger platform for the DRA to perform (Al-Sarkhi & Hanratty, 2001). The study showed that DR increased with decreasing the width of channel and by increasing the polymer concentration as shown in Figure 4-20 to Figure 4-27. The highest %FI(34.90%) was achieved at width 500  $\mu\text{m}$  with 500 ppm of Xanthan gum which is a clear clue about the commercial feasibility of the proposed DRA.

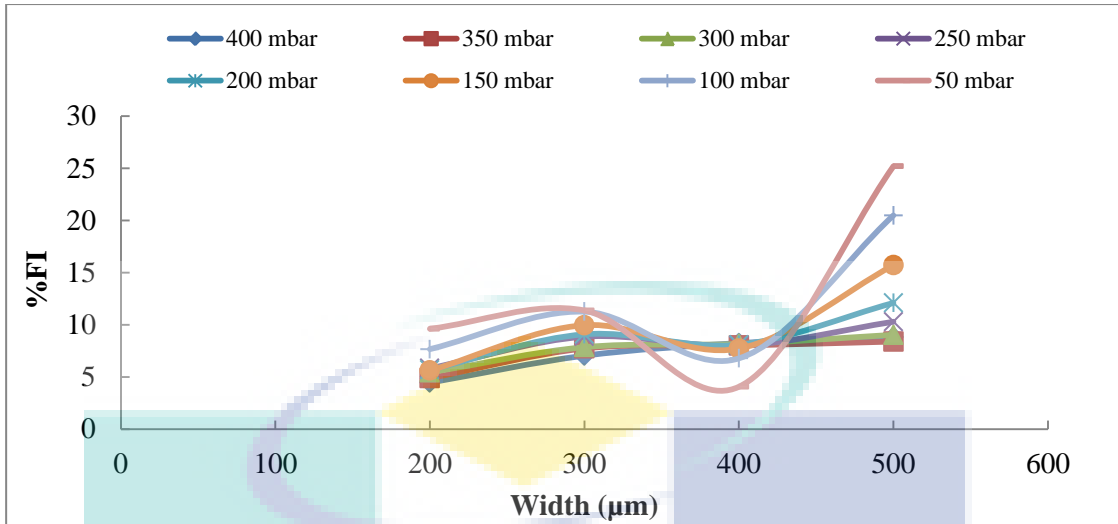


Figure 4-20 %FI of Xanthan gum in various width of micro-channel by varying the operating pressure having the concentration of 20 ppm.

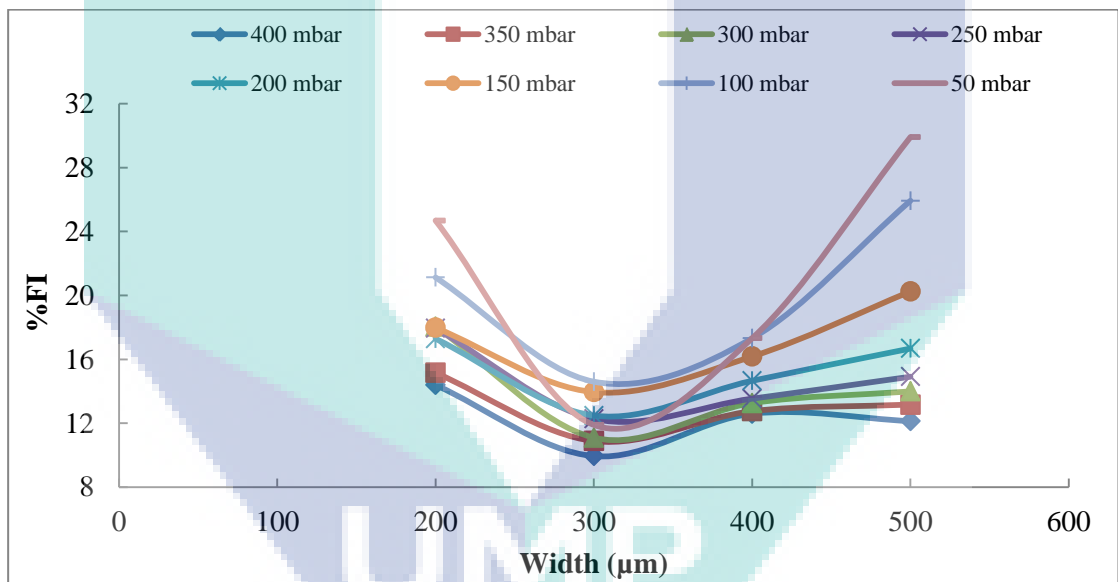


Figure 4-21 %FI of Xanthan gum in various width of micro-channel by varying the operating pressure having the concentration of 50 ppm.

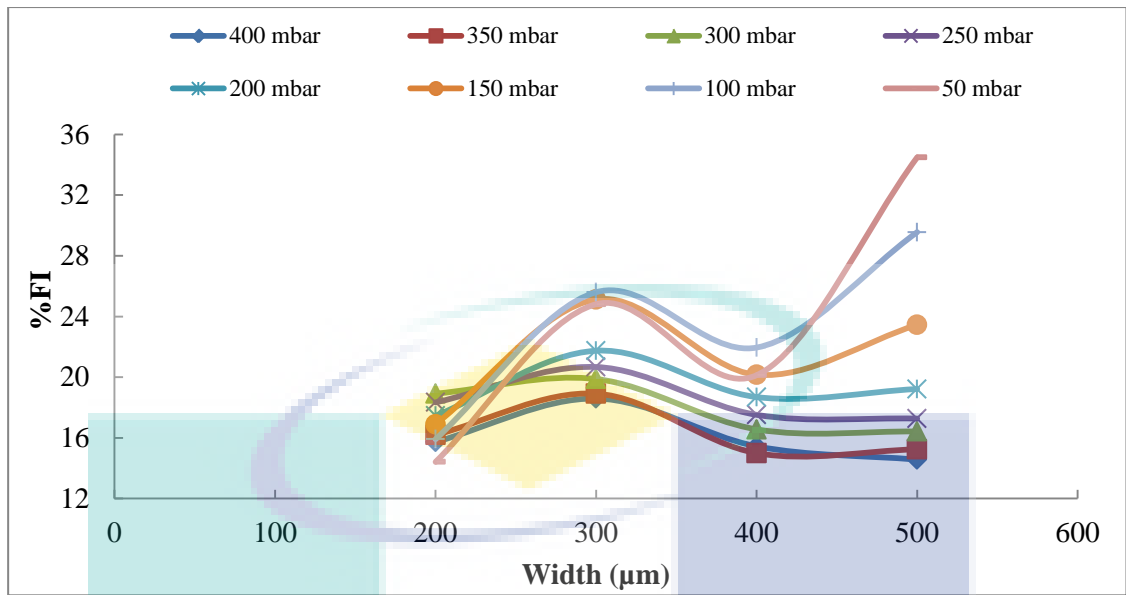


Figure 4-22 %FI of Xanthan gum in various width of micro-channel by varying the operating pressure having the concentration of 100 ppm.

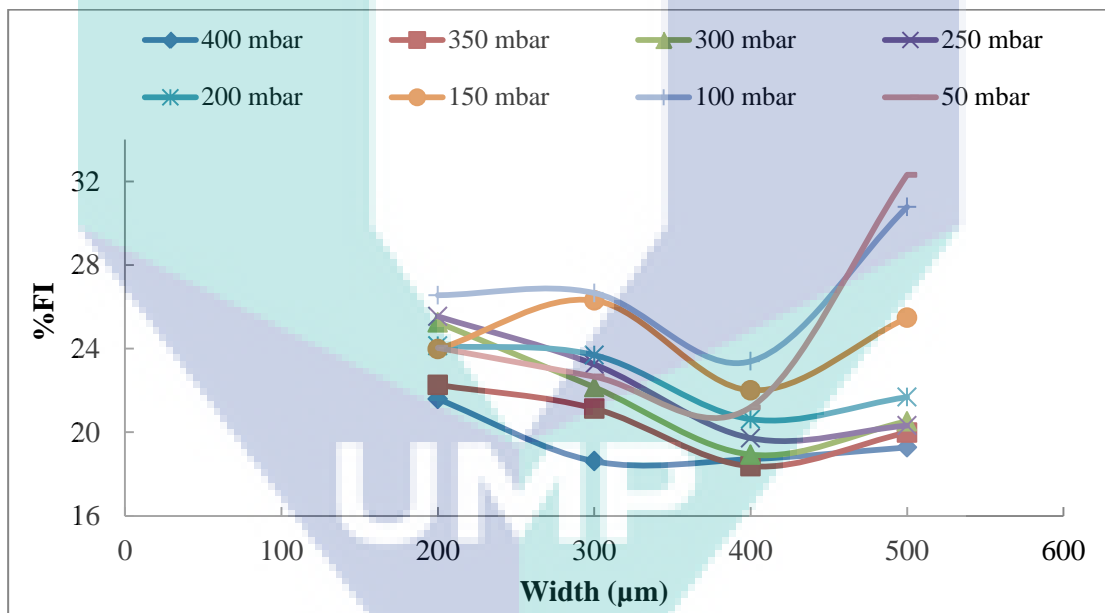


Figure 4-23 %FI of Xanthan gum in various width of micro-channel by varying the operating pressure having the concentration of 150 ppm.

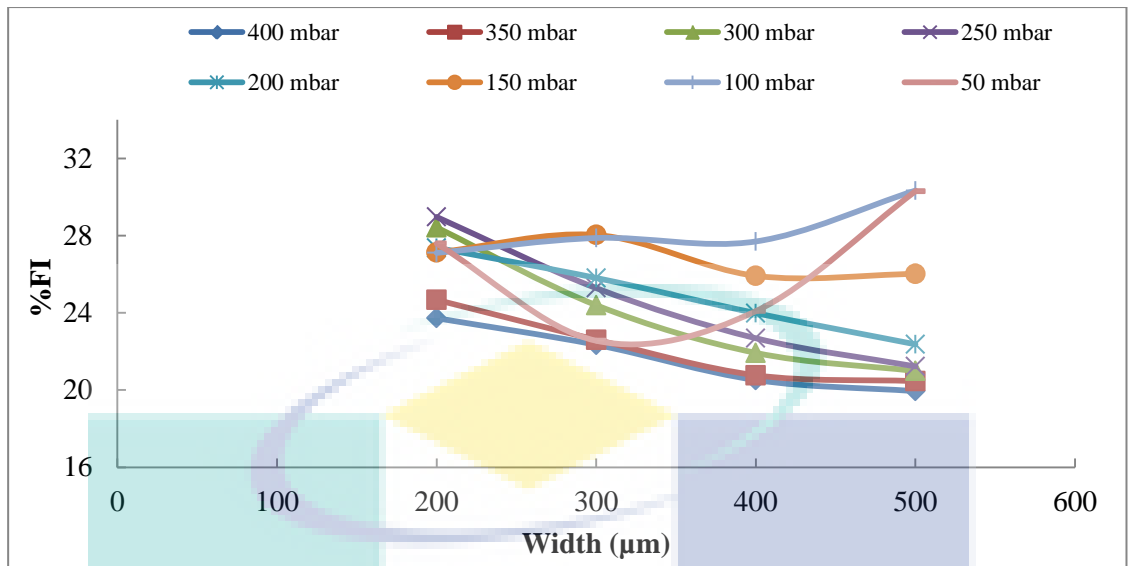


Figure 4-24 %FI of Xanthan gum in various width of micro-channel by varying the operating pressure having the concentration of 200 ppm.

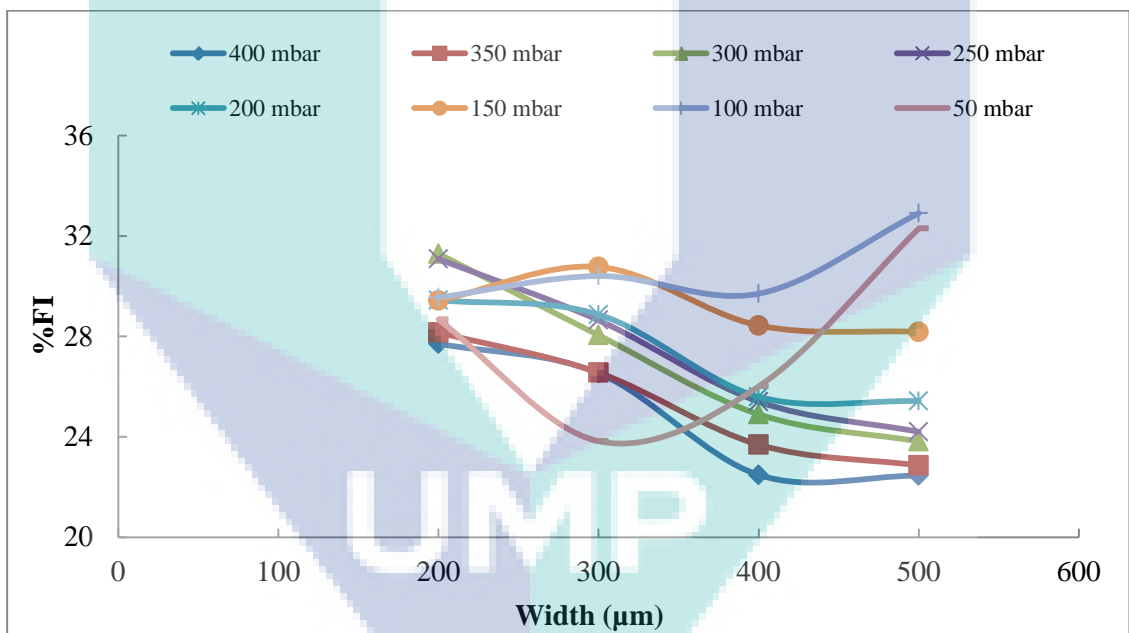


Figure 4-25 %FI of Xanthan gum in various width of micro-channel by varying the operating pressure having the concentration of 300 ppm.

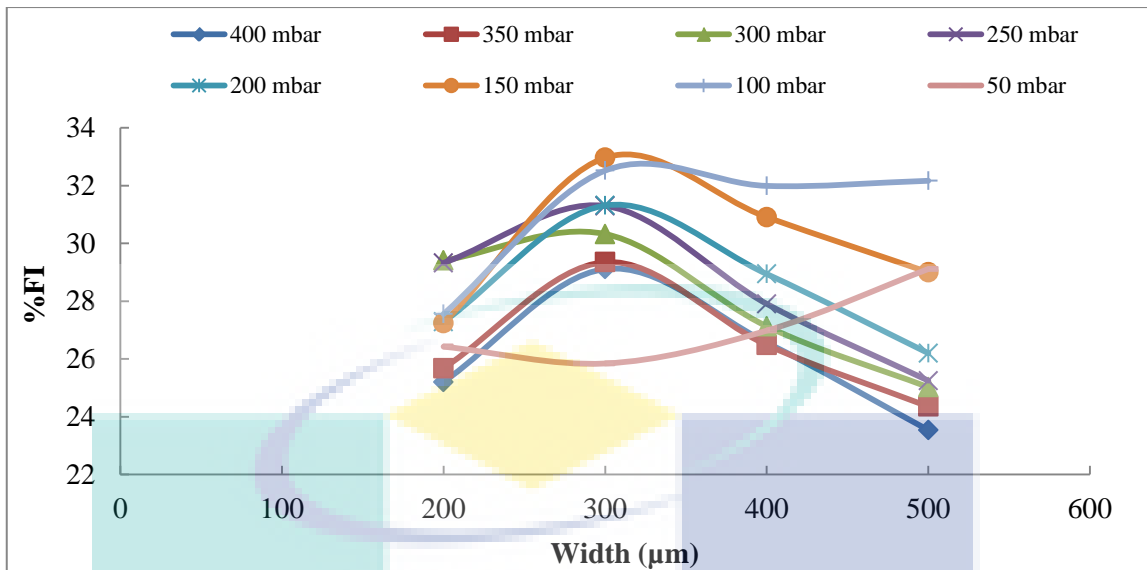


Figure 4-26 %FI of Xanthan gum in various width of micro-channel by varying the operating pressure having the concentration of 400 ppm.

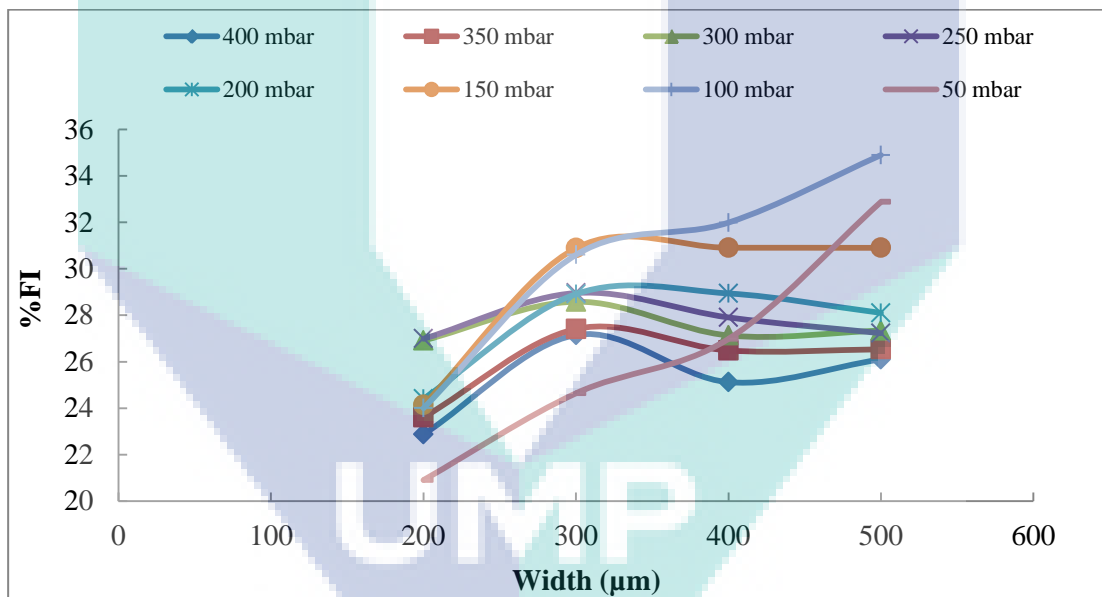


Figure 4-27 %FI of Xanthan gum in various width of micro-channel by varying the operating pressure having the concentration of 500 ppm.

#### 4.2.4 Summary

From the result above, the maximum % FI are summarized in Table 4-1. From the table, Xanthan gum achieved the maximum %FI in micro-channel having the width with 500 µm, which is 34.90% at the concentration of 500 ppm.

Table 4-1 The maximum %FI achieved by DRA.

No.	Micro-channel	Concentration (ppm)	Operating pressure (mbar)	Max. % FI (%)
1	70 mm	200	50	33.14
2	60 mm	500	100	33.98
3	40 mm	500	100	32.45
4	40 mm	500	100	31.42
5	500 $\mu\text{m}$	500	100	34.90
6	300 $\mu\text{m}$	400	150	32.97
7	200 $\mu\text{m}$	300	300	31.92

#### 4.2.5 Flow Enhancement for Passive Micromixer

Pressure ranging from 200 mbar to 900 mbar were applied on each micromixer as initial pressure to flow the fluid within the micromixer. The flow profile was being analyzed via the flow enhancement method. Through this method, the flowrate recorded by from each micromixer were being compared with the control micromixer (absence of riblets) to analyze the flow behavior.

Figure 4-28 illustrates the flow enhancement performance of the microchannels with different microriblets dimensions. At lower operating pressure, which is 200 mbar in this case, the %FI was in positive region indicating that the micro-structures embedded along the channel wall reduced the skin friction of the fluid flow thus increased the velocity within the system. From the results, the flow enhancement performance increased up to 98% from 14.5% to 28.73% when increasing the microriblets size from 20 to 60  $\mu\text{m}$ . However, increasing the microriblets size beyond 60  $\mu\text{m}$  showed negative effect on the flow enhancement performance where the %FI dropped slightly to 25.95% and 20.65% for the microriblets size of 80 and 100  $\mu\text{m}$ , respectively. A similar behavior was also seen in higher operating pressure (300 – 900 mbar). It is believed that the presence of micro-riblets in this case will create a stagnant liquid layer that replaces the solid surface in the case of smooth surface. The stagnant liquid layer depth trapped in the V-shaped valleys will depend on the dimensions of the grooves and its mobility will be effected as well with the surface tension– water mass relationship that get weaker when the groove is deeper. It is expected that, Increasing the space between the microriblets led to the formation of some secondary vortex that enter the gaps and increase the shear stress (Dean and Bhushan, 2010). Hence, the flow

enhancement performance was lower when utilized larger microriblets. The results also showed agreement with the literature where the optimum microriblets spacing was 30 – 70  $\mu\text{m}$  (Lee and Jang, 2005). In this present study, a maximum %FI of 28.73% was achieved from a microchannel with the 60  $\mu\text{m}$  microriblets at the operating pressure of 200 mbar.

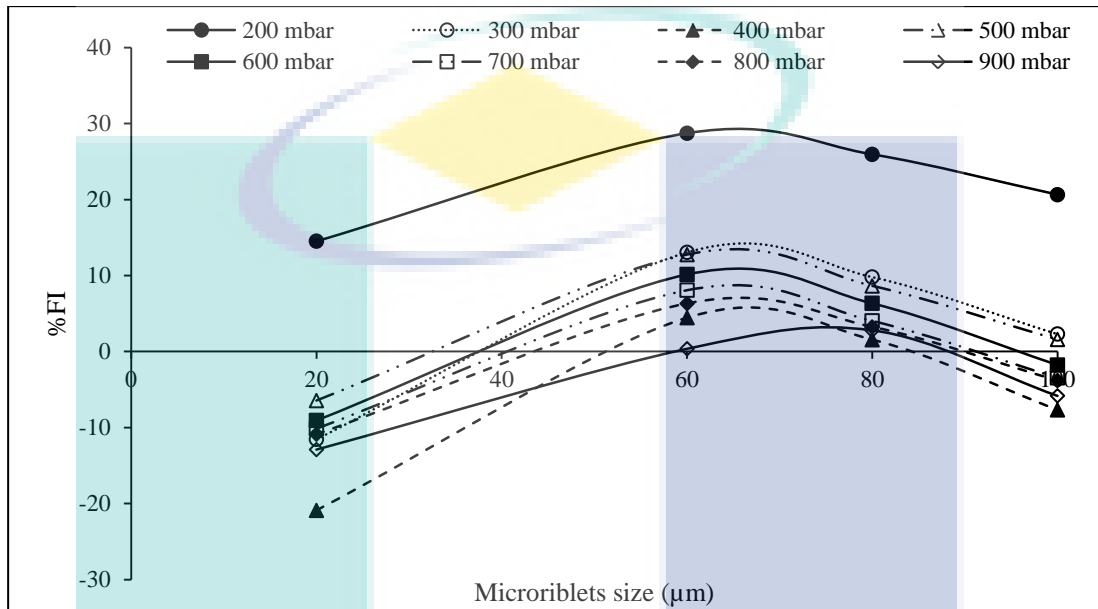


Figure 4-28 Flow enhancement of micromixer against pressure.

### 4.3 Result and Discussions for Micro-PIV

#### 4.3.1 The CCD Images

Y-shape micro-channel with 500 $\mu\text{m}$  as shown in Figure 4-29 is the most typical structure in the microfluidic chip. The measured region is divided into two sections because of the limited view scope of the microscope. The first section is located around the Y-shaped and the second section is located at the straight channel behind the Y-shaped where the CCD images are shown in Figure 4-30 and Figure 4-31. The trajectories of the tracer particles can be seen clearly in the figures. The velocities in the Y-shaped region and in the straight region are measured in the present work. The velocity field is obtained by calculating the displacement of particles and the time interval of the sequential exposures.

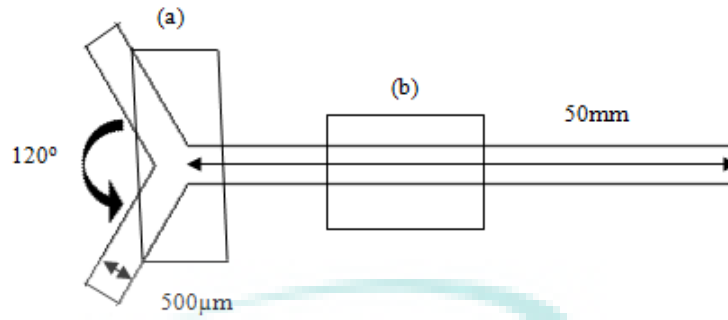


Figure 4-29 Schematic of the 500  $\mu\text{m}$  width micro-channel consist measured regions of (a) Y-shaped (b) straight channel

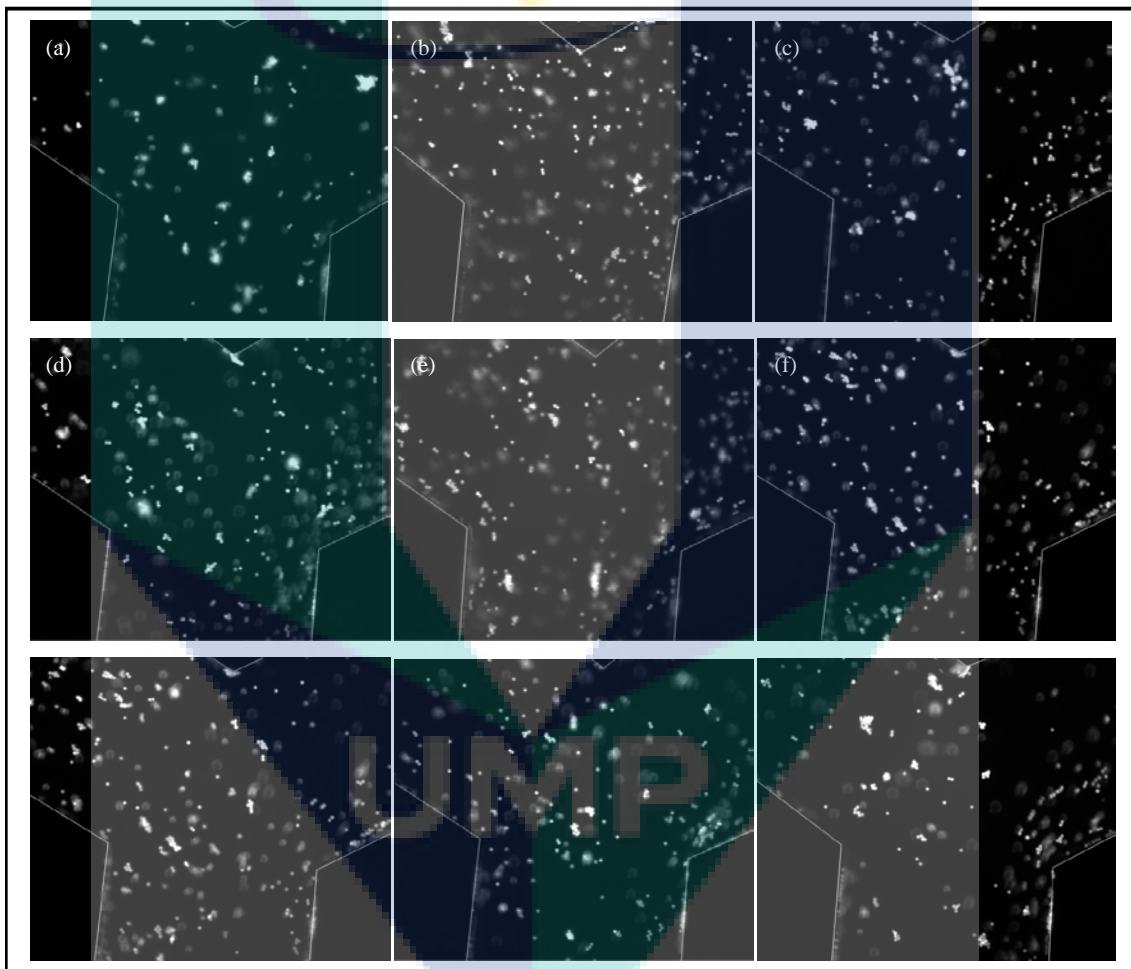


Figure 4-30 CCD images at the Y-shaped region having the (a) DI water and concentration of (b) 20 ppm (c) 50 ppm (d) 100 ppm (e) 150 ppm (f) 200 ppm (g) 300 ppm (h) 400 ppm, and (i) 500 ppm

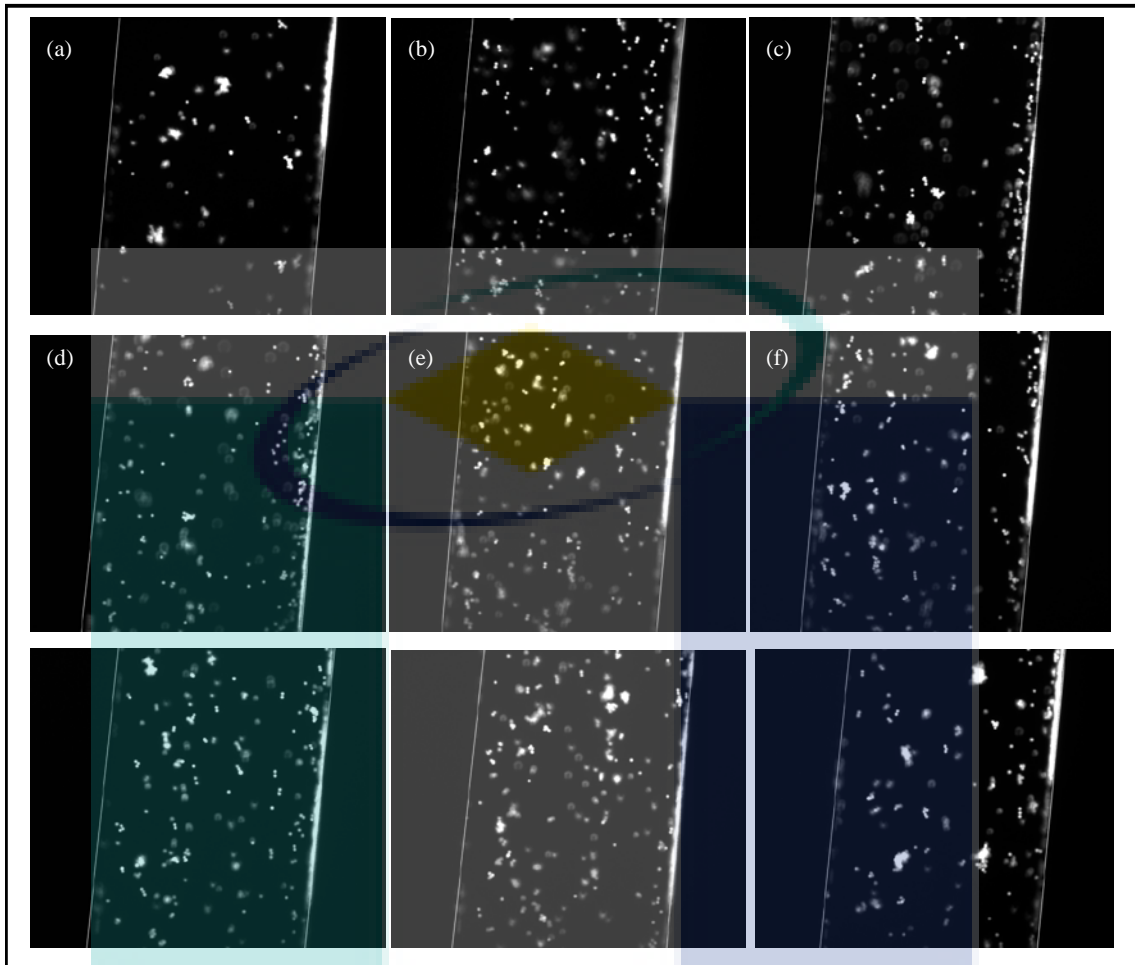
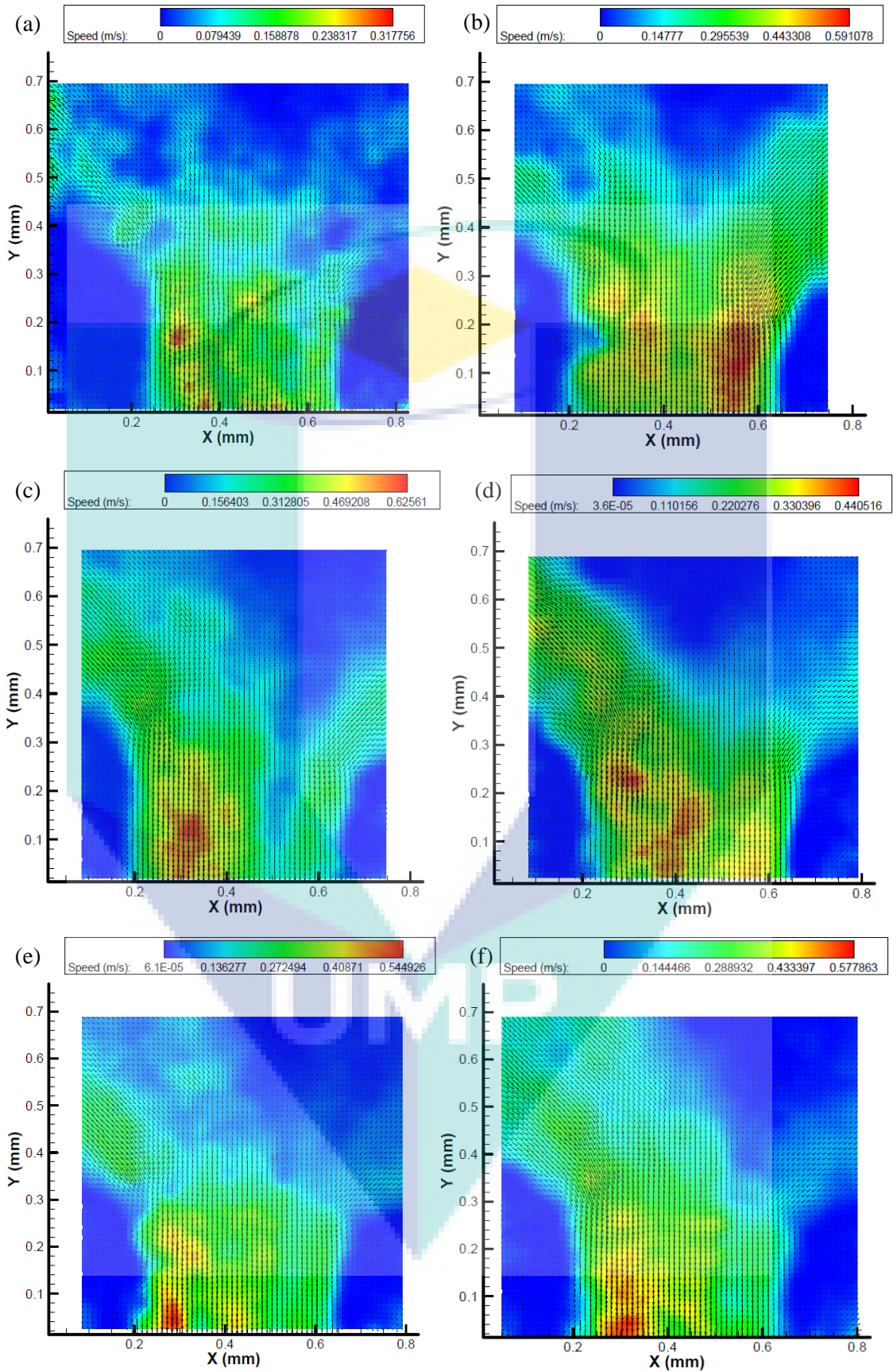


Figure 4-31 CCD images at the straight region having the (a) DI water and concentration of (b) 20 ppm (c) 50 ppm (d) 100 ppm (e) 150 ppm (f) 200 ppm (g) 300 ppm (h) 400 ppm, and (i) 500 ppm

### 4.3.2 Velocity Profiles for Active Micromixers

Based on the CCD images, the velocity vectors can be obtained by measuring the displacement of certain tracer particles in the interval time of the sequential CCD images. The velocity vectors around the Y-shaped and straight channel are shown in Figure 4-32 and Figure 4-33 respectively. The patterns of velocity vector in both regions are almost the same. Besides, both results are in good agreement with the maximum velocity increment being around 40%. In the regions close to the wall, all the values of velocity given by experiments are approximately between 0.07-0.17 m/s.



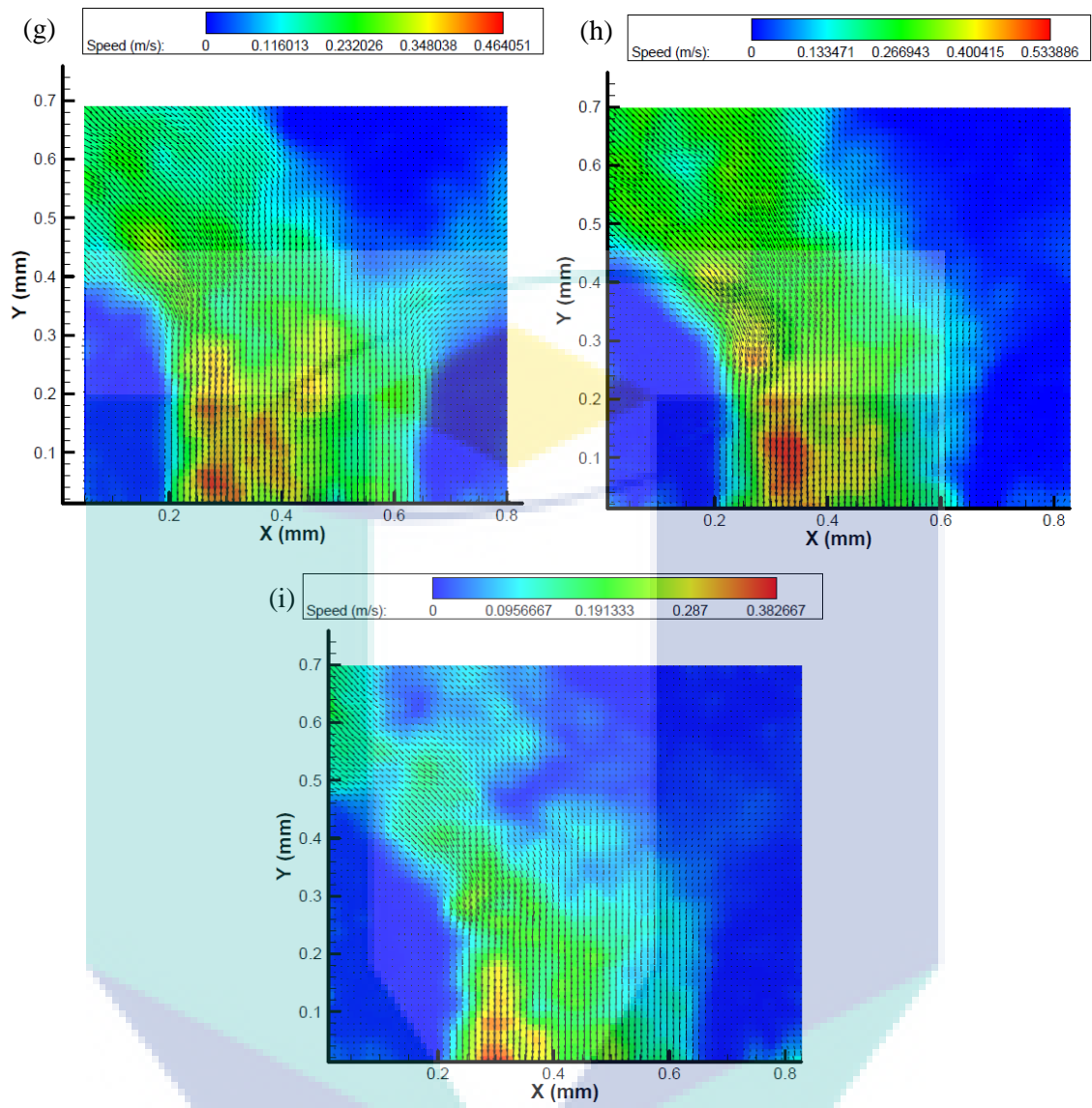
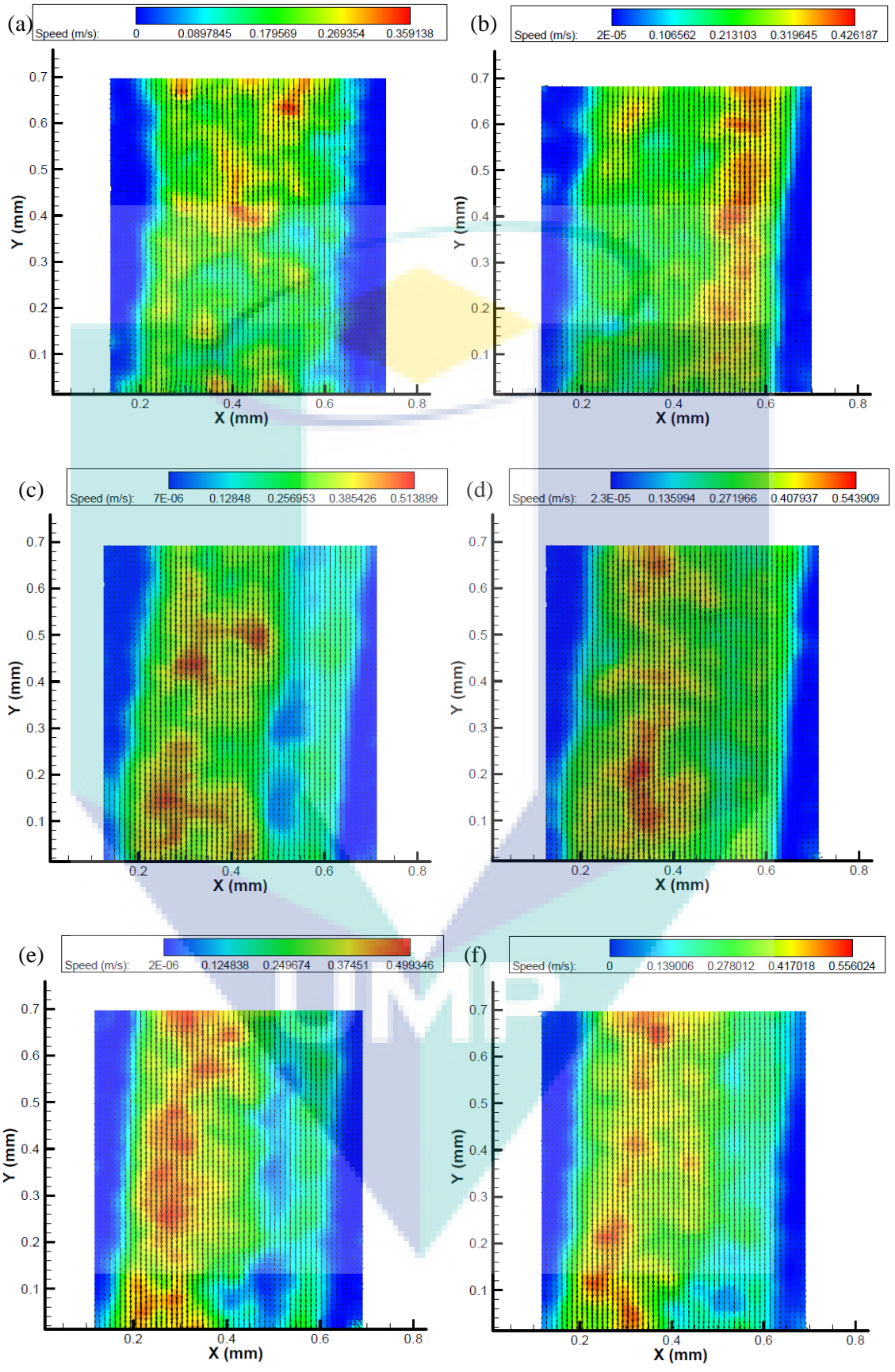


Figure 4-32 Velocity profiles at the Y-shaped region having the (a) DI water and concentration of (b) 20 ppm (c) 50 ppm (d) 100 ppm (e) 150 ppm (f) 200 ppm (g) 300 ppm (h) 400 ppm, and (i) 500 ppm



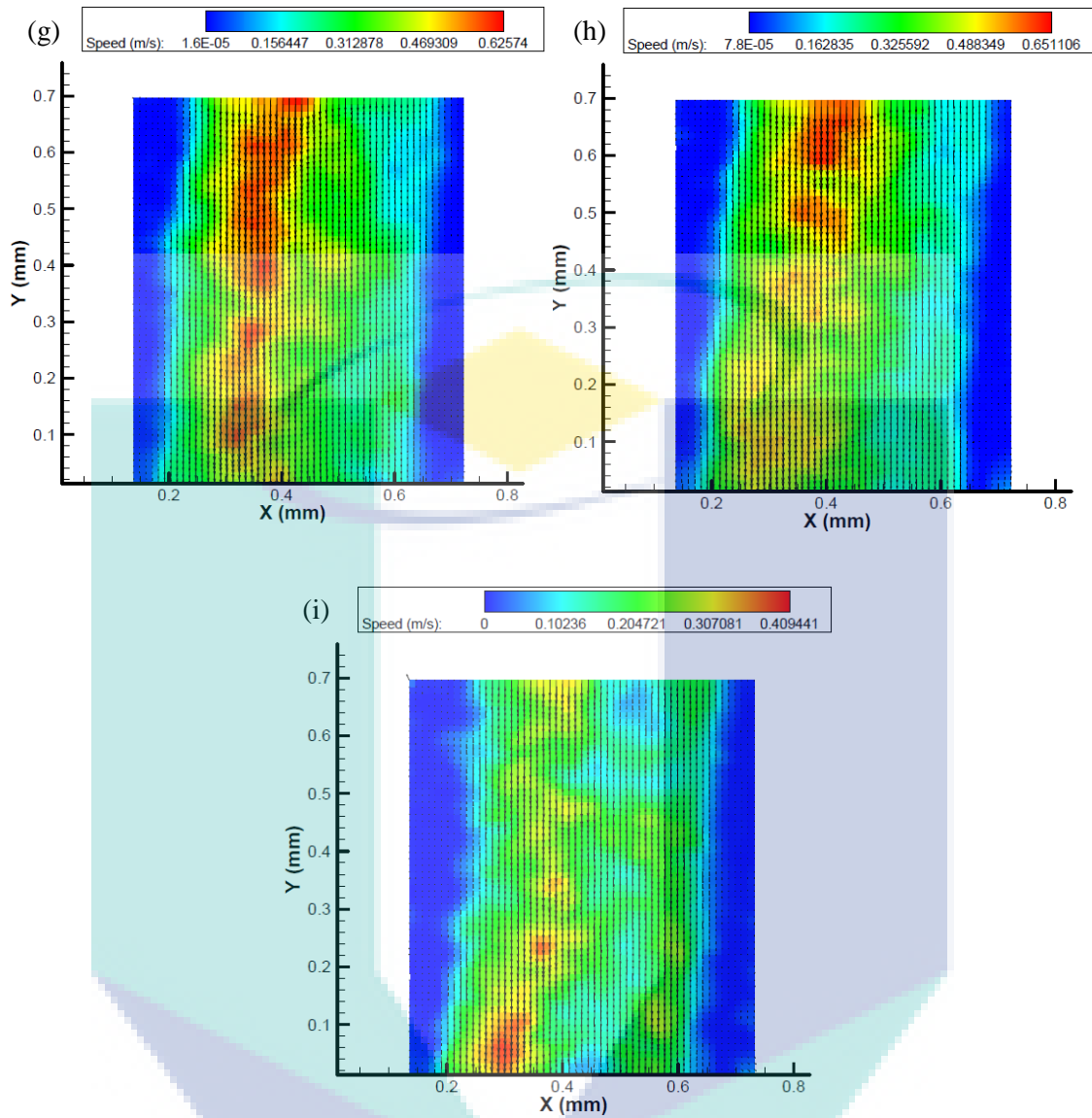


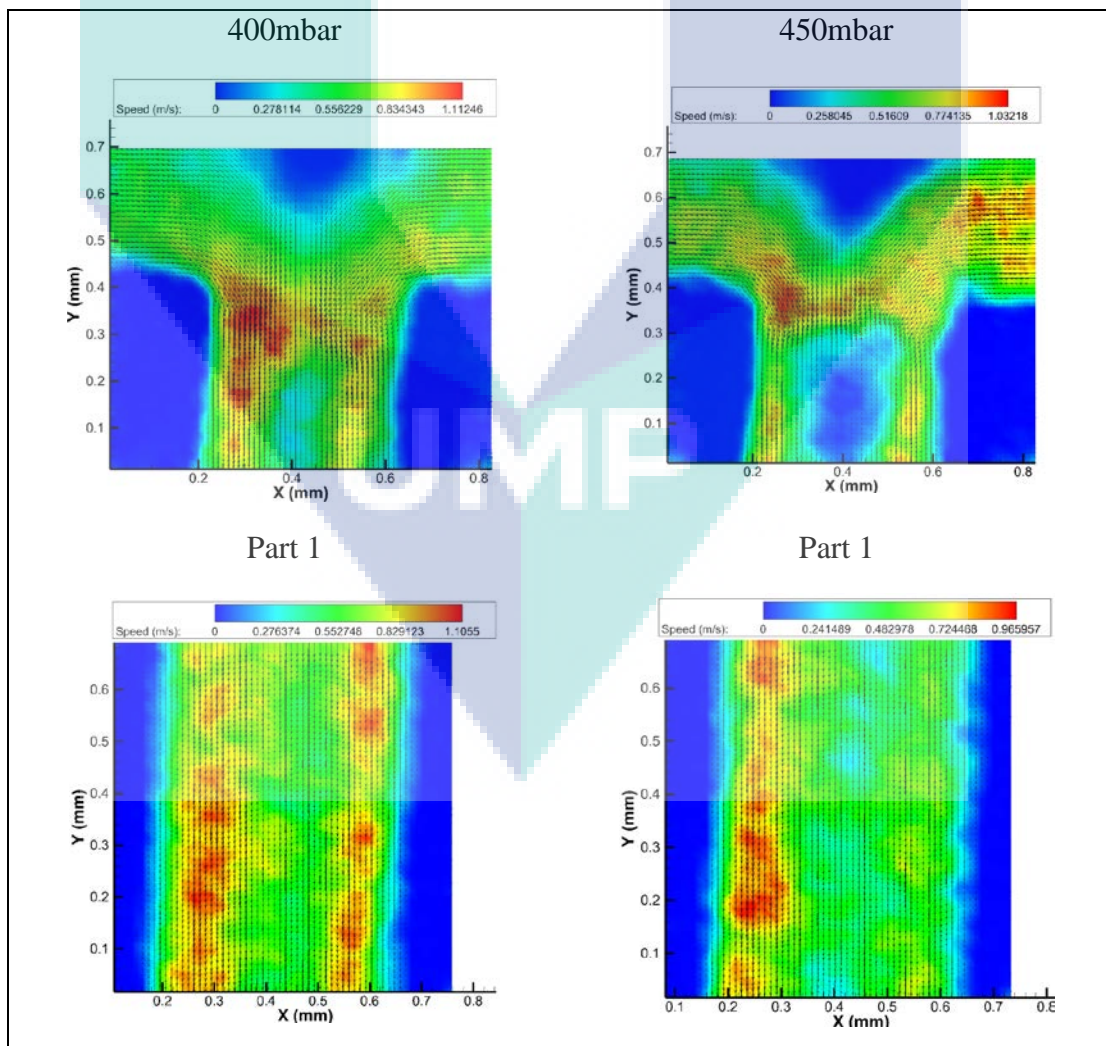
Figure 4-33 Velocity profiles at the straight channel region having the (a) DI water and concentration of (b) 20 ppm (c) 50 ppm (d) 100 ppm (e) 150 ppm (f) 200 ppm (g) 300 ppm (h) 400 ppm, and (i) 500 ppm

The original motivation of adding the DRA is to improve the flow enhancement performance. The experiment results of velocity vectors in the straight channel region are shown in Figure 4-33. Initially, the velocity recorded in the DI water was 0.36 m/s. It can be seen that the velocity profiles across the channel width varies along the velocity of flow. The large velocity gradient across the channel width appears in the region having the concentration of 400 ppm with the speed of 0.65 m/s, which is beneficial to the enhancement of the flow efficiency. The minimum value of velocity was obtained in the concentration of 500 ppm, which was 0.41 m/s. The additional of

the Xanthan gum as additives into the flow resulting in an increasing of the velocity flow where proven that the feasibility of Xanthan gum to be proposed as DRA. Theoretically speaking, the velocity increased significantly by increasing the concentration of the Xanthan gum which indicated that DR happened, and it reached the maximum velocity point at its optimum concentration.

Also, from the results, when the two streams of the liquid met at the intersection point, vortices were expected to occur which would increase the mixing performance. The formation of the vortices within the system was able to break the fluid streams into small eddies that increase the interfacial area which would reduce the diffusion distance between the molecules of the two streams. High velocity pockets were also observed at the active core of the fluid system. These formations of the high velocity regions were expected to induce the mixing performance within the micromixers.

### 4.3.3 Velocity Profiles for Passive Micromixers



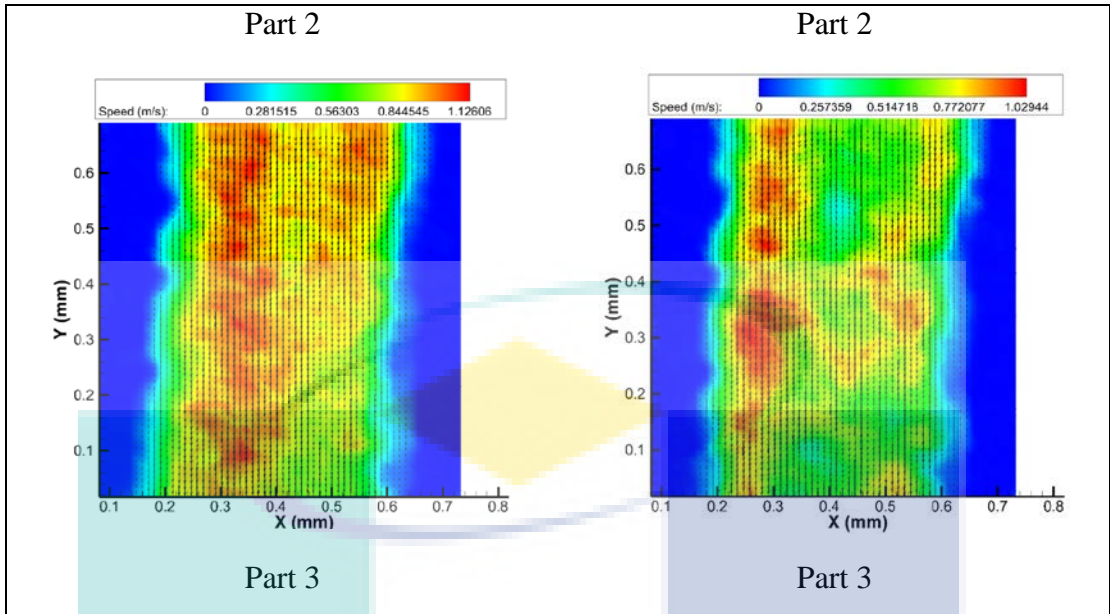
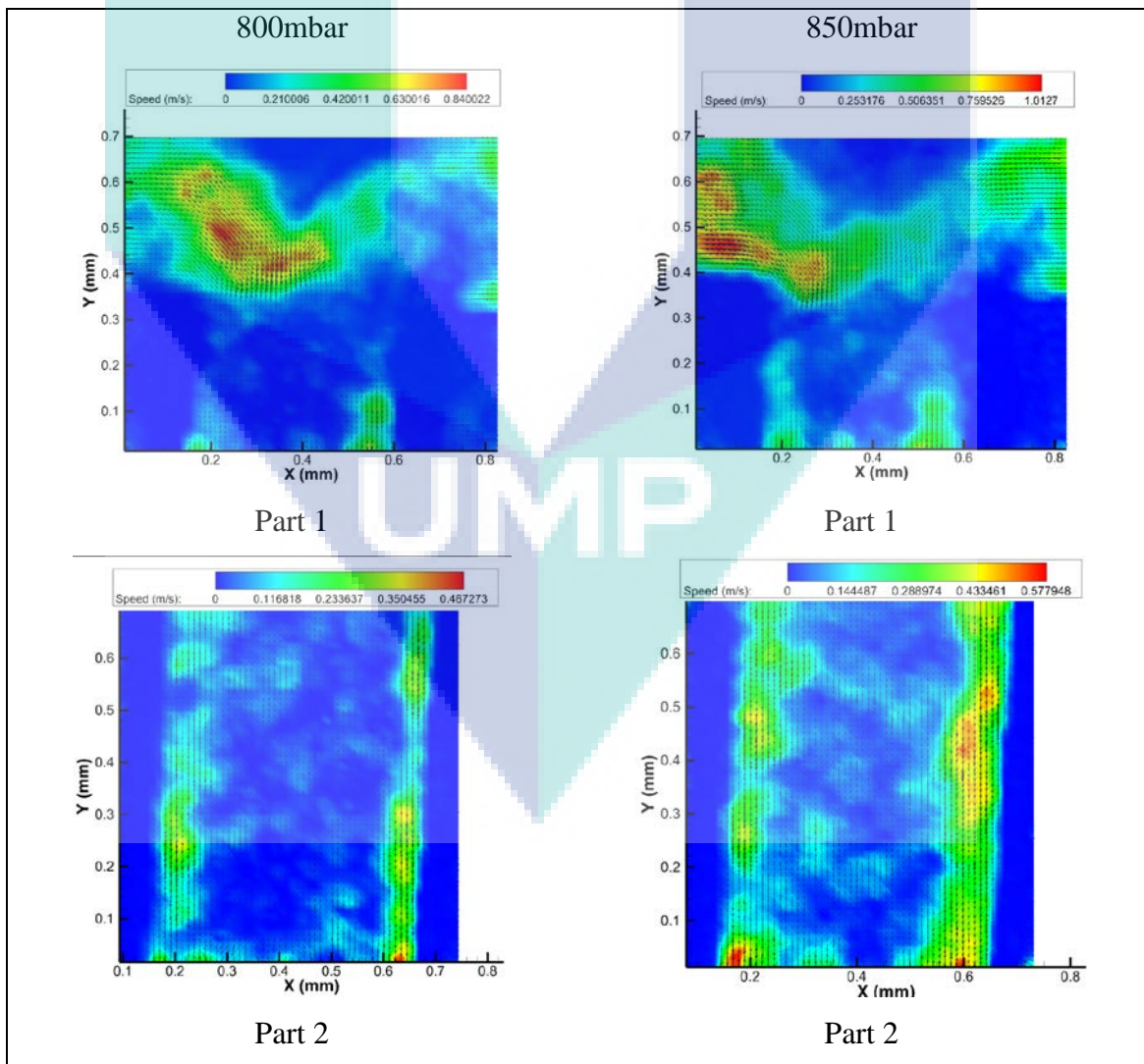


Figure 4-34 Image of  $\mu$ PIV of 60micron ribblets with inlet pressure of 400mbar and 450mbar respectively



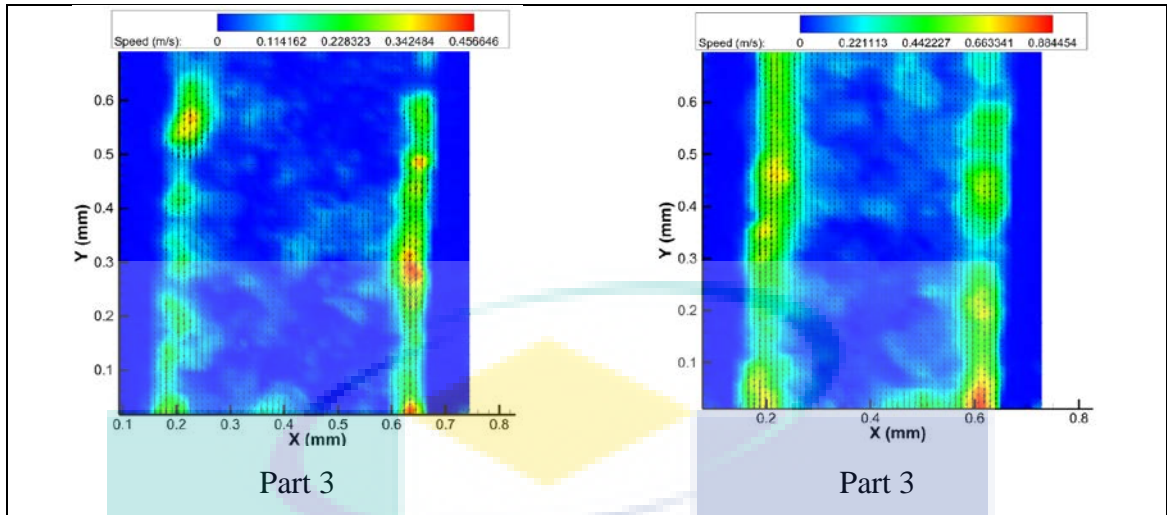


Figure 4-35 Image of  $\mu$ PIV of 60micron ribblets with inlet pressure of 800mbar and 850mbar respectively

From Figure 4-34 and Figure 4-35, it is seemed that there were no flow within the micromixer. However, this was not the case. Such behavior was due to the undetectable flow field in the middle of the micromixer by the  $\mu$ PIV because the flowrate was very high. The image showing only on the border as the it is still detectable. Theoretically, flow which are long the side happen to be slower due to the friction from the adhesion force between the fluid and the wall of the micromixer. Therefore, through image captured by the  $\mu$ PIV, it appeared to be as if flow only happen on the side of the wall.

Secondary vortices started to develop at the intersection of the two inlet channels where the vortex flow was generated. Secondary flow and the separation of the boundary layer at the junction where there are some discontinuities of the two-inlet micro channels of the T-mixer for all the cases is under study. This lateral flow can be applied to improve mixing performance. In addition, due to the nature of impingement at the intersection of two fluid streams flow separation occurred, and consequently, vortices were generated. Again, this resulted in enhanced mixing performance. The vortex tended to break the fluid stream into small eddies thereby increasing the interfacial area. These reduced the diffusion distance between the molecules of two fluids in a mixing process. This behavior became stronger as the separation area became larger.

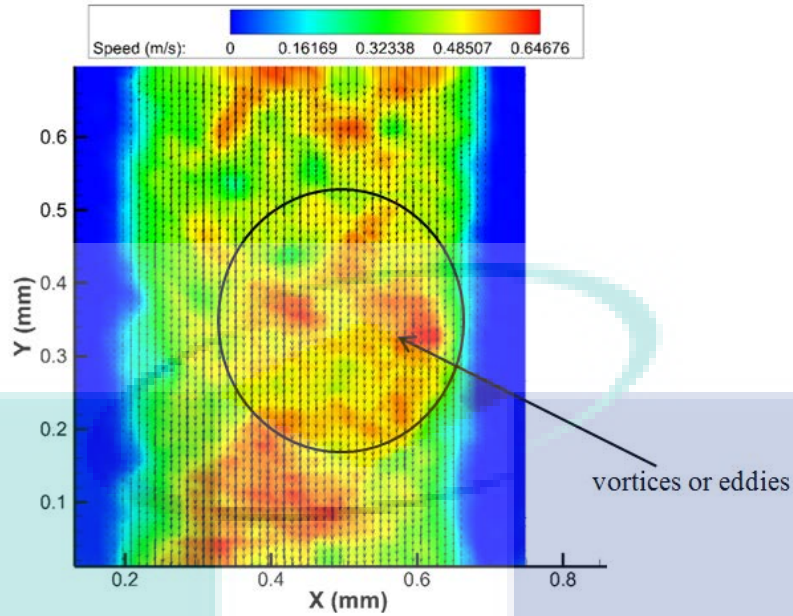


Figure 4-36 Image from  $\mu$ PIV of 40 micron ribblets of 250mbar inlet pressure at part 2 showing the formation of eddies.

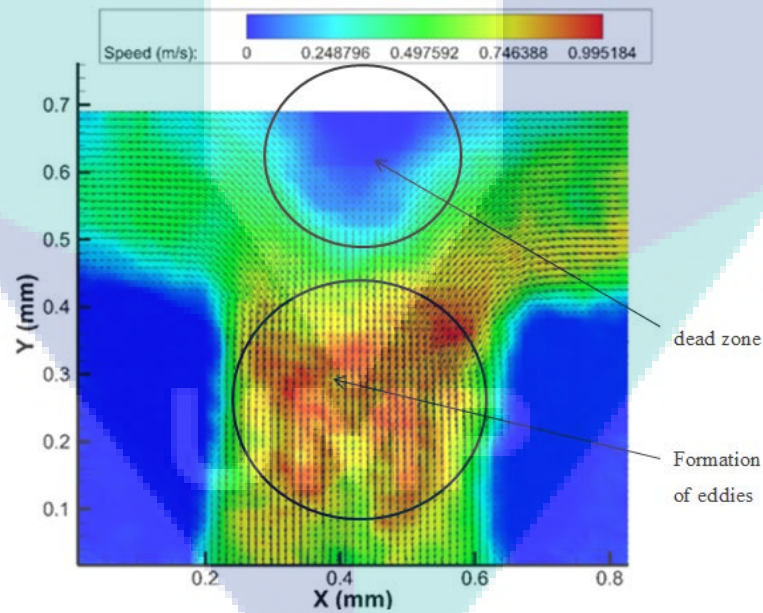
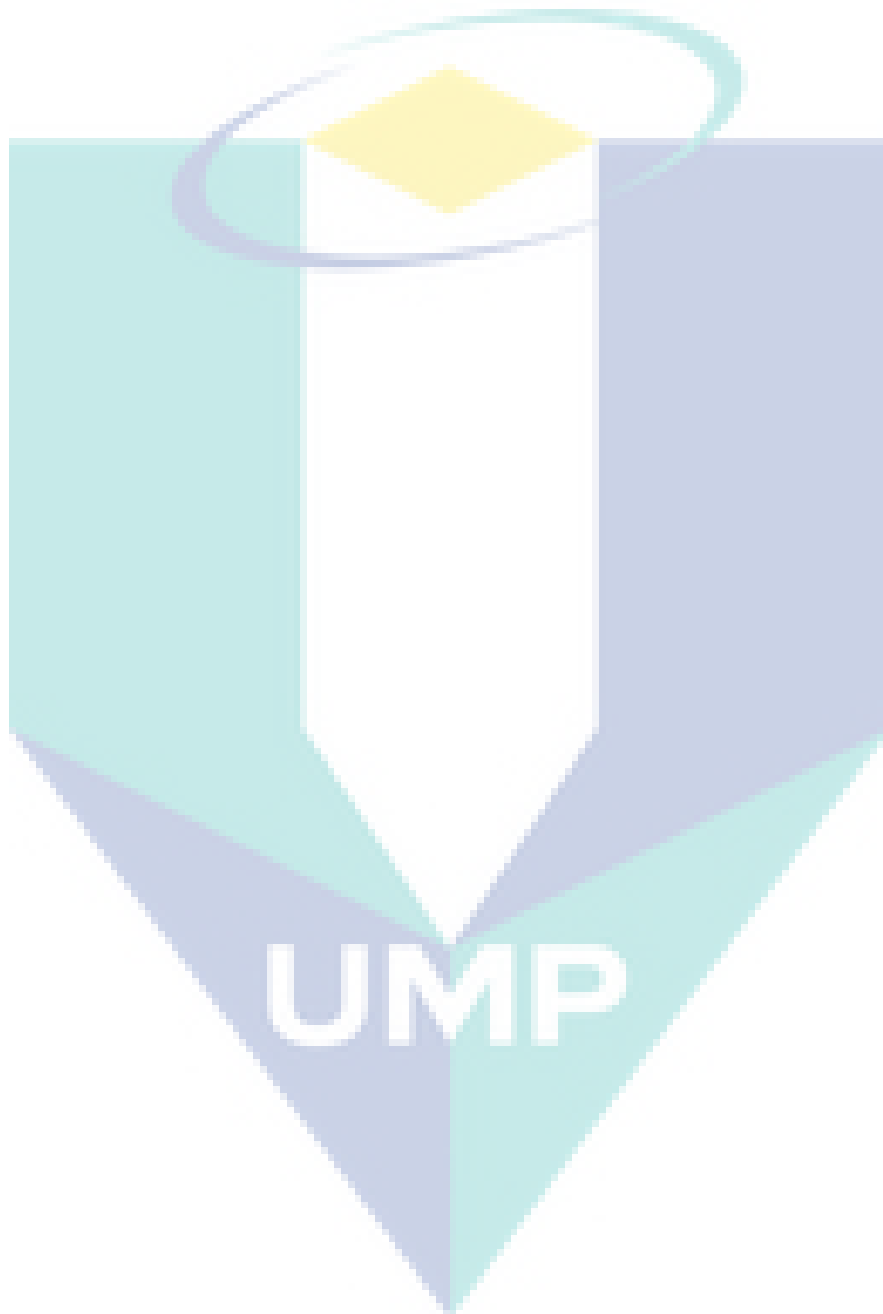


Figure 4-37 Image from  $\mu$ PIV of 60 micron ribblets of 350mbar inlet pressure having both dead zone and eddies formation

Near the intersection junction, a common stagnation (dead) zone was marked. This dead zone appears with almost the same size throughout all of the micromixer due to the similar design of T-shaped micromixer. In addition to this dead zone, a plug-like

velocity profile for all the cases with different velocity values was observed at the middle parts of the outlet channel.



## CHAPTER 5

### CONCLUSIONS AND RECOMMENDATIONS

#### 5.1 Conclusions

The intention of this study was to examine the performance of natural polymeric DRA in the enhancement of liquid flow in Y-shaped micromixers with various dimensions. The experimental results support Xanthan gum has the potential as a suitable alternative to synthetic polymer as it can enhance the flow performances. From the results, the %FI increased by increasing the additive concentration, length tail of micro-channels and decreasing in width of the micro-channels. The maximum %FI of 34.90% was achieved by 400 ppm of Xanthan gum at 100 mbar in micro-channel having the width of 500  $\mu\text{m}$ . Besides, 40% velocity increment was obtained by adding the Xanthan gum additives which tested using the  $\mu$ -PIV technique. Increasing the velocity in the system creates high velocity pockets at the active core of the fluid which is expected to enhance the mixing performance of the micromixers. Also, the two liquid streams met at the intersection point, resulting in the formation of vortices which able to break the fluid streams into smaller eddies thus reduce the diffusion distance between the molecules and increase the mixing performance. Hence, it is concluded that with the addition of DRA not only able to enhance the flow in the microchannel but also function as mixing enhancer in the miniature device.

Furthermore, the present work succeeded in presenting an alternative design (riblets) that is structured at the narrow walls of the micromixer to investigate a possible flow enhancement and liquid mixing to occur at the same time. The experimental results show that, the new design can enhance the flow in the micromixer when introducing a single water phase by 28.73% within the 60  $\mu\text{m}$  base-to-height ribletted micromixer at the operating pressure of 200 mbar. The micro-PIV images showed

clearly that the wall riblets at 20  $\mu\text{m}$  can create high-speed pockets that are able to enhance the mixing performance in the systems. It is believed that, the investigated microriblets (V-shape) created stagnant liquid layers in the grooves and this layer will replace or act-like the smooth wall surface but with different friction conditions. The size of the proposed riblets controls the wall friction where the balance between the mass of the trapped liquid and its apparent physical properties influences (viscosity and surface tension) the mobility of the liquid mass trapped in the groove. This will definitely result in the creation of the high speed pockets that are spotted using the  $\mu$ -PIV images and can control the mixing and flow enhancement performances in the proposed micromixer design.

## 5.2 Future work

From our findings, there are several recommendations for the future work that could provide a more complete idea on this topic. It is recommended to:

1. Explore and investigate on new natural polymeric additives where the resources are abundant not only in Malaysia but all over the world with high flow enhancement and mixing performance.
2. Investigate more parameters such as the molecular weight of the natural polymers that would influence the flow enhancement and mixing performance.
3. Investigate and suggest the mechanism of the flow enhancement using polymers. Researchers also can compare the mechanism of DR in laminar and turbulent flow when using polymers.

## REFERENCES

- Abate, A. R., Seiffert, S., Utada, A. S., Shum, A., Shah, R., Thiele, J., . . . Weitz, D. A. (2007). Microfluidic techniques for synthesizing particles. 1-21.
- Abdulbari, H. A., Letchmanan, K., & Yunus, R. M. (2011). Drag reduction characteristics using aloe vera natural mucilage: An experimental study. *Journal of Applied Sciences*, *11*, 1039-1043. doi:http://dx.doi.org/10.3923/jas.2011.1039.1043
- Abdulbari, H. A., & Ming, F. L. W. (2015). Drag reduction properties of nanofluids in microchannels *The Journal of Engineering Research (TJER)*, *12*(2), 60-67.
- Abdulbari, H. A., Nour, A. H., Kor, K., & Abdalla, A. N. (2011). Investigating the effect of solid particle addition on the turbulent multiphase flow in pipelines. *International Journal of the Physical Sciences*, *6*(15), 3672-3679. doi:http://dx.doi.org.10.5897/IJPS11.647
- Abdulbari, H. A., Wang Ming, F. L., & Mahmood, W. K. (2017). Insoluble additives for enhancing a blood-like liquid flow in micro-channels. *Journal of Hydrodynamics, Ser. B*, *29*(1), 144-153. doi:http://dx.doi.org/10.1016/S1001-6058(16)60726-6
- Abdulbari, H. A., Ahmad, M. A., & Yunus, R. B. M. (2010). Formulation of okra-natural mucilage as drag reducing agent in different size of galvanized iron pipes in turbulent water flowing system. *Journal of Applied Science*, *10*(23), 3105-3110. doi:http://dx.doi.org/10.3923/jas.2010.3105.3110
- Abdulbari, Hayder A., Siti Nuraffini , K., & A.H., Nour. (2012). Grafted natural polymer as new drag reducing agent: An experimental approach. *Chemical Industry & Chemical Engineering Quarterly*, *13*(3), 361-371. doi:http://dx.doi.org/10.2298/CICEQ111206012A
- Abubakar, A., Al-Wahaibi, T., Al-Wahaibi, Y., Al-Hashmi, A. R., & Al-Ajmi, A. (2014). Roles of drag reducing polymers in single- and multi-phase flows. *Chemical Engineering Research and Design*, *92*(11), 2153-2181. doi:http://dx.doi.org/10.1016/j.cherd.2014.02.031
- Abutarboush, R., Pappas, G., Arnaud, F., Auker, C., McCarron, R., Scultetus, A., & Moon-Massat, P. F. (2013). Effects of N-Acetyl-L-cysteine and hyaluronic acid on HBOC-201- induced systemic and cerebral vasoconstriction in the rat. *Current Drug Discovery Technologies*, *10*(4), 315-324. doi:http://dx.doi.org/10.2174/15701638113109990034

- Al-Sarkhi, A. (2010). Drag reduction with polymers in gas-liquid/liquid-liquid flows in pipes: A literature review. *Journal of Natural Gas Science and Engineering*, 2(1), 41-48. doi:<http://dx.doi.org/10.1016/j.jngse.2010.01.001>
- Al-Sarkhi, A. (2012). Effect of mixing on frictional loss reduction by drag reducing polymer in annular horizontal two-phase flows. *International Journal of Multiphase Flow*, 39(0), 186-192. doi:<http://dx.doi.org/10.1016/j.ijmultiphaseflow.2011.10.001>
- Al-Sarkhi, A., & Hanratty, T. J. (2001). Effect of pipe diameter on the performance of drag-reducing polymers in annular gas-liquid flows. *Chemical Engineering Research and Design*, 79(4), 402-408. doi:<http://dx.doi.org/10.1205/026387601750282328>
- Alavi, M., Büttgenbach, S., Schumacher, A., & Wagner, H. J. (1991, 24-27 June 1991). *Laser machining of silicon for fabrication of new microstructures*. Paper presented at the International Conference on Solid-State Sensors and Actuators, 1991.
- Alavi, M., Büttgenbach, S., Schumacher, A., & Wagner, H. J. (1992). Fabrication of microchannels by laser machining and anisotropic etching of silicon. *Sensors and Actuators A: Physical*, 32(1), 299-302. doi:[http://dx.doi.org/10.1016/0924-4247\(92\)80002-K](http://dx.doi.org/10.1016/0924-4247(92)80002-K)
- Alsabagh, A. M., Abdou, M. I., Ahmed, H. E.-s., Khalil, A. A.-s., & Aboulrous, A. A. (2015). Evaluation of some natural water-insoluble cellulosic material as lost circulation control additives in water-based drilling fluid. *Egyptian Journal of Petroleum*, 24(4), 461-468. doi:<http://dx.doi.org/10.1016/j.ejpe.2015.06.004>
- Angiography in India. Retrieved from <http://www.medgurus.org/angiography-in-india/>
- Aoki, N., Umei, R., Yoshida A. (2011). Design method for micromixers considering influence of channel confluence and bend on diffusion length. *Chemical Engineering Journal*, 167(2), 643-650. doi:<http://dx.doi.org/10.1016/j.cej.2010.08.084>
- Ashman, S., & Kandlikar, S. G. (2006). *A review of manufacturing processes for microchannel heat exchanger fabrication*. Paper presented at the Fourth International Conference on Nanochannels, Microchannels and Minichannels, Limerick, Ireland.
- Ashraf, M. W., Tayyaba, S., & Afzulpurkar, N. (2011). Micro electromechanical systems (MEMS) based microfluidic devices for biomedical applications. *International Journal of Molecular Sciences*, 12(6), 3648-3704. doi:<http://dx.doi.org/10.3390/ijms12063648>

- Barbulovic-N, I., Yang, H., Park, P. S., & Wheeler, A. R. (2008). Digital microfluidics for cell-based assays. *Lab Chip*, 8, 519-526. doi:http://dx.doi.org/10.1039/b717759c
- Becker, H., & Heim, U. (2000). Hot embossing as a method for the fabrication of polymer high aspect ratio structures. *Sensors and Actuators A: Physical*, 83(1-3), 130-135. doi:http://dx.doi.org/10.1016/S0924-4247(00)00296-X
- Becker, H., & Locascio, L. E. (2002). Polymer microfluidic devices. *Talanta*, 56(2), 267-287. doi:http://dx.doi.org/10.1016/S0039-9140(01)00594-X
- Beebe, D. J., Moore, J. S., Yu, Q., Liu, R. H., Kraft, M. L., Jo, B.-H., & Devadoss, C. (2000). Microfluidic tectonics: A comprehensive construction platform for microfluidic systems. *Proceedings of the National Academy of Sciences*, 97(25), 13488-13493. doi:http://dx.doi.org/10.1073/pnas.250273097
- Benzi, R. (2010). A short review on drag reduction by polymers in wall bounded turbulence. *Physica D: Nonlinear Phenomena*, 239(14), 1338-1345. doi:http://dx.doi.org/10.1016/j.physd.2009.07.013
- Bessa, K. L., Belletati, J. F., Dos Santos, L., Rossoni, L. V., & Ortiz, J. P. (2011). Drag reduction by polyethylene glycol in the tail arterial bed of normotensive and hypertensive rats. *Brazilian Journal of Medical and Biological Research*, 44, 767-777. doi:http://dx.doi.org/10.1590/S0100-879X2011007500071
- Bewersdorff, H.-W., & Singh, R. P. (1988). Rheological and drag reduction characteristics of xanthan gum solutions. *Rheologica Acta*, 27(6), 617-627. doi:http://dx.doi.org/10.1007/bf01337457
- Blick, E. (1969). Compliant coating skin friction experiments *7th Aerospace Sciences Meeting*: American Institute of Aeronautics and Astronautics.
- Boomsma, A., & Sotiropoulos, F. (2015). Riblet drag reduction in mild adverse pressure gradients: A numerical investigation. *International Journal of Heat and Fluid Flow*, 56, 251-260. doi:http://dx.doi.org/10.1016/j.ijheatfluidflow.2015.07.022
- Boussommier-Calleja, A., Li, R., Chen, M. B., Wong, S. C., & Kamm, R. D. (2016). Microfluidics: A new tool for modeling cancer-immune interactions. *Trends in Cancer*, 2(1), 6-19. doi:http://dx.doi.org/10.1016/j.trecan.2015.12.003
- Bozzi, A., Perrin, C., Austin, S., & Arce Vera, F. (2007). Quality and authenticity of commercial aloe vera gel powders. *Food Chemistry*, 103(1), 22-30. doi:http://dx.doi.org/10.1016/j.foodchem.2006.05.061
- Brands, J., Kliner, D., Lipowsky, H. H., Kameneva, M. V., Villanueva, F. S., & Pacella, J. J. (2013). New insights into the microvascular mechanisms of drag reducing

polymers: Effect on the cell-free layer. *PLOS ONE*, 8(10), e77252.  
doi:<http://dx.doi.org/10.1371/journal.pone.0077252>

- Brostow, W. (2008). Drag reduction in flow: Review of applications, mechanism and prediction. *Journal of Industrial and Engineering Chemistry*, 14(4), 409-416.  
doi:<http://dx.doi.org/10.1016/j.jiec.2008.07.001>
- Brostow, W., Lobland, H. E. H., Pal, S., & Singh, R. P. (2009). Polymeric flocculants for wastewater and industrial effluent treatment. *Journal of Materials Education*, 31(3-4), 157 - 166.
- Buchhave, P. (1992). Particle image velocimetry - Status and trends. *Experimental Thermal and Fluid Science*, 5, 586-604. doi:[http://dx.doi.org/10.1016/0894-1777\(92\)90016-X](http://dx.doi.org/10.1016/0894-1777(92)90016-X)
- Burger, E. D., Munk, W. R., & Wahl, H. A. (1982). Flow increase in the Trans Alaska pipeline through use of a polymeric drag-reducing additive. *JPT, Journal of Petroleum Technology*, 34(2), 377-386. doi:<http://dx.doi.org/10.2118/9419-PA>
- Calado, B., dosSantos, A., & Semiao V. (2016). Characterization of the mixing regimes of Newtonian fluid flows in asymmetrical T-shaped micromixers, *Experimental Thermal and Fluid Science*, 72, 218–227. doi:<http://dx.doi.org/10.1016/j.expthermflusci.2015.11.010>
- Catherine Rivet, H. L., Alison Hirsch, Sharon Hamilton, HangLu. (2011). Microfluidics for medical diagnostics and biosensors. *Chemical Engineering Science* 66, 1490–1507. doi:<http://dx.doi.org/10.1016/j.ces.2010.08.015>
- Ceccio, S. L., Dowling, D. R., Perlin, M., & Solomon, M. (2007). *Influence of surface roughness on polymer drag reduction*. Retrieved from Final Technical Report of HROO11-06-1-0057.
- Çetin, B., Koska, A. K., & Erdal, M. (2015). Warpige characterization of microchannels fabricated by injection molding. *Journal of Micro and Nano-Manufacturing*, 3(2), 021005-021005. doi:<http://dx.doi.org/10.1115/1.4029841>
- Chamorro, L. P., Arndt, R. E. A., & Sotiropoulos, F. (2013). Drag reduction of large wind turbine blades through riblets: Evaluation of riblet geometry and application strategies. *Renewable Energy*, 50, 1095-1105.  
doi:<http://dx.doi.org/10.1016/j.renene.2012.09.001>
- Chang, T.-L. (2013). Micromachining of microfluidic channels in glass by microjoule femtosecond laser pulses. *Microelectronic Engineering*, 110, 450-456.  
doi:<http://dx.doi.org/10.1016/j.mee.2013.03.142>

- Chang, Y. C., Yang, Y. S., & Sheh, J. L. (2006). A roller embossing process for rapid fabrication of microlens arrays on glass substrates. *Microsystem Technologies*, 12(8), 754-759. doi:http://dx.doi.org/10.1007/s00542-006-0103-5
- Chejara DR, Kondaveeti S, Prasad K, Siddhanta AK. (2013) Studies on the structure–property relationship of sodium alginate based thixotropic hydrogels. *RSC Advances*, 3(36), 15744 -15751. doi: http://dx.doi.org/10.1039/C3RA43070G
- Chen, J., & Wise, K. D. (1995). *A high-resolution silicon monolithic nozzle array for inkjet printing*. Paper presented at the The 8th International Conference on Solid-state Sensors and Actuators, and Eurosensors IX, Stockholm, Swede.
- Cheng, J.-Y., Wei, C.-W., Hsu, K.-H., & Young, T.-H. (2004). Direct-write laser micromachining and universal surface modification of PMMA for device development. *Sensors and Actuators B: Chemical*, 99(1), 186-196. doi:http://dx.doi.org/10.1016/j.snb.2003.10.022
- Chen, X., & Li, T. (2017). A novel passive micromixer designed by applying an optimization algorithm to the zigzag microchannel. *Chemical Engineering Journal*, 313, 1406–1414. https://doi.org/https://doi.org/10.1016/j.cej.2016.11.052
- Chinaud, M., Roumpea, E.-P., & Angeli, P. (2015). Studies of plug formation in microchannel liquid–liquid flows using advanced particle image velocimetry techniques. *Experimental Thermal and Fluid Science*, 69, 99-110. doi:http://dx.doi.org/10.1016/j.expthermflusci.2015.07.022
- Choi, K.-S., & Clayton, B. R. (2001). The mechanism of turbulent drag reduction with wall oscillation. *International Journal of Heat and Fluid Flow*, 22(1), 1-9. doi:http://dx.doi.org/10.1016/S0142-727X(00)00070-9
- Choi, K. S., Yang, X., Clayton, B. R., Glover, E. J., Atlar, M., Semenov, B. N., & Kulik, V. M. (1997). Turbulent drag reduction using compliant surfaces. *Proceedings of the Royal Society of London. Series A: Mathematical, Physical and Engineering Sciences*, 453(1965), 2229-2240. doi:http://dx.doi.org/10.1098/rspa.1997.0119
- Chung, C. K., & Lin, S. L. (2011). On the fabrication of minimizing bulges and reducing the feature dimensions of microchannels using novel CO<sub>2</sub> laser micromachining. *Journal of Micromechanics and Microengineering*, 21(6), 1-7. doi:http://dx.doi.org/10.1088/0960-1317/21/6/065023
- Cirillo, F., Leonardo, G., Renzulli, A., Crescenzi, B., Irace, C., Gnasso, A., & Cotrufo, M. (2002). Carotid atherosclerosis is associated with in-hospital mortality after cabg surgery. *International Journal of Angiology*, 11(4), 210-215. doi:http://dx.doi.org/10.1007/s00547-002-0912-z

- Cochrane, T., Earnshaw, J. C., & Love, A. H. G. (1981). Laser doppler measurement of blood velocity in microvessels. *Medical & Biological Engineering & Computing*, 19, 589-596. doi:http://dx.doi.org/10.1007/BF02442773
- Coelho, E. C., Barbosa, K. C. O., Soares, E. J., Siqueira, R. N., & Freitas, J. C. C. (2016). Okra as a drag reducer for high Reynolds numbers water flows. *Rheologica Acta*, 55(11), 983-991. doi:http://dx.doi.org/10.1007/s00397-016-0974-z
- Coleman, P. B., Ottenbreit, B. T., & Polimeni, P. I. (1987). Effects of a drag-reducing polyelectrolyte of microscopic linear dimension (Separan AP-273) on rat hemodynamics. *Circ Res*, 61(6), 787-796. doi:https://doi.org/10.1161/01.RES.61.6.787
- Cortes-Quiroz, C. A., Azarbadegan, A., Zangeneh, M., & Goto, A. (2010). Analysis and multi-criteria design optimization of geometric characteristics of grooved micromixer. *Chemical Engineering Journal*, 160(3), 852-864. https://doi.org/https://doi.org/10.1016/j.cej.2010.02.029
- Cotoia, A., Kameneva, M. V., Marascalco, P. J., Fink, M. P., & Delude, R. L. (2009). Drag-reducing hyaluronic acid increases survival in profoundly hemorrhaged rats. *Shock*, 31(3), 258-261. doi:http://dx.doi.org/10.1097/SHK.0b013e31817fc434
- Dallas, V., Vassilicos, J. C., & Hewitt, G. F. (2010). Strong polymer-turbulence interactions in viscoelastic turbulent channel flow. *Physical Review E*, 82(6), 066303.
- Daly, A. R., Sobajima, H., Olia, S. E., Takatani, S., & Kameneva, M. V. (2010). Application of drag-reducing polymer solutions as test fluids for in vitro evaluation of potential blood damage in blood pumps. *American Society of Artificial Internal Organs Journal*, 56(1), 6-11. doi:http://dx.doi.org/10.1097/MAT.0b013e3181c8e281
- de Bessa, K. L., & Ortiz, J. P. (2006). Drag reduction in vascular system. *ABCM Symposium Series in Bioengineering*, 1.
- De Gennes, P.G. (1990), *Introduction to polymer dynamics*. Cambridge University Press.
- De Rosa, I. M., Kenny, J. M., Puglia, D., Santulli, C., & Sarasini, F. (2010). Morphological, thermal and mechanical characterization of okra (*Abelmoschus esculentus*) fibres as potential reinforcement in polymer composites. *Composites Science and Technology*, 70(1), 116-122. doi:http://dx.doi.org/10.1016/j.compscitech.2009.09.013

- deMello, A. J. (2006). Control and detection of chemical reactions in microfluidic systems. *Nature*, 442(7101), 394-402. doi:http://dx.doi.org/10.1038/nature05062
- Diehl, B., & Teichmuller, E. (1998). Aloe vera, quality inspection and identification. *Agro Food Industry Hi-Tech*, 9 (1), 14-16.
- Dintenfass, L. (1969). Blood rheology in pathogenesis of the coronary heart disease. *American Heart Journal*, 77, 139-147 doi:http://dx.doi.org/10.1016/0002-8703(69)90139-2
- Dosunmu, I. T., & Shah, S. N. (2014). Turbulent flow behavior of surfactant solutions in straight pipes. *Journal of Petroleum Science and Engineering*, 124, 323-330. doi:http://dx.doi.org/10.1016/j.petrol.2014.09.025
- Driels, M. R., & Ayyash, S. (1976). Drag reduction in laminar flow. *Nature*, 259(5542), 389-390. doi:http://dx.doi.org/10.1038/259389a0
- Drzazga, M., Gierczycki, A., Dzido, G., & Lemanowicz, M. (2013). Influence of nonionic surfactant addition on drag reduction of water based nanofluid in a small diameter pipe. *Chinese Journal of Chemical Engineering*, 21(1), 104-108. doi:http://dx.doi.org/10.1016/S1004-9541(13)60447-4
- El-Samni, O. A., Chun, H. H., & Yoon, H. S. (2007). Drag reduction of turbulent flow over thin rectangular riblets. *International Journal of Engineering Science*, 45(2-8), 436-454. doi:http://dx.doi.org/10.1016/j.ijengsci.2007.03.002
- Eshrati, M., Al-Hashmi, A. R., Al-Wahaibi, T., Al-Wahaibi, Y., Al-Ajmi, A., & Abubakar, A. (2015). Drag reduction using high molecular weight polyacrylamides during multiphase flow of oil and water: A parametric study. *Journal of Petroleum Science and Engineering*, 135, 403-409. doi:http://dx.doi.org/10.1016/j.petrol.2015.09.028
- Eshrati, M., Al-Wahaibi, T., Al-Hashmi, A. R., Al-Wahaibi, Y., Al-Ajmi, A., & Abubakar, A. (2017). Experimental study of drag reduction of polymer-polymer mixtures in horizontal dispersed oil-water flow. *Experimental Thermal and Fluid Science*, 83, 169-176. doi:http://dx.doi.org/10.1016/j.expthermflusci.2017.01.006
- Eskin, D. (2017). Modeling an effect of pipe diameter on turbulent drag reduction. *Chemical Engineering Science*, 162, 66-68. doi:http://dx.doi.org/10.1016/j.ces.2016.12.052
- Farooq, U., Malviya, R., & Sharma, P. K. (2013). Extraction and characterization of okra mucilage as pharmaceutical excipient. *Academic Journal of Plant Sciences*, 6(4), 168-172. doi:http://dx.doi.org/10.5829/idosi.ajps.2013.6.4.82292

- Faruqui, F. I., Otten, M. D., & Polimeni, P. I. (1987). Protection against atherogenesis with the polymer drag-reducing agent Separan AP-30. *Circulation*, 75(3), 627-635. doi:http://dx.doi.org/10.1161/01.cir.75.3.627
- Faustino, V., Catarino, S. O., Lima, R., & Minas, G. (2016). Biomedical microfluidic devices by using low-cost fabrication techniques: A review. *Journal of Biomechanics*, 49(11), 2280-2292. doi:http://dx.doi.org/10.1016/j.jbiomech.2015.11.031
- Feng, G.-H., & Tsai, M.-Y. (2010). Acoustic emission sensor with structure-enhanced sensing mechanism based on micro-embossed piezoelectric polymer. *Sensors and Actuators A: Physical*, 162(1), 100-106. doi:http://dx.doi.org/10.1016/j.sna.2010.06.019
- Fink, J. K. (2003). Chapter 12 - Drag reducers. In J. K. Fink (Ed.), *Oil Field Chemicals* (pp. 166-173). Burlington: Gulf Professional Publishing.
- Fiorini, G. S., & Chiu, D. T. (2005). Disposable microfluidic devices: Fabrication, function, and application. *BioTechniques*, 38, 429-446. doi:http://dx.doi.org/10.2144/05383RV02
- Forrest, F., & Grierson, G. A. (1931). Friction losses in cast iron pipe carrying paper stock. *Paper Trade Journal*, 92(22), 39-41.
- Fossum, E., Høieggen, A., & Moan, A. (1997). Whole blood viscosity, blood pressure and cardiovascular risk factors in healthy blood donors. *Blood Pressure*, 6, 161-165. doi:http://dx.doi.org/10.3109/08037059709061932
- Friend, J., & Yeo, L. (2010). Fabrication of microfluidic devices using polydimethylsiloxane. *Biomicrofluidics*, 4. doi:http://dx.doi.org/10.1063/1.3259624
- Fu, G., Tor, S. B., Hardt, D. E., & Loh, N. H. (2011). Effects of processing parameters on the micro-channels replication in microfluidic devices fabricated by micro injection molding. *Microsystem Technologies*, 17(12), 1791-1798. doi:http://dx.doi.org/10.1007/s00542-011-1363-2
- Gad-el-Hak, M. (1998). Compliant coatings: The simpler alternative. *Experimental Thermal and Fluid Science*, 16(1-2), 141-156. doi:http://dx.doi.org/10.1016/S0894-1777(97)10006-1
- Gad-El-Hak, M. (2003). Drag reduction using compliant walls. In P. W. Carpenter & T. J. Pedley (Eds.), *Flow Past Highly Compliant Boundaries and in Collapsible Tubes: Proceedings of the IUTAM Symposium held at the University of Warwick, United Kingdom, 26-30 March 2001* (pp. 191-229). Dordrecht: Springer Netherlands.

- Gampert, B., & Wagner, P. (1985). *The influence of polymer additives on velocity and temperature fields* (B. Gampert Ed.): Springer-Verlag Berlin Heidelberg.
- García-González, V., Delgado-Coello, B., Pérez-Torres, A., & Mas-Oliva, J. (2015). Reality of a vaccine in the prevention and treatment of atherosclerosis. *Archives of Medical Research*, 46(5), 427-437. doi:http://dx.doi.org/10.1016/j.arcmed.2015.06.004
- Goh, K. K. T., Matia-Merino, L., Chiang, J. H., Quek, R., Soh, S. J. B., & Lentle, R. G. (2016). The physico-chemical properties of chia seed polysaccharide and its microgel dispersion rheology. *Carbohydrate Polymers*, 149, 297-307. doi:http://dx.doi.org/10.1016/j.carbpol.2016.04.126
- Gowda, D. C., Neelisiddaiah, B., & Anjaneyalu, Y. V. (1979). Structural studies of polysaccharides from aloe vera. *Carbohydrate Research*, 72, 201-205. doi:http://dx.doi.org/10.1016/S0008-6215(00)83936-1
- Gray, J. (1936). Studies in animal locomotion. IV. The propulsive powers of the dolphin. *Journal of Experimental Biology*, 13(2), 192-199.
- Greene, H. L., Mostardi, R. F., & Nokes, R. F. (1980). Effects of drag reducing polymers on initiation of atherosclerosis. *Polymer Engineering & Science*, 20(7), 499-504. doi:http://dx.doi.org/10.1002/pen.760200710
- Grünberger, A., Wiechert, W., & Kohlheyer, D. (2014). Single-cell microfluidics: opportunity for bioprocess development. *Current Opinion in Biotechnology*, 29, 15-23. doi:http://dx.doi.org/10.1016/j.copbio.2014.02.008
- Guo, L., Feng, J., Fang, Z., Xu, J., & Lu, X. (2015). Application of microfluidic “lab-on-a-chip” for the detection of mycotoxins in foods. *Trends in Food Science & Technology*, 46(2, Part A), 252-263. doi:http://dx.doi.org/10.1016/j.tifs.2015.09.005
- Harpole, G. M., & Eninger, J. E. (1991, 12-14 Feb 1991). *Micro-channel heat exchanger optimization*. Paper presented at the Semiconductor Thermal Measurement and Management Symposium, 1991. SEMI-THERM VII. Proceedings., Seventh Annual IEEE.
- Harrison, D. J., Manz, A., Fan, Z., Luedi, H., & Widmer, H. M. (1992). Capillary electrophoresis and sample injection systems integrated on a planar glass chip. *Anal Chem*, 64(17), 1926-1932. doi:http://dx.doi.org/10.1021/ac00041a030
- Haywood, J. R., Shaffer, R. A., Fastenow, C., Fink, G. D., & Brody, M. J. (1981). Regional blood flow measurement with pulsed Doppler flowmeter in conscious rat. *American Journal of Physiology Heart and Circulatory Physiology*, 241, H273-H278.

- Henri, J., Han, G., Meint de, B., Miko, E., & Jan, F. (1996). A survey on the reactive ion etching of silicon in microtechnology. *Journal of Micromechanics and Microengineering*, 6(1), 14. doi:http://dx.doi.org/10.1088/0960-1317/6/1/002
- Hessel, V., Löwe, H., & Schönfeld F. (2005). Micromixers—a review on passive and active mixing principles. *Chemical Engineering Science*, 60(8-9), 2479–2501. doi:http://dx.doi.org/ 10.1016/j.ces.2004.11.033
- Hofmann, S., Stern, P., & Myska, J. (1994). Rheological behavior and birefringence investigations on drag-reducing surfactant solutions of tallow-(tris-hydroxyethyl)-ammonium acetate/sodiumsalicylate mixtures. *Rheologica Acta*, 33(5), 419-430. doi:http://dx.doi.org/10.1007/bf00366584
- Hong, C. H., Choi, H. J., Zhang, K., Renou, F., & Grisel, M. (2015). Effect of salt on turbulent drag reduction of xanthan gum. *Carbohydrate Polymers*, 121, 342-347. doi:http://dx.doi.org/10.1016/j.carbpol.2014.12.015
- Hong, C. H., Zhang, K., Choi, H. J., & Yoon, S. M. (2010). Mechanical degradation of polysaccharide guar gum under turbulent flow. *Journal of Industrial and Engineering Chemistry*, 16(2), 178-180. doi:http://dx.doi.org/10.1016/j.jiec.2009.09.073
- Hossain, S., Ansari, M. A., Husain, A., & Kim, K.-Y. (2010). Analysis and optimization of a micromixer with a modified Tesla structure. *Chemical Engineering Journal*, 158(2), 305–314. https://doi.org/https://doi.org/10.1016/j.cej.2010.02.002
- Hossain, S., Ansari, M. A., & Kim, K.-Y. (2009). Evaluation of the mixing performance of three passive micromixers. *Chemical Engineering Journal*, 150(2), 492–501. https://doi.org/https://doi.org/10.1016/j.cej.2009.02.033
- Hoyt, J. W. (1965). *A turbulent-flow rheometer*. Paper presented at the Symposium on Rheology, Marris.
- Hoyt, J. W. (1971). Blood transfusion fluids having reduced turbulent friction properties: Google Patents.
- Hoyt, J. W., & Fabula, A. G. (1964). *The effect of additives on fluid friction*. Paper presented at the 5th Symposium on Naval Hydrodynamics, Bergen, Norway.
- Hsieh, S.-S., Lin, J.-W., & Chen, J.-H. (2013). Mixing efficiency of Y-type micromixers with different angles. *International Journal of Heat and Fluid Flow*, 44, 130-139. doi:http://dx.doi.org/10.1016/j.ijheatfluidflow.2013.05.011
- Huang, C., Liu, D., & Wei, J. (2016). Experimental study on drag reduction performance of surfactant flow in longitudinal grooved channels. *Chemical*

- Huang, Y., Liu, S., Yang, W., & Yu, C. (2010). Surface roughness analysis and improvement of PMMA-based microfluidic chip chambers by CO<sub>2</sub> laser cutting. *Applied Surface Science*, 256(6), 1675-1678. doi:<http://dx.doi.org/10.1016/j.apsusc.2009.09.092>
- Huntson, D. L., & Reischman, M. M. (1975). The role of polydispersity in the mechanism of drag reduction. *The Physics of Fluids*, 18(12), 1626-1629. doi:<http://aip.scitation.org/doi/abs/10.1063/1.861080>
- Hutchison, K. J., Campbell, J. D., & Karpinski, E. (1989). Decreased poststenotic flow disturbance during drag reduction by polyacrylamide infusion without increased aortic blood flow. *Microvasc Res*, 38(1), 102-109. doi:[http://dx.doi.org/10.1016/0026-2862\(89\)90019-8](http://dx.doi.org/10.1016/0026-2862(89)90019-8)
- Iaccarino, G., Shaqfeh, E. S. G., & Dubief, Y. (2010). Reynolds-averaged modeling of polymer drag reduction in turbulent flows. *Journal of Non-Newtonian Fluid Mechanics*, 165(7-8), 376-384. doi:<http://dx.doi.org/10.1016/j.jnnfm.2010.01.013>
- Insull Jr, W. (2009). The pathology of atherosclerosis: Plaque development and plaque responses to medical treatment. *The American Journal of Medicine*, 122(1, Supplement), S3-S14. doi:<http://dx.doi.org/10.1016/j.amjmed.2008.10.013>
- Interthal, W., & Wilski, H. (1985). Drag reduction experiments with very large pipes. *Colloid and Polymer Science*, 263(3), 217-229. doi:<http://dx.doi.org/10.1007/bf01415508>
- Ishizuka, M., Mizuno, J., Harada, T., & Shoji, S. (2004). *Fabrication of fine plastic microchannel by using hot embossing*. Paper presented at the Proceedings - Electrochemical Society.
- Jakeway, C. S., de Mello, J. A., & Russell, L. E. Miniaturized total analysis systems for biological analysis. *Fresenius' Journal of Analytical Chemistry*, 366(6), 525-539. doi:<http://dx.xoi/org/10.1007/s002160051548>
- Jang Min, P., Kyoung Duck, S., & Tai Hun, K. (2010). A chaotic micromixer using obstruction-pairs. *Journal of Micromechanics and Microengineering*, 20(1), 15023.
- Japper-Jaafar, A., Escudier, M. P., & Poole, R. J. (2009). Turbulent pipe flow of a drag-reducing rigid "rod-like" polymer solution. *Journal of Non-Newtonian Fluid Mechanics*, 161(1-3), 86-93. doi:<http://dx.doi.org/10.1016/j.jnnfm.2009.04.008>

- Jen, C.-P., Wu, C.-Y., Lin, Y.-C., & Wu, C.-Y. (2003). Design and simulation of the micromixer with chaotic advection in twisted microchannels. *Lab on a Chip*, 3(2), 77. <https://doi.org/10.1039/b211091a>
- Jeon, W., & Shin, C. B. (2009). Design and simulation of passive mixing in microfluidic systems with geometric variations. *Chemical Engineering Journal*, 152(2), 575–582. <https://doi.org/10.1016/j.cej.2009.05.035>
- Jiang, F., Drese, K. S., Hardt, S., Küpper, M., & Schönfeld, F. (2004). Helical flows and chaotic mixing in curved micro channels. *AIChE Journal*, 50(9), 2297–2305. <https://doi.org/10.1002/aic.10188>
- Johnson, T. J., Ross, D., Gaitan, M., & Locascio, L. E. (2001). Laser modification of preformed polymer microchannels: Application to reduce band broadening around turns subject to electrokinetic flow. *Anal Chem*, 73(15), 3656-3661. [doi:http://dx.doi.org/10.1021/ac010269g](http://dx.doi.org/10.1021/ac010269g)
- Jovanovic, J., Zhou, W., Rebrov, E. V., Nijhuis, T. A., Hessel, V., & Schouten, J. C. (2011). Liquid- liquid slug flow: hydrodynamics and pressure drop. *Chemical Engineering Science*, 66(1), 42-54. [doi:http://dx.doi.org/10.1016/j.ces.2010.09.040](http://dx.doi.org/10.1016/j.ces.2010.09.040)
- Kalanuria, A. A., Nyquist, P., & Ling, G. (2012). The prevention and regression of atherosclerotic plaques: emerging treatments. *Vascular Health and Risk Management*, 8, 549-561. [doi:http://dx.doi.org/10.2147/VHRM.S27764](http://dx.doi.org/10.2147/VHRM.S27764)
- Kamarulizam, H. A. A. B. S. N., & Man, R. C. (2011). Investigating drag reduction characteristic using Okra Mucilage as new drag reduction agent. *Journal of Applied Sciences*, 11, 2554-2561. [doi:http://dx.doi.org/10.3923/jas.2011.2554.2561](http://dx.doi.org/10.3923/jas.2011.2554.2561)
- Kamarulizam, S. N. b. (2012). *Formulation a dual effect natural drag reduction agent*. (Master Degree), University Malaysia Pahang, University Malaysia Pahang.
- Kamarulizam, S. N. B., Bari, H. A. A., & Arumugam, N. D. (2011, 27-29 May 2011). *Studying the potential of slag waste particle as suspended solid drag reducing agent*. Paper presented at the Communication Software and Networks (ICCSN), 2011 IEEE 3rd International Conference on.
- Kameneva, M., Borovetz, H., Chapman, T., Griffith, B., & Repko, B. (2003). Artificial blood fluids and microflow drag reducing factors for enhanced blood circulation: Google Patents.
- Kameneva, M. V. (2012). Microrheological effects of drag-reducing polymers in vitro and in vivo. *International Journal of Engineering Science*, 59, 168-183. [doi:http://dx.doi.org/10.1016/j.ijengsci.2012.03.014](http://dx.doi.org/10.1016/j.ijengsci.2012.03.014)

- Kameneva, M. V., Wu, Z. J., Uraysh, A., Repko, B., Litwak, K. N., Billiar, T. R., . . . Borovetz, H. S. (2004). Blood soluble drag-reducing polymers prevent lethality from hemorrhagic shock in acute animal experiments. *Biorheology*, *41*, 53–64.
- Kang, S.-W., Chen, J.-S., & Hung, J.-Y. (1998). Surface roughness of (110) orientation silicon based micro heat exchanger channel. *International Journal of Machine Tools and Manufacture*, *38*(5–6), 663–668. doi:http://dx.doi.org/10.1016/S0890-6955(97)00115-6
- Kaplan, W., Elderstig, H., & Veider, C. (1994). *A novel fabrication method of capillary tubes on quartz for chemical analysis applications*. Paper presented at the Micro Electro Mechanical Systems, 1994, MEMS '94, Proceedings, IEEE Workshop on.
- Karami, H. R., & Mowla, D. (2012). Investigation of the effects of various parameters on pressure drop reduction in crude oil pipelines by drag reducing agents. *Journal of Non-Newtonian Fluid Mechanics*, *177–178*, 37–45. doi:http://dx.doi.org/10.1016/j.jnnfm.2012.04.001
- Kaur, H., Singh, G., & bt. Jaafar, A. (2013). *Study of drag reduction ability of naturally produced polymers from a local plant source*. Paper presented at the International Petroleum Technology Conference, Beijing, China.
- Kawaguchi, Y., Segawa, T., Feng, Z., & Li, P. (2002). Experimental study on drag-reducing channel flow with surfactant additives—spatial structure of turbulence investigated by PIV system. *International Journal of Heat and Fluid Flow*, *23*(5), 700–709. doi:http://dx.doi.org/10.1016/S0142-727X(02)00166-2
- Kelley, D. H., & Ouellette, N. T. (2011). Separating stretching from folding in fluid mixing. *Nat Phys*, *7*(6), 477–480. https://doi.org/http://www.nature.com/nphys/journal/v7/n6/abs/nphys1941.html#supplementary-information
- Khadom, A. A., & Abdul-Hadi, A. A. (2014). Performance of polyacrylamide as drag reduction polymer of crude petroleum flow. *Ain Shams Engineering Journal*, *5*(3), 861–865. doi:http://dx.doi.org/10.1016/j.asej.2014.04.005
- Khodaparast, S., Borhani, N., & Thome, J. R. (2014). Application of micro particle shadow velocimetry  $\mu$ PSV to two-phase flows in microchannels. *International Journal of Multiphase Flow*, *62*, 123–133. doi:http://dx.doi.org/10.1016/j.ijmultiphaseflow.2014.02.005
- Kim, B. S., Kwak, B. S., Shin, S., Lee, S., Kim, K. M., Jung, H.-I., & Cho, H. H. (2011). Optimization of microscale vortex generators in a microchannel using advanced response surface method. *International Journal of Heat and Mass Transfer*, *54*(1), 118–125. https://doi.org/https://doi.org/10.1016/j.ijheatmasstransfer.2010.09.061

- Kim, C. A., Choi, H. J., Kim, C. B., & Jhon, M. S. (1998). Drag reduction characteristics of polysaccharide xanthan gum. *Macromolecular Rapid Communications*, 19(8), 419-422. doi:[http://dx.doi.org/10.1002/\(SICI\)1521-3927\(19980801\)19:8<419::AID-MARC419>3.0.CO;2-0](http://dx.doi.org/10.1002/(SICI)1521-3927(19980801)19:8<419::AID-MARC419>3.0.CO;2-0)
- Kim, D. S., Lee, S. H., Kwon, T. H., & Ahn, C. H. (2005). A serpentine laminating micromixer combining splitting/recombination and advection. *Lab on a Chip*, 5(7), 739–747. <https://doi.org/10.1039/B418314B>
- Kim, H. M., Moon, M. A., & Kim, K. Y. (2011). Multi-objective optimization of a cooling channel with staggered elliptic dimples. *Energy*, 36(5), 3419-3428. doi:<http://dx.doi.org/10.1016/j.energy.2011.03.043>
- Kim, N.-J., Kim, S., Lim, S. H., Chen, K., & Chun, W. (2009). Measurement of drag reduction in polymer added turbulent flow. *International Communications in Heat and Mass Transfer*, 36(10), 1014-1019. doi:<http://dx.doi.org/10.1016/j.icheatmasstransfer.2009.08.002>
- Kim, N.-J., Lee, J.-Y., Yoon, S.-M., Kim, C.-B., & Hur, B.-K. (2000). Drag reduction rates and degradation effects in synthetic polymer solution with surfactant additives. *Journal of Industrial and Engineering Chemistry*, 6(6), 412-418.
- Kimerling, T. E., Liu, W., Kim, B. H., & Yao, D. (2006). Rapid hot embossing of polymer microfeatures. *Microsystem Technologies*, 12(8), 730-735. doi:<http://dx.di.org/10.1007/s00542-006-0098-y>
- Klank, H., Kutter, J. P., & Geschke, O. (2002). CO<sub>2</sub>-laser micromachining and back-end processing for rapid production of PMMA-based microfluidic systems. *Lab Chip*, 2(4), 242-246. doi:<http://dx.doi.org/10.1039/B206409J>
- Kobets, G. F., Zav'yalova, V. S., & Komarova, M. L. (1969). The effect of fish mucus on turbulent friction. *Bionika*, 3(80).
- Koerner, T., Brown, L., Xie, R., & Oleschuk, R. D. (2005). Epoxy resins as stamps for hot embossing of microstructures and microfluidic channels. *Sensors and Actuators B: Chemical*, 107(2), 632-639. doi:<http://dx.doi.org/10.1016/j.snb.2004.11.035>
- Konstantinou, D., Shirazi, A., Sadri, A., & Young, E. W. K. (2016). Combined hot embossing and milling for medium volume production of thermoplastic microfluidic devices. *Sensors and Actuators B: Chemical*, 234, 209-221. doi:<http://dx.doi.org/10.1016/j.snb.2016.04.147>
- Kozminsky, M., Wang, Y., & Nagrath, S. (2016). The incorporation of microfluidics into circulating tumor cell isolation for clinical applications. *Current Opinion in Chemical Engineering*, 11, 59-66. doi:<http://dx.doi.org/10.1016/j.coche.2016.01.005>

- Kramer, M. O. (1960). Boundary layer stabilization by distributed damping. *Journal of the American Society for Naval Engineers*, 72(1), 25-34. doi:http://dx.doi.org/10.1111/j.1559-3584.1960.tb02356.x
- Krope, A., & Lipus, L. C. (2010). Drag reducing surfactants for district heating. *Applied Thermal Engineering*, 30(8-9), 833-838. doi:http://dx.doi.org/10.1016/j.applthermaleng.2009.12.012
- Kulicke, W. M., Kötter, M., & Gräger, H. (1989). Drag reduction phenomenon with special emphasis on homogeneous polymer solutions *Polymer Characterization/Polymer Solutions*, (Vol. 89, pp. 1-68): Springer Berlin Heidelberg.
- Le Brun, N., Zadrazil, I., Norman, L., Bismarck, A., & Markides, C. N. (2016). On the drag reduction effect and shear stability of improved acrylamide copolymers for enhanced hydraulic fracturing. *Chemical Engineering Science*, 146, 135-143. doi:http://dx.doi.org/10.1016/j.ces.2016.02.009
- Le The, H., Le Thanh, H., Dong, T., Ta, B. Q., Tran-Minh, N., & Karlsen, F. (2015). An effective passive micromixer with shifted trapezoidal blades using wide Reynolds number range. *Chemical Engineering Research and Design*, 93, 1-11. doi:http://dx.doi.org/10.1016/j.cherd.2014.12.003
- Lee, A. J., Mowbray, P. I., & Lowe, G. D. (1998). Blood viscosity and evaluated carotid intima-media thickness in men and women. *Circulation*, 97, 1467-1473. doi:https://doi.org/10.1161/01.CIR.97.15.1467
- Lee, S. H., & Mudawar, I. (2016). Investigation of flow boiling in large micro-channel heat exchangers in a refrigeration loop for space applications. *International Journal of Heat and Mass Transfer*, 97, 110-129. doi:http://dx.doi.org/10.1016/j.ijheatmasstransfer.2016.01.072
- Lewis, S. J. (2009). Prevention and treatment of atherosclerosis: a practitioner's guide for 2008. *American Journal of Medicine*, 122(1 Suppl), S38-50. doi:http://dx.doi.org/10.1016/j.amjmed.2008.10.016
- Li, F.-C., Kawaguchi, Y., Yu, B., Wei, J.-J., & Hishida, K. (2008). Experimental study of drag-reduction mechanism for a dilute surfactant solution flow. *International Journal of Heat and Mass Transfer*, 51(3-4), 835-843. doi:http://dx.doi.org/10.1016/j.ijheatmasstransfer.2007.04.048
- Li, F.-C., Yu, B., Wei, J.-J., & Kawaguchi, Y. (2012). *Turbulent drag reduction by surfactant additives*. Singapore: John Wiley & Sons Singapore Pte. Ltd.
- Lienhart, H., Breuer, M., & Köksoy, C. (2008). Drag reduction by dimples? – A complementary experimental/numerical investigation. *International Journal of*

- Lim, S. T., Park, S. J., Chan, C. K., & Choi, H. J. (2005). Turbulent drag reduction characteristics induced by calf-thymus DNA. *Physica A: Statistical Mechanics and its Applications*, 350(1), 84-88.  
doi:<http://dx.doi.org/10.1016/j.physa.2004.11.034>
- Lin, C.-Y., Meng, H.-C., & Fu, C. (2011). A PDMS self-vortical micromixer without obstructions. *The Open Chemical Engineering Journal*, 5, 7-12.
- Lin, Y., Gerfen, G. J., Rousseau, D. L., & Yeh, S. R. (2003). Ultrafast microfluidic mixer and freeze-quenching device. *Analytical Chemistry*, 75(20), 5381-5386.  
<https://doi.org/10.1021/ac0346205>
- Liu, Y., Ganser, D., Schneider, A., Liu, R., Grodzinski, P., & Kroutchinina, N. (2001). Microfabricated polycarbonate CE devices for DNA analysis. *Analytical Chemistry*, 73(17), 4196-4201. doi:<http://dx.doi.org/10.1021/ac010343v>
- Liu, Y., Rauch, C. B., Stevens, R. L., Lenigk, R., Yang, J., Rhine, D. B., & Grodzinski, P. (2002). DNA Amplification and Hybridization Assays in Integrated Plastic Monolithic Devices. *Analytical Chemistry*, 74(13), 3063-3070.  
doi:<http://dx.doi.org/10.1021/ac020094q>
- Lu, C.-S., Chen, J.-J., Liao, J.-H., & Hsieh, T.-Y. (2009). Flow and concentration analysis inside a microchannel with lightning grooves at two floors. *Journal of Biomechatronics Engineering*, 2, 13-32.
- Lumley, J. L. (1969). Drag reduction by additives. *Annual Review of Fluid Mechanics*, 1, 367-384. doi:<http://dx.doi.org/10.1146/annurev.fl.01.010169.002055>
- Lumley, J. L. (1973). Drag reduction in turbulent flow by polymer additives. *Journal of Polymer Science: Macromolecular Reviews*, 7(1), 263-290.  
doi:<http://dx.doi.org/10.1002/pol.1973.230070104>
- Hung, L.-H., & Lee, A. P. (2007). Microfluidic devices for the synthesis of nanoparticles and biomaterials. *Journal of Medical and Biological Engineering*, 27(1), 1-6.
- Macias, C. A., Kameneva, M. V., Tenhunen, J. J., Puyana, J. C., & Fink, M. P. (2004). Survival in a rat model of lethal hemorrhagic shock is prolonged following resuscitation with a small volume of a solution containing a drag-reducing polymer derived from aloe vera. *Shock*, 22(2), 151-156.  
doi:<http://dx.doi.org/10.1097/01.shk.0000131489.83194.1a>
- MacKinnon, S., McDermid, S., Bonorand, L., Peckham, T., Wang, K., & Li, J. (2007). United States Patent No. WO2008048317 A1

- Mäkelä, T., Haatainen, T., Majander, P., & Ahopelto, J. (2007). Continuous roll to roll nanoimprinting of inherently conducting polyaniline. *Microelectronic Engineering*, 84(5–8), 877-879. doi:<http://dx.doi.org/10.1016/j.mee.2007.01.131>
- Malcher, T., & Gzyl-Malcher, B. (2012). Influence of polymer–surfactant aggregates on fluid flow. *Bioelectrochemistry*, 87, 42-49. doi:<http://dx.doi.org/10.1016/j.bioelechem.2012.01.011>
- Malviya, R. (2011). Extraction characterization and evaluation of selected mucilage as pharmaceutical excipient. *Polymers in Medicine*, 41(3), 39-44.
- Mann, D. L., Zipes, D. P., Libby, P., & Bonow, R. O. (2011). *Braunwald's heart disease - a textbook of cardiovascular medicine* (9th ed.). Philadelphia, PA: Elsevier Saunders.
- Manz, A., Miyahara, Y., Miura, J., Watanabe, Y., Miyagi, H., & Sato, K. (1990). Design of an open-tubular column liquid chromatograph using silicon chip technology. *Sensors and Actuators B: Chemical*, 1(1), 249-255. doi:[http://dx.doi.org/10.1016/0925-4005\(90\)80210-Q](http://dx.doi.org/10.1016/0925-4005(90)80210-Q)
- Marhefka, J., & Kameneva, M. (2016). Natural drag-reducing polymers: Discovery, characterization and potential clinical applications. *Fluids*, 1(2), 6.
- Marhefka, J., Velankar, S., Chapman, T., & Kameneva, M. (2008). Mechanical degradation of drag reducing polymers in suspensions of blood cells and rigid particles. *Biorheology*, 45(5), 599-609.
- Marhefka, J. N. (2007). *Study of drag reducing polymers and mechanisms of their intravascular effect*. Doctoral Dissertation. University of Pittsburgh. Retrieved from <http://d-scholarship.pitt.edu/6497/>
- Marhefka, J. N., Zhao, R., Wu, Z., Velankar, S. S., Antaki, J. F., & Kameneva, M. V. (2009). Drag reducing polymers improve tissue perfusion via modification of the RBC traffic in microvessels. *Biorheology*, 46(4), 281-292. doi:<http://dx.doi.org/10.3233/BIR-2009-0543>
- Martin, C. R., & Aksay, I. A. (2005). Microchannel molding: A soft lithography-inspired approach to micrometer-scale patterning. *Journal of Materials Research*, 20(8), 1995 - 2003. doi:<http://dx.doi.org/10.1557/JMR.2005.0251>
- Martin, J. R., & Shapella, B. D. (2003). The effect of solvent solubility parameter on turbulent flow drag reduction in polyisobutylene solutions. *Experiments in Fluids*, 34(5), 535-539. doi:<http://dx.doi.org/10.1007/s00348-002-0564-y>
- Martin, S., & Bhushan, B. (2016). Modeling and optimization of shark-inspired riblet geometries for low drag applications. *Journal of Colloid and Interface Science*, 474, 206-215. doi:<http://dx.doi.org/10.1016/j.jcis.2016.04.019>

- Martynova, L., Locascio, L. E., Gaitan, M., Kramer, G. W., Christensen, R. G., & MacCrehan, W. A. (1997). Fabrication of plastic microfluid channels by imprinting methods. *Analytical Chemistry*, 69(23), 4783-4789. doi:http://dx.doi.org/10.1021/ac970558y
- Matras, Z., & Kopiczak, B. (2015). Intensification of drag reduction effect by simultaneous addition of surfactant and high molecular polymer into the solvent. *Chemical Engineering Research and Design*, 96, 35-42. doi:http://dx.doi.org/10.1016/j.cherd.2015.02.006
- Mavros, P., Ricard, A., Xuereb, C., & Bertrand, J. (2011). A study of the effect of drag-reducing surfactants on flow patterns in stirred vessels. *Chemical Engineering Research and Design*, 89(1), 94-106. doi:http://dx.doi.org/10.1016/j.cherd.2010.04.016
- McCormick, R. M., Nelson, R. J., Alonso-Amigo, M. G., Benvegna, D. J., & Hooper, H. H. (1997). Microchannel electrophoretic separations of DNA in injection-molded plastic substrates. *Analytical Chemistry*, 69(14), 2626-2630. doi:http://dx.doi.org/10.1021/ac9701997
- McDonald, J. C., & Whitesides, G. M. (2002). Poly(dimethylsiloxane) as a material for fabricating microfluidic devices. *Accounts of Chemical Research*, 35(7), 491-499. doi:http://dx.doi.org/10.1021/ar010110q
- Mecomber, J. S., Hurd, D., & Limbach, P. A. (2005). Enhanced machining of micron-scale features in microchip molding masters by CNC milling. *International Journal of Machine Tools and Manufacture*, 45(12-13), 1542-1550. doi:http://dx.doi.org/10.1016/j.ijmachtools.2005.01.016
- Mecomber, J. S., Stalcup, A. M., Hurd, D., Halsall, H. B., Heineman, W. R., Seliskar, C. J., . . . Limbach, P. A. (2006). Analytical performance of polymer-based microfluidic devices fabricated by computer numerical controlled machining. *Analytical Chemistry*, 78(3), 936-941. doi:http://dx.doi.org/10.1021/ac051523y
- Mela, P., van den Berg, A., Fintschenko, Y., Cummings, E. B., Simmons, B. A., & Kirby, B. J. (2005). The zeta potential of cyclo-olefin polymer microchannels and its effects on insulative (electrodeless) dielectrophoresis particle trapping devices. *Electrophoresis*, 26(9), 1792-1799. doi:http://dx.doi.org/10.1002/elps.200410153
- Mendes, A.C., et al., (2012). Fabrication of phospholipid-xanthan microcapsules by combining microfluidics with self-assembly. *Acta Biomaterialia*, 9(5), 6675 - 6685. doi: https://doi.org/10.1016/j.actbio.2013.01.035
- Metwally, K., Robert, L., Salut, R., & Khan-Malek, C. (2012). SU-8-based rapid tooling for thermal roll embossing. *Microsystem Technologies*, 18(11), 1863-1869. doi:http://dx.doi.org/10.1007/s00542-012-1534-9

- Miller, M. (2009). An emerging paradigm in atherosclerosis: focus on subclinical disease. *Postgraduate Medical Journal*, *121*(2), 49-59. doi:<http://dx.doi.org/10.3810/pgm.2009.03.1976>
- Min, T., Yul Yoo, J., Choi, H., & Joseph, D. D. (2003). Drag reduction by polymer additives in a turbulent channel flow. *Journal of Fluid Mechanics*, *486*, 213-238. doi:10.1017/S0022112003004610
- Ming, F. L. W., Abdulbari, H. A., Latip, N. B. A., & Heidarini, S. (2016). Insoluble nano-powders additives enhancing the flow of liquid in microchannel: Effect of particle size. *ARPJ Journal of Engineering and Applied Sciences*, *11*(4), 2146-2152.
- Morgan, A. J. L., Naylor, J., Gooding, S., John, C., Squires, O., Lees, J., . . . Porch, A. (2013). Efficient microwave heating of microfluidic systems. *Sensors and Actuators B: Chemical*, *181*, 904-909. doi:<http://dx.doi.org/10.1016/j.snb.2013.02.099>
- Mostardi, R. A., Greene, H. L., Nokes, R. F., Thomas, L. C., & Lue, T. (1976). The effect of drag reducing agents on stenotic flow disturbances in dogs. *Biorheology*, *13*(2), 137-141.
- Mostardi, R. A., Thomas, L. C., Greene, H. L., VanEssen, F., & Nokes, R. F. (1978). Suppression of atherosclerosis in rabbits using drag reducing polymers. *Biorheology*, *15*(1), 1-14.
- Mozaffarian, D., Benjamin, E. J., Go, A. S., Arnett, D. K., Blaha, M. J., Cushman, M., . . . Turner, M. B. (2015). Heart disease and stroke statistics—2015 update: A report from the American Heart Association. *Circulation*, *131*(4), e29-e322. doi:<http://dx.doi.org/10.1161/cir.0000000000000152>
- Muijlwijk, K., Berton-Carabin, C., & Schroën, K. (2016). Cross-flow microfluidic emulsification from a food perspective. *Trends in Food Science & Technology*, *49*, 51-63. doi:<http://dx.doi.org/10.1016/j.tifs.2016.01.004>
- Mukherjee, I., & Rosolen, M. (2013). Thermal transitions of gelatin evaluated using DSC sample pans of various seal integrities. *Journal of Thermal Analysis and Calorimetry*, *114*(3), 1161-1166. doi:<http://dx.doi.org/10.1007/s10973-013-3166-4>
- Mulligan, C. N. (2005). Environmental applications for biosurfactants. *Environmental Pollution*, *133*(2), 183-198. doi:<http://dx.doi.org/10.1016/j.envpol.2004.06.009>
- Muluneh, M., & Issadore, D. (2013). Hybrid soft-lithography/laser machined microchips for the parallel generation of droplets. *Lab Chip*, *13*(24), 4750-4754. doi:<http://dx.doi.org/10.1039/c3lc50979f>

- Nam, Y., Kim, M., & Kim, T. (2014). Pneumatically controlled multi-level microchannel for separation and extraction of microparticles. *Sensors and Actuators B: Chemical*, *190*, 86-92. doi:http://dx.doi.org/10.1016/j.snb.2013.08.024
- Nesyn, G. V., Konovalov, K. B., Vetrova, O. V., & Menshov, P. (2015). Laboratory evaluation of the drag reduction additives effectiveness. *Procedia Chemistry*, *15*, 371-377. doi:http://dx.doi.org/10.1016/j.proche.2015.10.059
- Neumann, D., & Dinkelacker, A. (1991). Drag measurements on V-grooved surfaces on a body of revolution in axial flow. *Applied Scientific Research*, *48*(1), 105-114. doi:http://dx.doi.org/10.1007/bf01998668
- Ng, S. H., & Wang, Z. F. (2008). Hot roller embossing for microfluidics: process and challenges. *Microsystem Technologies*, *15*(8), 1149-1156. doi:http://dx.doi.org/10.1007/s00542-008-0722-0
- Nimafar, M., Viktorov, V., & Martinelli, M. (2012). Experimental comparative mixing performance of passive micromixers with H-shaped sub-channels. *Chemical Engineering Science*, *76*, 37-44. doi:http://dx.doi.org/10.1016/j.ces.2012.03.036
- Nugen, S. R., Asiello, P. J., & Baeumner, A. J. (2008). Design and fabrication of a microfluidic device for near-single cell mRNA isolation using a copper hot embossing master. *Microsystem Technologies*, *15*(3), 477-483. doi:http://dx.doi.org/10.1007/s00542-008-0694-0
- Ogaji, I. J., & Hoag, S. W. (2014). Novel extraction and application of okra gum as a film coating agent using theophylline as a model drug. *Journal of Advanced Pharmaceutical Technology & Research*, *5*(2), 70-77. doi:http://dx.doi.org/10.4103/2231-4040.133427
- Oliver, D. R., & Bakhtiyarov, S. I. (1983). Drag reduction in exceptionally dilute polymer solutions. *Journal of Non-Newtonian Fluid Mechanics*, *12*(1), 113-118. doi:http://dx.doi.org/10.1016/0377-0257(83)80008-1
- Ottino, J. M., & Wiggins, S. (2004). Introduction: Mixing in microfluidics. *Philosophical Transactions of the Royal Society A: Mathematical, Physical and Engineering Sciences*, *362*(1818), 923-935. https://doi.org/10.1098/rsta.2003.1355
- Pacella, J. J., Kameneva, M. V., Csikari, M., Lu, E., & Villanueva, F. S. (2006). A novel hydrodynamic approach to the treatment of coronary artery disease. *European Heart Journal*, *27*, 2362-2369. doi:http://dx.doi.org/10.1093/eurheartj/ehl165
- Pacella, J. J., Lu, E., Gretton, J., Fischer, D., Kameneva, M. V., & Villanueva, F. S. (2004). Drag reduction by polymer infusion: A new mechanism to enhance

microcirculatory perfusion for the treatment of ischemia. *Journal of the American College of Cardiology*, 43(5, Supplement 2), A290. doi:[http://dx.doi.org/10.1016/S0735-1097\(04\)91227-2](http://dx.doi.org/10.1016/S0735-1097(04)91227-2)

- Paoletti, F., Gretillat, M. A., & Rooij, N. F. d. (1996, 11-15 Feb 1996). *A silicon micromachined vibrating gyroscope with piezoresistive detection and electromagnetic excitation*. Paper presented at the Micro Electro Mechanical Systems, 1996, MEMS '96, Proceedings. An Investigation of Micro Structures, Sensors, Actuators, Machines and Systems. IEEE, The Ninth Annual International Workshop on.
- Park, S.-R., & Wallace, J. M. (1994). Flow alteration and drag reduction by riblets in a turbulent boundary layer. *AIAA Journal*, 32(1), 31-38. doi:<http://dx.doi.org/10.2514/3.11947>
- Pereira, A. S., Andrade, R. M., & Soares, E. J. (2013). Drag reduction induced by flexible and rigid molecules in a turbulent flow into a rotating cylindrical double gap device: Comparison between Poly (ethylene oxide), Polyacrylamide, and Xanthan Gum. *Journal of Non-Newtonian Fluid Mechanics*, 202, 72-87. doi:<http://dx.doi.org/10.1016/j.jnnfm.2013.09.008>
- Petrie, H. L., Deutsch, S., Brungart, T. A., & Fontaine, A. A. (2003). Polymer drag reduction with surface roughness in flat-plate turbulent boundary layer flow. *Experiments in Fluids*, 35(1), 8-23. doi:<http://dx.doi.org/10.1007/s00348-003-0589-x>
- Pitts, K. L., & Fenech, M. (2013). Micro-particle image velocimetry for velocity profile measurements of micro blood flows. *Journal of Visualized Experiments*, 74. doi:<http://dx.doi.org/10.3791/50314>
- Polimeni, P. I., Ottenbreit, B., & Coleman, P. (1985). Enhancement of aortic blood flow with a linear anionic macropolymer of extraordinary molecular length. *Journal of Molecular and Cellular Cardiology*, 17(7), 721-724. doi:[http://dx.doi.org/10.1016/S0022-2828\(85\)80072-9](http://dx.doi.org/10.1016/S0022-2828(85)80072-9)
- Poole, R., Alfateh, M., & Gauntlett A. (2013). Bifurcation in a T-channel junction: Effects of aspect ratio and shear-thinning. *Chemical Engineering Science*, 104, 839-848. doi:<http://dx.doi.org/10.1016/j.ces.2013.10.006>
- Prajapati, K. (2009). *Interactions between drag reducing polymers and surfactants* University of Waterloo. Retrieved from <http://hdl.handle.net/10012/4758>
- Prasad, A. K. (2000). Particle image velocimetry. *Current Science*, 79(1), 51-60.
- Pribush, A., Hatzkelzon, L., Meyerstein, D., & Meyerstein, N. (2013). The mechanism of the polymer-induced drag reduction in blood. *Colloids and Surfaces B:*

- Puryear, F. W. (1962). Boundary layer control-drag reduction by use of compliant coatings: Defense Technical Information Center.
- Qi, Y., Kesselman, E., Hart, D. J., Talmon, Y., Mateo, A., & Zakin, J. L. (2011). Comparison of oleyl and elaidyl isomer surfactant-counterion systems in drag reduction, rheological properties and nanostructure. *Journal of Colloid and Interface Science*, 354(2), 691-699. doi:http://dx.doi.org/10.1016/j.jcis.2010.10.067
- Qin, D., Xia, Y., & Whitesides, G. M. (2010). Soft lithography for micro- and nanoscale patterning. *Nature Protocols*, 5(3), 491-502. doi:http://dx.doi.org/10.1038/nprot.2009.234
- Raffaghello, L., Lee, C., Safdie, F. M., Wei, M., Madia, F., Bianchi, G., & Longo, V. D. (2008). Starvation-dependent differential stress resistance protects normal but not cancer cells against high-dose chemotherapy. *Proceedings of the National Academy of Sciences of the United States of America*, 105(24), 8215-8220. doi:http://dx.doi.org/10.1073/pnas.0708100105
- Redha, Z. M., Baldock, S. J., Fielden, P. R., Goddard, N. J., Brown, B. J. T., Haggett, B. G. D., . . . Birch, B. J. (2009). Hybrid Microfluidic Sensors Fabricated by Screen Printing and Injection Molding for Electrochemical and Electrochemiluminescence Detection. *Electroanalysis*, 21(3-5), 422-430. doi:http://dx.doi.org/10.1002/elan.200804415
- Reis, L. G., Oliveira, I. P., Pires, R. V., & Lucas, E. F. (2016). Influence of structure and composition of poly(acrylamide-g-propylene oxide) copolymers on drag reduction of aqueous dispersions. *Colloids and Surfaces A: Physicochemical and Engineering Aspects*, 502, 121-129. doi:http://dx.doi.org/10.1016/j.colsurfa.2016.05.022
- Resch, K. L., Ernst, E., Matrai, A., & Paulsen, H. F. (1992). Fibrinogen and viscosity as risk factors for subsequent cardiovascular event in stroke survivors. *Annals of Internal Medicine*, 117, 371-375. doi:http://dx.doi.org/10.7326/0003-4819-117-5-371
- Resende, P. R., Kim, K., Younis, B. A., Sureshkumar, R., & Pinho, F. T. (2011). A FENE-P  $k-\epsilon$  turbulence model for low and intermediate regimes of polymer-induced drag reduction. *Journal of Non-Newtonian Fluid Mechanics*, 166(12-13), 639-660. doi:http://dx.doi.org/10.1016/j.jnnfm.2011.02.012
- Reston, R. R., & Kolesar, E. S. (1994). Silicon-micromachined gas chromatography system used to separate and detect ammonia and nitrogen dioxide. I. Design, fabrication, and integration of the gas chromatography system. *Journal of*

- Rodriguez, I., Spicar-Mihalic, P., Kuyper, C. L., Fiorini, G. S., & Chiu, D. T. (2003). Rapid prototyping of glass microchannels. *Analytica Chimica Acta*, 496(1-2), 205-215. doi:http://dx.doi.org/10.1016/S0003-2670(03)01000-6
- Rohlf, W., Haustein, H. D., Garbrecht, O., & Kneer, R. (2012). Insights into the local heat transfer of a submerged impinging jet: Influence of local flow acceleration and vortex-wall interaction. *International Journal of Heat and Mass Transfer*, 55(25-26), 7728-7736. doi:http://dx.doi.org/10.1016/j.ijheatmasstransfer.2012.07.081
- Romoli, L., Tantussi, G., & Dini, G. (2011). Experimental approach to the laser machining of PMMA substrates for the fabrication of microfluidic devices. *Optics and Lasers in Engineering*, 49(3), 419-427. doi:http://dx.doi.org/10.1016/j.optlaseng.2010.11.013
- Rosen, M. W., & Cornford, N. E. (1971). Fluid friction of fish slimes. *Nature*, 234(5323), 49-51. doi:http://dx.doi.org/10.1038/234049a0
- Rossier, J. S., Vollet, C., Carnal, A., Lagger, G., Gobry, V., Girault, H. H., . . . Reymond, F. (2002). Plasma etched polymer microelectrochemical systems. *Lab Chip*, 2(3), 145-150. doi:http://dx.doi.org/10.1039/b204063h
- Rózański, J. (2011). Flow of drag-reducing surfactant solutions in rough pipes. *Journal of Non-Newtonian Fluid Mechanics*, 166(5-6), 279-288. doi:http://dx.doi.org/10.1016/j.jnnfm.2010.12.005
- Sakai, T., Repko, B. M., Griffith, B. P., Waters, J. H., & Kameneva, M. V. (2007). Infusion of a drag-reducing polymer extracted from aloe vera prolonged survival time in a rat model of acute myocardial ischaemia. *British Journal of Anaesthesia*, 98(1), 23-28. doi:http://dx.doi.org/10.1093/bja/ael307
- Salim, A., Fourar, M., Pironon, J., & Sausse, J. (2008). Oil-water two phase flow in microchannels: flow patterns and pressure drop measurements. *The Canadian Journal of Chemical Engineering*, 86(6), 978-988. doi:http://dx.doi.org/10.1002/cjce.20108
- Sampaio, D., Lopes, D., & Semiao V. (2015). Horse and dog blood flows in PDMS rectangular microchannels: Experimental characterization of the plasma layer under different flow conditions. *Experimental Thermal and Fluid Science*, 68, 205-215. doi:http://dx.doi.org/10.1016/j.expthermflusci.2015.04.020
- Santiago, J., Wereley, S., Meinhart, C., Beebe, D., & Adrian, R. (1998). A micro particle image velocimetry system. *Experiments in Fluids*, 25, 316-319. doi:http://dx.doi.org/10.1007/s003480050235

- Sarkar, A., Narváez, A., & Harting, J. (2012). Optimization of chaotic micromixers using finite time Lyapunov exponents. In W. E. Nagel, D. B. Kröner, & M. M. Resch (Eds.), *High Performance Computing in Science and Engineering '11: Transactions of the High Performance Computing Center, Stuttgart (HLRS) 2011* (pp. 325–336). Berlin, Heidelberg: Springer Berlin Heidelberg. [https://doi.org/10.1007/978-3-642-23869-7\\_24](https://doi.org/10.1007/978-3-642-23869-7_24)
- Savins, J. G. (1967). A stress-controlled drag-reduction phenomenon. *Rheologica Acta*, 6(4), 323-330. doi:<http://dx.doi.org/10.1007/BF01984629>
- Schaller, T., Bohn, L., Mayer, J., & Schubert, K. (1999). Microstructure grooves with a width of less than 50 [mu]m cut with ground hard metal micro end mills. *Precision Engineering*, 23, 229-235. doi:[http://dx.doi.org/10.1016/S0141-6359\(99\)00011-2](http://dx.doi.org/10.1016/S0141-6359(99)00011-2)
- Schonfeld, F., Hessel, V., & Hofmann, C. (2004). An optimised split-and-recombine micro-mixer with uniform “chaotic” mixing. *Lab on a Chip*, 4(1), 65–69. <https://doi.org/10.1039/B310802C>
- Schwartz, B., & Robbins, H. (1976). Chemical etching of Silicon IV . Etching technology. *Journal of Electrochemical Society*, 123(12), 1903-1909. doi:<http://dx.doi.org/10.1149/1.2132721>
- Seki, J., Sasaki, Y., Oyama, T., & Yamamoto, J. (1996). Fiber-optic laser-Doppler anemometer microscope applied to the cerebral microcirculation in rats. *Biorheology*, 33, 463-470. doi:[http://dx.doi.org/10.1016/S0006-355X\(97\)00034-6](http://dx.doi.org/10.1016/S0006-355X(97)00034-6)
- Shah, R. K., Shum, H. C., Rowat, A. C., Lee, D., Agresti, J. J., Utada, A. S., . . . Weitz, D. A. (2008). Designer emulsions using microfluidics. *Materials Today*, 11(4), 18-27. doi:[http://dx.doi.org/10.1016/S1369-7021\(08\)70053-1](http://dx.doi.org/10.1016/S1369-7021(08)70053-1)
- Shah, S. N., & Zhou, Y. (2003). An experimental study of drag reduction of polymer solutions in coiled tubing. *SPE Production & Facilities*, 18(4), 280-287. doi:<http://dx.doi.org/10.2118/87231-PA>
- Shan, X., Jin, L., Soh, Y. C., & Lu, C. W. (2009). A polymer-metal hybrid flexible mould and application for large area hot roller embossing. *Microsystem Technologies*, 16(8), 1393-1398. doi:<http://dx.doi.org/10.1007/s00542-009-0991-2>
- Shanshool, J., & Al-Qamaje, H. M. T. (2008). *Effect of molecular weight on turbulent drag reduction with polyisobutylene*. Paper presented at the The 1stRegional Conference of Eng. Sci. NUCEJ Spatial ISSUE.

- Shenoy, A. V. (1984). A review on drag reduction with special reference to micellar systems. *Colloid and Polymer Science*, 262(4), 319-337. doi:http://dx.doi.org/10.1007/BF01410471
- Shih-Jeh, W., Hsiang-Chen, H., & Wen-Jui, F. (2014). Novel design and fabrication of a geometrical obstacle-embedded micromixer with notched wall. *Japanese Journal of Applied Physics*, 53(9), 97201.
- Shih-Jung, L., & Yau-Chia, C. (2007). A novel soft-mold roller embossing method for the rapid fabrication of micro-blocks onto glass substrates. *Journal of Micromechanics and Microengineering*, 17(1), 172. doi:http://dx.doi.org/10.1088/0960-1317/17/1/022
- Sifferman, T. R., & Greenkorn, R. A. (1981). Drag reduction in three distinctly different fluid systems. *Society of Petroleum Engineers Journal*, 21(6), 663-669. doi:http://dx.doi.org/10.2118/8722-PA
- Singh, R. P., Jain, S. K., & Lan, N. (1991). *Drag reduction, flocculation and rheological characteristics of grafted polysaccharides*. Paper presented at the Polymer Science Contemporary Themes, New Delhi.
- Skote, M., Mishra, M., & Wu, Y. (2015). Drag reduction of a turbulent boundary layer over an oscillating wall and its variation with Reynolds number. *International Journal of Aerospace Engineering*, 2015, 9. doi:http://dx.doi.org/10.1155/2015/891037
- Sohn, J. I., Kim, C. A., Choi, H. J., & Jhon, M. S. (2001). Drag-reduction effectiveness of xanthan gum in a rotating disk apparatus. *Carbohydrate Polymers*, 45(1), 61-68. doi:http://dx.doi.org/10.1016/S0144-8617(00)00232-0
- Sokolova, I. A., Shakhnazarov, A. A., Timkina, M. I., Poliakova, M. S., Priezzhev, A. V., Proskurin, S. G., . . . Bikkulova, K. F. (1993). A decrease in the hydrodynamic resistance in the mesenteric arterioles of rats injected with the polyethylene oxide polyox WSR-301. *Bulletin of Experimental Biology and Medicine*, 116(11), 552-555. doi:http://dx.doi.org/10.1007/BF00805173
- Stamhuis, E. J. (2006). Basics and principles of particle image velocimetry (PIV) for mapping biogenic and biologically relevant flows. *Aquatic Ecology*, 40, 463-479. doi:http://dx.doi.org/10.1007/s10452-005-6567-z
- Stary, H. C., Chandler, A. B., Dinsmore, R. E., Fuster, V., Glagov, S., Jr, W. I., . . . Wissler, R. W. (2015). *A definition of advanced types of atherosclerotic lesions and a histological classification of atherosclerosis*. Retrieved from A Report From the Committee on Vascular Lesions of the Council on Arteriosclerosis, American Heart Association:

- Stone, H. A., Stroock, A. D., & Ajdari, A. (2004). Engineering flows in small devices: Microfluidics toward a lab-on-a-chip. *Annual Review of Fluid Mechanics*, 36, 381-411. doi:<http://dx.doi.org/10.1146/annurev.fluid.36.050802.122124>
- Suksamranchit, S., & Sirivat, A. (2007). Influence of ionic strength on complex formation between poly(ethylene oxide) and cationic surfactant and turbulent wall shear stress in aqueous solution. *Chemical Engineering Journal*, 128(1), 11-20. doi:<http://dx.doi.org/10.1016/j.cej.2006.10.003>
- Sumpio, B. E., Upchurch, G. R., & Johnson, G. (1989). The influence of perfusate viscosity, RBC deformability and drag on the function of an isolated perfused rat kidney. *Journal of Surgical Research*, 46(1), 4-8. doi:[http://dx.doi.org/10.1016/0022-4804\(89\)90174-1](http://dx.doi.org/10.1016/0022-4804(89)90174-1)
- Sun, Y., Wu, Q., Wei, M., Bai, B., & Ma, Y. (2014). Experimental study of friction reducer flows in microfracture. *Fuel*, 131(0), 28-35. doi:<http://dx.doi.org/10.1016/j.fuel.2014.04.050>
- Talmadge, J., Chavez, J., Jacobs, L., Munger, C., Chinnah, T., Chow, J. T., . . . Yates, K. (2004). Fractionation of Aloe vera L. inner gel, purification and molecular profiling of activity. *International Immunopharmacology*, 4(14), 1757-1773. doi:<http://dx.doi.org/10.1016/j.intimp.2004.07.013>
- Tamano, S., Ikarashi, H., Morinishi, Y., & Taga, K. (2015). Drag reduction and degradation of nonionic surfactant solutions with organic acid in turbulent pipe flow. *Journal of Non-Newtonian Fluid Mechanics*, 215, 1-7. doi:<http://dx.doi.org/10.1016/j.jnnfm.2014.10.011>
- Tang, G. H., Lu, Y. B., Zhang, S. X., Wang, F. F., & Tao, W. Q. (2012). Experimental investigation of non-Newtonian liquid flow in microchannels. *Journal of Non-Newtonian Fluid Mechanics*, 173-174(0), 21-29. doi:<http://dx.doi.org/10.1016/j.jnnfm.2012.02.001>
- Tarn, M. D., & Pamme, N. (2014). *Microfluidics Reference Module in Chemistry, Molecular Sciences and Chemical Engineering*: Elsevier.
- Tay, A., Pavesi, A., Yazdi, S. R., Lim, C. T., & Warkiani, M. E. (2016). Advances in microfluidics in combating infectious diseases. *Biotechnology Advances*, 34(4), 404-421. doi:<http://dx.doi.org/10.1016/j.biotechadv.2016.02.002>
- Terry, S. C., Jerman, J. H., & Angell, J. B. (1979). A gas chromatographic air analyzer fabricated on a silicon wafer. *Ieee Transactions On Electron Devices*, 26(12), 1880-1886. doi:<http://dx.doi.org/10.1109/T-ED.1979.19791>
- Thais, L., Gatski, T. B., & Mompean, G. (2013). Analysis of polymer drag reduction mechanisms from energy budgets. *International Journal of Heat and Fluid Flow*, 43(0), 52-61. doi:<http://dx.doi.org/10.1016/j.ijheatfluidflow.2013.05.016>

- Tian, M., Fang, B., Jin, L., Lu, Y., Qiu, X., Jin, H., & Li, K. (2015). Rheological and drag reduction properties of hydroxypropyl xanthan gum solutions. *Chinese Journal of Chemical Engineering*, 23(9), 1440-1446. doi:http://dx.doi.org/10.1016/j.cjche.2015.04.003
- Ting, C. J., Huang, M. C., Tsai, H. Y., Chou, C. P., & Fu, C. C. (2008). Low cost fabrication of the large-area anti-reflection films from polymer by nanoimprint/hot-embossing technology. *Nanotechnology*, 19(20), 205301. doi:http://dx.doi.org/10.1088/0957-4484/19/20/205301
- Tjerkstra, R. W., Boer, M. D., Berenschot, E., Gardeniers, J. G. E., Berg, A. v. d., & Elwenspoek, M. (1997a, 26-30 Jan 1997). *Etching technology for microchannels*. Paper presented at the Micro Electro Mechanical Systems, 1997. MEMS '97, Proceedings, IEEE., Tenth Annual International Workshop on.
- Tjerkstra, R. W., Boer, M. d., Berenschot, E., Gardeniers, J. G. E., Berg, A. v. d., & Elwenspoek, M. C. (1997b). Etching technology for chromatography microchannels. *Electrochimica Acta*, 42(20-22), 3399-3406. doi:http://dx.doi.org/10.1109/MEMSYS.1997.581790
- Toth, K., Kesmarky, G., & Vekasi, J. (1999). Hemorheological and hemodynamic parameters in patients with essential hypertension and their modification by alpha-1 inhibitor drug treatment. *Clinical Hemorheology and Microcirculation*, 21, 209-216.
- Truong, V.-T. (2001). *Drag Reduction Technologies*. Australia: DSTO Aeronautical and Maritime Research Laboratory
- Truter, L. A., Ordonsky, V., Schouten, J. C., & Nijhuis, T. A. (2016). The application of palladium and zeolite incorporated chip-based microreactors. *Applied Catalysis A: General*, 515, 72-82. doi:http://dx.doi.org/10.1016/j.apcata.2016.01.039
- Tsao, C.-W., Chen, T.-Y., Woon, W. Y., & Lo, C.-J. (2012). Rapid polymer microchannel fabrication by hot roller embossing process. *Microsystem Technologies*, 18(6), 713-722. doi:http://dx.doi.org/10.1007/s00542-012-1513-1
- Tsaoulidis, D., Dore, V., Angeli, P., Plechkova, N. V., & Seddon, K. R. (2013). Flow patterns and pressure drop of ionic liquid-water two-phase flows in microchannels. *International Journal of Multiphase Flow*, 54, 1-10. doi:http://dx.doi.org/10.1016/j.ijmultiphaseflow.2013.02.002
- Tseng, L.-Y., Yang, A.-S., Lee, C.-Y., & Hsieh, C.-Y. (2011). CFD-based optimization of a diamond-obstacles inserted micromixer with boundary protrusions. *Engineering Applications of Computational Fluid Mechanics*, 5(2), 210-222. https://doi.org/10.1080/19942060.2011.11015365

- Tuan, N. A., & Mizunuma, H. (2013). High-shear drag reduction of surfactant solutions. *Journal of Non-Newtonian Fluid Mechanics*, 198(0), 71-77. doi:http://dx.doi.org/10.1016/j.jnnfm.2013.05.002
- Unthank, J. L., Lalka, S. G., Nixon, J. C., & Sawchuk, A. P. (1992). Improvement of flow through arterial stenoses by drag reducing agents. *Journal of Surgical Research*, 53(6), 625-630. doi:http://dx.doi.org/10.1016/0022-4804(92)90265-2
- Ushida, A., Hasegawa, T., Kudou, S., Kawami, M., Uchiyama, H., & Narumi, T. (2011). Flow properties of several types of liquid flows through micro-orifices. *Journal of Fluid Science and Technology*, 6(6), 802-811. doi:http://dx.doi.org/10.1299/jfst.6.802
- Ushida, A., Hasegawa, T., & Narumi, T. (2010). Drag reduction for liquid flow through micro-apertures. *Journal of Non-Newtonian Fluid Mechanics*, 165(21-22), 1516-1524. doi:http://dx.doi.org/10.1016/j.jnnfm.2010.07.015
- van Nesselrooij, M., Veldhuis, L. L. M., van Oudheusden, B. W., & Schrijer, F. F. J. (2016). Drag reduction by means of dimpled surfaces in turbulent boundary layers. *Experiments in Fluids*, 57(9), 142. doi:http://dx.doi.org/10.1007/s00348-016-2230-9
- Velten, T., Schuck, H., Haberer, W., & Bauerfeld, F. (2009). Investigations on reel-to-reel hot embossing. *The International Journal of Advanced Manufacturing Technology*, 47(1), 73-80. doi:http://dx.doi.org/10.1007/s00170-009-1975-1
- Virk, P. S. (1975). Drag reduction fundamentals. *AIChE Journal*, 21(4), 625-656. doi:http://dx.doi.org/10.1002/aic.690210402
- Viswanath, P. R. (2002). Aircraft viscous drag reduction using riblets. *Progress in Aerospace Sciences*, 38(6-7), 571-600. doi:http://dx.doi.org/10.1016/S0376-0421(02)00048-9
- Vlachogiannis, M., & Hanratty, T. J. (2004). Influence of wavy structured surfaces and large scale polymer structures on drag reduction. *Experiments in Fluids*, 36, 685-700. doi:http://dx.doi.org/10.1007/s00348-003-0745-3
- Walsh, E., Muzychka, Y., Walsh, P., Egan, V., & Punch, J. (2009). Pressure drop in two phase slug/bubble flows in mini scale capillaries. *International Journal of Multiphase Flow*, 35(10), 879-884. doi:http://dx.doi.org/10.1016/j.ijmultiphaseflow.2009.06.007
- Walsh, M. (1982). Turbulent boundary layer drag reduction using riblets. *20th Aerospace Sciences Meeting: American Institute of Aeronautics and Astronautics*.

- Walsh, M., & Lindemann, A.. (1984). Optimization and application of riblets for turbulent drag reduction. *22nd Aerospace Sciences Meeting: American Institute of Aeronautics and Astronautics*.
- Walsh, M. J. (1983). Riblets as a viscous drag reduction technique. *AIAA Journal*, 21(4), 485-486. doi:http://dx.doi.org/10.2514/3.60126
- Wang, H., Iovenitti, P., Harvey, E., & Masood, S. (2002). Optimizing layout of obstacles for enhanced mixing in microchannels. *Smart Materials and Structures*, 11(5), 662–667. https://doi.org/10.1088/0964-1726/11/5/306
- Weibel, D. B., & Whitesides, G. M. (2006). Applications of microfluidics in chemical biology. *Current Opinion in Chemical Biology*, 10(6), 584-591. doi:http://dx.doi.org/10.1016/j.cbpa.2006.10.016
- White, C. M., & Mungal, M. G. (2008). Mechanics and prediction of turbulent drag reduction with polymer additives. *Annual Review of Fluid Mechanics*, 40(1), 235-256. doi:http://dx.doi.org/10.1146/annurev.fluid.40.111406.102156
- Wong, I., & Ho, C.-M. (2009). Surface molecular property modifications for poly(dimethylsiloxane) (PDMS) based microfluidic devices. *Microfluidics and Nanofluidics*, 7(3), 291-306. doi:http://dx.doi.org/10.1007/s10404-009-0443-4
- Xia, G., Liu, Q., Qi, J., & Xu, J. (2008). Influence of surfactant on friction pressure drop in a manifold microchannel. *International Journal of Thermal Sciences*, 47(12), 1658-1664. doi:http://dx.doi.org/10.1016/j.ijthermalsci.2008.01.014
- Xiao, R., & Zheng, Y. (2016). Overview of microalgal extracellular polymeric substances (EPS) and their applications. *Biotechnology Advances*, 34(7), 1225-1244. doi:http://dx.doi.org/10.1016/j.biotechadv.2016.08.004
- Xu, J., Locascio, L., Gaitan, M., & Lee, C. S. (2000). Room-temperature imprinting method for plastic microchannel fabrication. *Analytical Chemistry*, 72(8), 1930-1933. doi:http://dx.doi.org/10.1021/ac991216q
- Yang, A.-S., Chuang, F.-C., Chen, C.-K., Lee, M.-H., Chen, S.-W., Su, T.-L., & Yang, Y.-C. (2015). A high-performance micromixer using three-dimensional Tesla structures for bio-applications. *Chemical Engineering Journal*, 263(Supplement C), 444–451. https://doi.org/https://doi.org/10.1016/j.cej.2014.11.034
- Yang, S.-Q., & Ding, D. (2013). Drag reduction induced by polymer in turbulent pipe flows. *Chemical Engineering Science*, 102(0), 200-208. doi:http://dx.doi.org/10.1016/j.ces.2013.07.048
- Yeo, L. P., Ng, S. H., Wang, Z., Wang, Z., & de Rooij, N. F. (2009). Micro-fabrication of polymeric devices using hot roller embossing. *Microelectronic Engineering*, 86(4–6), 933-936. doi:http://dx.doi.org/10.1016/j.mee.2008.12.021

- Yeo, L. P., Ng, S. H., Wang, Z. F., Xia, H. M., Wang, Z., & Thang, V. S. (2010). Investigation of hot roller embossing for microfluidic devices. *Journal of Micromechanics and Microengineering*, 20(1), 1-10. doi:<http://dx.doi.org/10.1088/0960-1317/20/1/015017>
- Ying, X., Zhang, L., Xu, H., Ren, Y.-L., Luo, Q., Zhu, H.-W., . . . Xuan, J. (2016). Efficient Fischer–Tropsch microreactor with innovative aluminizing pretreatment on stainless steel substrate for Co/Al<sub>2</sub>O<sub>3</sub> catalyst coating. *Fuel Processing Technology*, 143, 51-59. doi:<http://dx.doi.org/10.1016/j.fuproc.2015.11.005>
- You, X.-y., & Guo, L.-x. (2010). Analysis of EDL effects on the flow and flow stability in microchannels. *Journal of Hydrodynamics, Ser. B*, 22(5), 725-731. doi:[http://dx.doi.org/10.1016/S1001-6058\(09\)60109-8](http://dx.doi.org/10.1016/S1001-6058(09)60109-8)
- Youdan, G. (2014). Flow characteristics of microchannel melts during injection molding of microstructure medical components. *Journal of Chemical and Pharmaceutical Research*, 6(5), 112-117
- Yu, B., & Kawaguchi, Y. (2006). Parametric study of surfactant-induced drag-reduction by DNS. *International Journal of Heat and Fluid Flow*, 27(5), 887-894. doi:<http://dx.doi.org/10.1016/j.ijheatfluidflow.2006.03.013>
- Yu, B., Li, F., & Kawaguchi, Y. (2004). Numerical and experimental investigation of turbulent characteristics in a drag-reducing flow with surfactant additives. *International Journal of Heat and Fluid Flow*, 25(6), 961-974. doi:<http://dx.doi.org/10.1016/j.ijheatfluidflow.2004.02.029>
- Zaharuddin, N. D., Noordin, M. I., & Kadivar, A. (2014). The use of Hibiscus esculentus (okra) gum in sustaining the release of propranolol hydrochloride in a solid oral dosage form. *BioMed Research International*, 2014, 8. doi:<http://dx.doi.org/10.1155/2014/735891>
- Zakaria, A. N. B., & Nabil, A. (2012). *Drag reducing agent for water system using natural polymer (hibiscus leaves)*. (Bachelor Degree), Universiti Teknologi Petronas. Retrieved from <http://utpedia.utp.edu.my/5638/1/Ahmed%20Nabil%2011878%20FYP%20Dissertation.pdf>
- Zhang, C., Xing, D., & Li, Y. (2007). Micropumps, microvalves, and micromixers within PCR microfluidic chips: Advances and trends. *Biotechnology Advances*, 25(5), 483–514. doi:<https://doi.org/10.1016/j.biotechadv.2007.05.003>
- Zhang, J., Sahli, M., Gelin, J. C., & Barrière, T. (2015). Roll manufacturing of polymer microfluidic devices using a roll embossing process. *Sensors and Actuators A: Physical*, 230, 156-169. doi:<http://dx.doi.org/10.1016/j.sna.2015.03.002>

- Zhang, K., Lim, G. H., & Choi, H. J. (2016). Mechanical degradation of water-soluble acrylamide copolymer under a turbulent flow: Effect of molecular weight and temperature. *Journal of Industrial and Engineering Chemistry*, 33, 156-161. doi:<http://dx.doi.org/10.1016/j.jiec.2015.09.031>
- Zhao, C.-X. (2013). Multiple flow microfluidics for the production of single or multiple emulsions for drug delivery. *Advanced Drug Delivery Reviews*, 1420–1446. doi:<http://dx.doi.org/10.1016/j.addr.2013.05.009>
- Zhao, D. S., Roy, B., McCormick, M. T., Kuhr, W. G., & Brazill, S. A. (2003). Rapid fabrication of a poly(dimethylsiloxane) microfluidic capillary gel electrophoresis system utilizing high precision machining. *Lab Chip*, 3(2), 93-99. doi:<http://dx.doi.org/10.1039/b300577a>
- Zhao, R., Marhefka, J. N., Antaki, J. F., & Kameneva, M. V. (2010). Drag-reducing polymers diminish near-wall concentration of platelets in microchannel blood flow. *Biorheology*, 47(3-4), 193-203. doi:<http://dx.doi.org/10.3233/bir-2010-0570>
- Zhou, Y., Shah, S. N., & Gujar, P. V. (2006). Effects of coiled tubing curvature on drag reduction of polymeric fluids. *Society of Petroleum Engineers*, 21(01). doi:<http://dx.doi.org/10.2118/89478-PA>
- Zhu, Y., & Fang, Q. (2013). Analytical detection techniques for droplet microfluidics—A review. *Analytica Chimica Acta*, 787, 24-35. doi:<http://dx.doi.org/10.1016/j.aca.2013.04.064>
- Ziaie, B., Baldi, A., Lei, M., Gu, Y., & Siegel, R. A. (2004). Hard and soft micromachining for BioMEMS: review of techniques and examples of applications in microfluidics and drug delivery. *Advanced Drug Delivery Reviews*, 56(2), 145-172. doi:<http://dx.doi.org/10.1016/j.addr.2003.09.001>

## APPENDIX A PUBLICATIONS AND AWARDS

### Journals

- ❖ Hayder. A. Abdulbari, Fiona W. M. Ling, Z. Hassan, and J.T. Heng, *Experimental Investigations on Biopolymer in Enhancing the Liquid Flow in Microchannel*, *Advances in Polymer Technology* (accepted) [IF: 2.073]
- ❖ Hayder A. Abdulbari and Fiona W.M. Ling, *Hibiscus Mucilage for Enhancing the Flow in Blood-Stream-Like Microchannel System*, *Chemical Engineering Communications* Vol. 204 (2017) 1282-1298 [IF: 1.433]
- ❖ Fiona W.M. Ling and Hayder A. Abdulbari, *Drag reduction by natural polymeric additives in PMDS microchannel: Effect of types of additives*, *MATEC Web of Conference*, 111, 2017.
- ❖ Fiona W.M. Ling, Wafaa K. Mahmood and Hayder A. Abdulbari, *Rapid Prototyping of Microfluidics Devices using Xurography Method*, *MATEC Web of Conference*, 111, 2017.
- ❖ Fiona W.M. Ling and Hayder A. Abdulbari, *Enhancing the Flow in Microchannel using Natural Polymeric Additives*, *Indian Journal of Science and Technology (IJST)*, 2017. 10(7). [Q2]
- ❖ Fiona Ling Wang Ming, Hayder A. Abdulbari, Noraishah Bt Abdul Latip and Somaye Heidarinik, *Insoluble Nanopowders Additives Enhancing the Flow of Liquid in Microchannel: Effect of Particle Size*, *Journal of Engineering and Applied Science* Vol. 11, No. 4 (2016) 2146-2152 [Q3]
- ❖ Hayder A. Abdulbari, Fiona Ling Wang Ming, Wafaa K. Mahmooda, *Insoluble Additives for Enhancing a Blood-Like liquid Flow in Micro-Channels*, *Journal of Hydrodynamics* Vol. 29, No. 1 (2017) 144-153 [IF: 0.776]
- ❖ H.A. Abdulbari and F.L.W. Ming, *Drag Reduction Properties of Nanofluids in Microchannels*, *The Journal of Engineering Research (TJER)* Vol. 12, No. 2 (2015) 60-67

## Honors & Awards

- ❖ Gold Medal, Creation, Innovation, Technology & Research Exposition (CITREX), 2018
- ❖ Gold Medal, 13th annual of Seoul International Invention Fair (SIIF), 2017
- ❖ Special Award, The International Conference and Exposition on Inventions by Institutions of Higher Learning (PECIPTA), 2017
- ❖ Gold Medal, The International Conference and Exposition on Inventions by Institutions of Higher Learning (PECIPTA), 2017
- ❖ Best Paper Award, FluidsChE 2017 (Microfluidics)
- ❖ Gold Medal, Creation, Innovation, Technology & Research Exposition (CITREX), 2017
- ❖ Silver Medal, Creation, Innovation, Technology & Research Exposition (CITREX), 2017
- ❖ Bronze Medal, Creation, Innovation, Technology & Research Exposition (CITREX), 2016

## Conferences

- ❖ ICCEIB 2018, Kuala Lumpur, 1-2 August, 2018
- ❖ FluidsChe 2017, Kota Kinabalu, Sabah, 4 – 6 April, 2017